CHARACTERIZATION OF THE INFLUENCE OF APPLIED EXTRACELLULAR FIELDS ON EPILEPTIFORM ACTIVITIES IN THE DENTATE GYRUS OF THE RAT

by

Collette N. O'Reilly

B.Sc. (Kines.), Simon Fraser University, 1988

THESIS SUBMITTED IN PARTIAL FULFILLMENT

OF THE REQUIREMENTS FOR THE DEGREE OF

MASTER OF SCIENCE

in the

School of Kinesiology

SIMON FRASER UNIVERSITY
January 1994

APPROVAL

NAME: Collette O'Reilly

DEGREE: Master of Science Kinesiology

TITLE OF THESIS: Characterization of the Influence of Applied Extracellular Fields on Epileptiform Activities in the Dentate Gyrus of the Rat

EXAMINING COMMITTEE:

Chair: Dr. Glen Tibbits

Dr. Tom Richardson
Senior Supervisor

Dr. Kerry Delaney
Supervisory Committee

Dr. John Church
External Examiner
University of British Columbia
Department of Anatomy

Date Approved: 10 JAN 94

PARTIAL COPYRIGHT LICENSE

Title of Thesis/Project/Extended Essay

CHARACTERIZATION OF THE INFLUENCE OF APPLIED EXTRACELLULAR FIELDS ON EPILEPTIFORM ACTIVITIES IN THE DENTATE GYRUS OF THE RAT.

Author: _____
(signature)

COLLETTE O'REILLY
(name)

JAN. 28/94
(date)

ABSTRACT

The epilepsies are neurological disorders that affect approximately 2% of the population. A growing body of evidence implicates extracellular field effects as contributing to the generation of epileptiform events. Most of this evidence is based on the finding that epileptiform bursts occur in the hippocampus during synaptic blockade by reducing the extracellular $[Ca^{2+}]$. This low $[Ca^{2+}]_o$ seizure activity is confined to area CA1, whereas bursting is rarely observed in the dentate gyrus. The differing propensity of these two regions to exhibit seizures may be due to a lower level of excitability of granule cells, rather than other differences in intrinsic neuronal characteristics. This hypothesis was tested by depolarizing the granule cell population with the application of appropriate extracellular fields. This treatment resulted in low $[Ca^{2+}]_o$ antidromic bursts in the dentate gyrus in 100% of the experimental trials (n=24). This finding suggests that the physiological properties required for epileptiform discharge exist in the seizure resistant dentate gyrus and that the mechanisms underlying these events are non-synaptic. Larger depolarizing field intensities resulted in non-antidromic, field induced population bursts in the dentate gyrus in 100% of the experimental trials (n=24). This finding demonstrates that, when the granule cell population is uniformly depolarized with extracellular fields, seizure activity can be initiated. Finally, the antidromic bursts

of the dentate gyrus were compared to those of CA1 and found to have similar spike amplitudes, spike amplitude patterns, and patterns of discharge. The similarities found between the bursting in these two tissues suggest that common mechanisms may underlie these epileptiform events. The relationship between extracellular fields and the antidromic population response was also investigated. A useful predictive equation for this relationship is reported ($m=0.133+\backslash-0.001$, $p<0.0001$). The tissue generated extracellular voltage gradients present during antidromic spikes are appropriate in magnitude and polarity to depolarize the transmembrane potential of individual granule cells and similar gradients are known to synchronize the discharge of large populations of neurons in CA1. The findings indicate that a large component of the population response to antidromic stimulation is actually recruited through non-synaptic mechanisms. The results of this thesis project suggest that non-synaptic mechanisms may have widespread influences on neuronal excitability.

ACKNOWLEDGEMENTS

The author wishes to thank Dr. Tom Richardson for his supervision and guidance throughout this project. Recognition is also extended to Dr. Kerry Delaney and Mr. Tim Phillips for their consultation and assistance in completing this thesis. For their support, Roderick and Joan O'Reilly are acknowledged as contributors to this work.

TABLE OF CONTENTS

LIST OF TABLES

LIST OF FIGURES

1.0 - INTRODUCTION

The disabling condition of epilepsy is manifested as cortical seizures that range clinically from the relatively small disturbances of the *petite mal* seizure, to the life threatening episodes of the *grand mal*. Salient to all neural activities categorized as "epileptiform" is the abnormal, intense, synchronous, and self sustained discharge of large populations of cortical neurons (Jackson, 1870; Yaari, 1988). A major challenge of researchers investigating the basic mechanisms involved in the pathology of epilepsy is to understand the genesis of this synchrony. Much of this research has focused on the hippocampal formation as this structure demonstrates a strong propensity for highly synchronous epileptic events (Haas, Jefferys,1984; Yaari et al,1983; Taylor, Dudek, 1982; Traynelis, Dingledine, 1988) and hippocampal sclerosis is the most common pathological correlate of human temporal lobe epilepsy.

Area one of the cornu ammons (CA1) of the hippocampal formation is often reported as a seizure prone region in human temporal lobe epilepsy (Houser, 1992) and in animal models of epilepsy (Anderson et al,1978; Taylor, Dudek,1982; Albrecht et al, 1989; TaylorDudek 1984; Schweitzer et al, 1992; Roper et al, 1992). This apparent propensity of the CA1 to exhibit seizure activity is in stark contrast to the dentate gyrus which is remarkably seizure resistant (Fricke,

Prince 1984; Albrecht et al 1989; Schweitzer et al 1992; Lothman 1991; Lothman et al 1991,1992). The fact that the dentate gyrus is selectively spared from the extensive neuronal loss often reported in histological examination of epileptic tissues supports this speculation (Babb et al, 1984; Babb, Brown, 1987; Franck, Roberts, 1990; Kim et al, 1990; Sagar, Oxbury, 1987; Urban et al, 1993). As these two tissues exist in close proximity to one another, have laminar structures, and both are part of the hippocampal tri-synaptic network (Heinemann et al, 1992; Schwartzkroin et al, 1992) this difference in seizure propensity has lead to speculation that the dentate gyrus is naturally "protected" from developing seizure activity. If so, then identifying this unique protective mechanism could open new avenues for treatment of seizures in humans.

The dentate gyrus is under strong synaptic inhibition from basket cells distributed in all regions of the dentate gyrus as well as hilar interneurons (Scharfman, 1992). It is postulated that this inhibition results in the resistance of the dentate gyrus to epileptiform activity in animal models of epilepsy and various forms of human temporal lobe epilepsy.

One of the few models of epilepsy in the dentate gyrus is maximal dentate activation (MDA). In these recent *in vivo* studies, maximal high frequency stimulation of the perforant path from the enthorinal cortex can resulted in epileptiform discharge of the dentate gyrus (Stinger et al

1989; Stringer, Lothman, 1989; Stringer, Lothman, 1990; Stringer et al, 1991). Unlike human epilepsy, cell loss in the dentate gyrus is marked with MDA (Stringer, Lothman, 1989; Stringer et al, 1991; Stringer, Lothman,1992). Lothman proposed that high frequency stimulation evokes seizure activity in the MDA model by overcoming the strong inhibition in the dentate gyrus (Lothman, 1991; Lothman et al, 1991,1992).

The *in vitro* slice preparation of the hippocampus is frequently used for studies into epileptic mechanisms as it provides direct access to the neuronal elements within the hippocampus in a highly controlled experimental environment. Furthermore, several forms of experimentally induced seizure activity occurs in the hippocampal slice. While initial attempts to produce robust epileptiform activity in the dentate gyrus failed (example Somjen 1985), more recently, the epileptiform events of the MDA model were replicated in the dentate gyrus of the *in vitro* hippocampal slice (Schweitzer et al 1992).

While synaptic mechanisms clearly play a role in the generation of seizure activity, robust epileptiform activity can occur under conditions of synaptic blockade. When Ca^{2+} is not added to the perfusing medium of *in vitro* hippocampal slices, robust, prolonged epileptiform events developed. These events consist of spontaneous bursts of population spikes involving the entire CA1 neuronal population

(Anderson et al,1978; Taylor, Dudek,1984; Snow, Dudek,1984; Jefferys, Haas, 1982; Schweitzer et al 1992).

Field effects, a specific form of non-synaptic inter-neuronal communication, are known to contribute to population synchronization and recruitment during low $[Ca^{2+}]_o$ bursts in CA1 (Taylor, Dudek, 1982). Area CA1 and the dentate gyrus have in common many of the structural characteristics important to the generation of field effects (Korn, Faber, 1989).

On a macroscopic level, both CA1 and the dentate gyrus are highly organized structures. Their somata are tightly packed into single discrete layers and the spatially distended dendritic arbors of neighboring cells branch off parallel to one another and perpendicular to the somatic layers. Upon electrophysiological examination, orthodromic and antidromic stimulation of these populations produces remarkably similar extracellular population responses. In both regions, the extracellular space is unusually small, while the extracellular resistivity is unusually high (McBain et al, 1990).

Despite these similarities, and the fact that the granule cells of the dentate gyrus are sensitive to field effects (Jefferys, 1981; O'Reilly, Richardson 1992; O'Reilly, Richardson 1993), during low $[Ca^{2+}]_o$ (zero added Ca^{2+}) perfusions, the dentate gyrus rarely demonstrates spontaneous or antidromically evoked epileptiform events, while these events are readily observed in the CA1

(O'Reilly, Richardson 1993; Schweitzer et al 1992; Roper et al, 1992).

Considerable evidence exists that non-synaptic mechanisms contribute to the neuronal excitation and neuronal synchronization of epileptiform events (Richardson et al,1984a; Jefferys, Haas, 1982; Haas, Jefferys,1984; Yaari et al,1983; Snow, Dudek,1984; Schweitzer et al 1992). Other possible non-synaptic mechanisms contributing to seizure activity include excitatory interconnections via gap junctions, altered extracellular $[K^+]_o$, and extracellular field effects.

Each of these non-synaptic mechanisms, along with synaptic mechanisms, probably contributes to seizure activity, however, no one mechanism in isolation is adequate to explain all of the available data. Based on these observations, and the fact that synaptic inhibition is blocked, the absence of seizure activity in the dentate gyrus leads to speculation as to what keeps this tissue from developing epileptiform discharges. This thesis was undertaken to identify what conditions are necessary for the dentate gyrus to exhibit robust epileptiform activity in the hope that this approach will shed some light on how the dentate gyrus normally resists seizure activity.

Note: Recently the term "ephaptics" has been discouraged in favor of the more descriptive term "extracellular field effects". While the terminology in this area continues to evolve, for the purposes of this

document, "ephaptic interactions", "ephaptics", "extracellular field effects", and "field effects" will be used interchangeably. The author's use of other terms is described in Appendix A - Terminology and Definitions.

2.0 - OVERVIEW

Research into other more widely understood human pathologies, dictates that no one isolated mechanism is likely to be solely responsible for such a complex phenomenon as the epileptic seizure. Coverage of the background material relevant to the specific goals of this thesis are reviewed here. Refer to Appendix B: "History of Ephaptic Interactions" for a detailed account of the scientific milestones in this area.

In this thesis project, field effects were used as a tool to depolarize and hyperpolarize entire populations of neurons. Field effects occur when extracellular currents flowing along the dendro-somatic axis of an active neuron have an effect on the state of excitability of a neighboring neuronal membrane (See Figure 1 and for a review Faber and Korn (1989)).

When a cell fires an action potential a voltage gradient is established along the length of the neuron as current flows in the extracellular space. If a non-active neuron is situated within this region of extracellular current it will be directly depolarized or hyperpolarized, dependent on its physical alignment to the active cell.

The majority of current will travel along the path of least resistance, which, in this case, is the extracellular space. However, current will also flow through the intracellular path offered by a cell situated within its

Figure 1 Field Effects / Ephaptic Interactions

Field effects between two populations of neighboring neurons are illustrated. The arrows depict current flow induced by an active population of neurons (bottom). The current sink at the soma generated by the firing of an action potential results in a current source in the dendrites of this population (bottom). Current will return via the path of least resistance offered by the extracellular space, however, some of this current will also flow via the path offered by the inactive cell population (top) and results in a depolarization of the somatic membrane of the inactive cells. Field effects generated by synchronous discharge of the tissue are maximal at the peak negativity of an extrasomatic population potential (left) and the corresponding positive extradendritic potential (right). This current flow is exaggerated when 1) the extracellular resistance is high, 2) the dendrites are uninsulated and spatially extended, and 3) the cells within the population are organized in parallel. These conditions are seen in CA1 of the hippocampal formation and the dentate gyrus.

Dentate Voltage Gradient - Antidromic

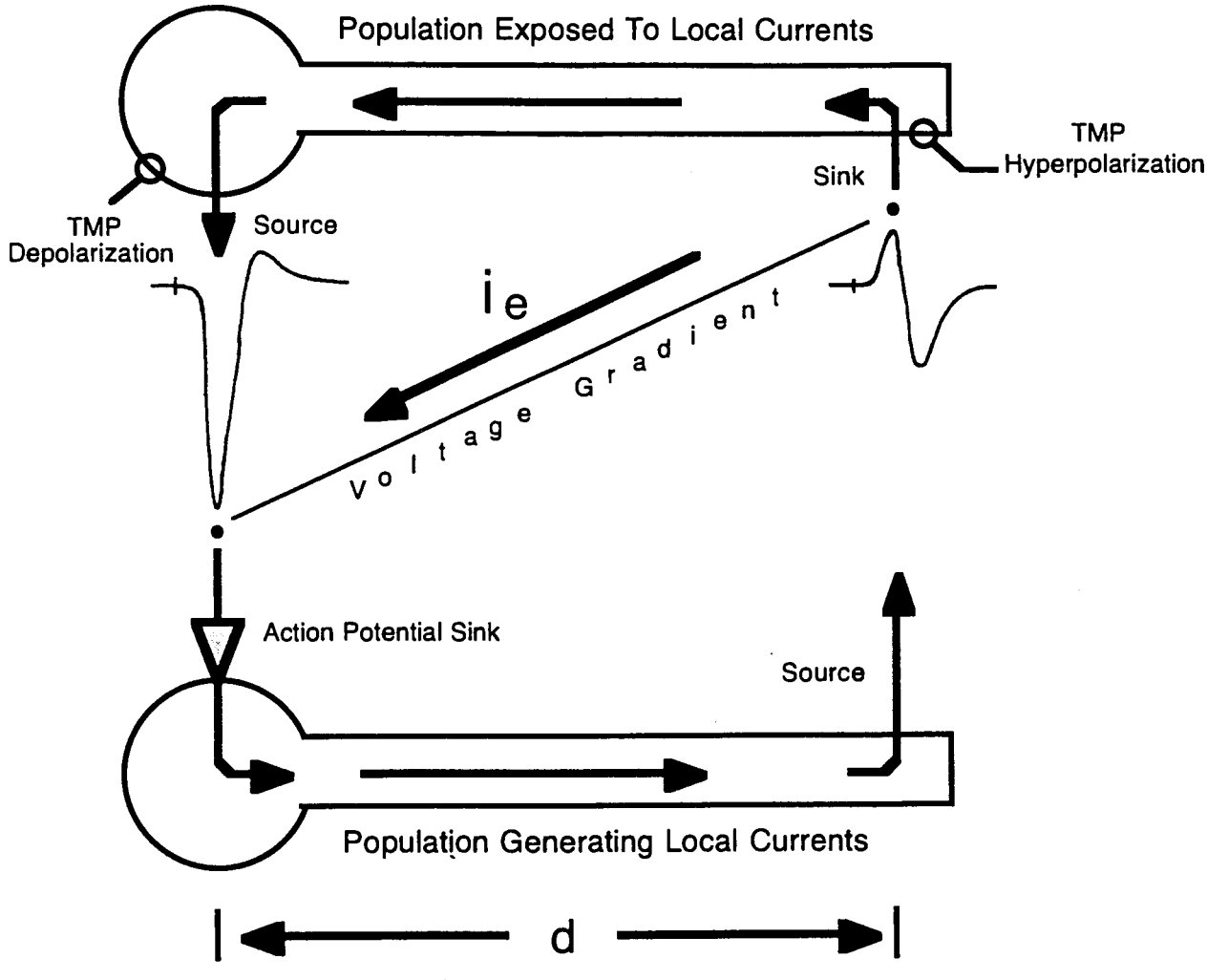

field. This current will pass into this cell, flow along its axis a finite distance and then return to the extracellular space. This results in a change to the membrane potential of the cell. The current flow and effect can be expanded to include a whole population of cells.

Field effects have a set of criteria which augment their effectiveness. The conditions which favor a significant influence of field effects are 1) a high extracellular resistance, 2) a dense approximation of un-insulated neurons, and 3) the parallel alignment of the neurons within a population in physical space (Green 1964; Green, Maxwell 1961; Yim et al 1986; Dudek, Traub, 1988; Korn, Faber 1989).

In the hippocampal formation and the dentate gyrus, all three of these criteria are met. An active pyramidal or granule cell population produces extracellular currents that are depolarizing to neighboring cells.

2.1 - Hippocampal Anatomy

The experiments reported in this thesis were carried out in the hippocampal slice preparation. This section reviews the cellular organization and synaptic interconnections of this structure.

In areas of the cornu ammons (CA1, CA2, and CA3) this anatomy includes the alveus, stratum oriens (SO), stratum pyramidal (SP), stratum radiatum (SR), and the stratum

lacunosum molecular layer (SLM). In the dentate gyrus the layers extend from the hippocampal fissure to the molecular layer (ML), granule cell layer (GC), and the dentate hilus. (See Figure 2.)

The alveus is a glossy white complex of myelinated axons which originate from the pyramidal cells of CA1-CA2. These axons project in one direction to the entorhinal cortex and in the opposite direction along the alveus and leave the hippocampus via the fornix and fimbria.

The stratum oriens contains the basal dendrites of the hippocampal pyramidal cells whose cell bodies make up stratum pyramidale. In the hippocampal slice of the rat, SO has an approximate width of 160 um +\- 18.4 um (Richardson et al.1987).

When stratum pyramidale is considered as a whole, its approximate width in the hippocampal slice of the rat is 44 um +\- 2.9 um (Richardson et al.1987). The extracellular space of the CA1 pyramidal cell layer is reported to comprise 7% of the tissue volume (Heinemann, 1983; Heinemann, 1982), while other regions of mammalian brain are roughly 20% extracellular space by volume (Heinemann, 1982). An Extracellular Volume Fraction (ECVF) for CA1 of 11.9% has been reported more recently (McBain et al,1990).

The soma of pyramidal cells are conical, 20-40um at the apical end and 40-60um in height (Shepherd, 1990). The prominent single apical dendrite (5-10um in diameter) bifurcates at 75-100um into stratum radiatum (Shepherd,

Figure 2 Hippocampal Anatomy

Both the hippocampal orientation in the rat brain and the intrinsic anatomy of the hippocampal slice are shown. The hippocampus and dentate gyrus are highly organized structures with well defined layers. Pyramidal cells of cornu ammons (CA1, CA2, CA3) and granule cells of the dentate gyrus are interconnected via the hippocampal tri-synaptic loop. The upper blade of the dentate gyrus is the site for the studies described in this project.

Hippocampal Anatomy

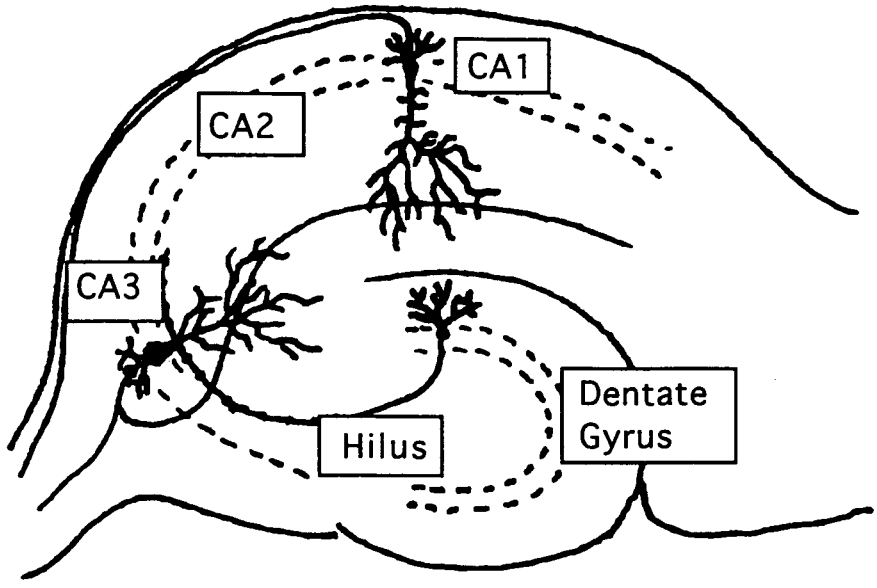

1990). Beyond this point the dendritic arbor spreads laterally an average of 50-100 um (Richardson et al.1987). Several basal dendrites with diameters of 3-6um arborize over 200-300um to form the stratum oriens (Shepherd, 1990).

Inhibitory basket cells are concentrated in stratum pyramidale providing synaptic feedback to the pyramidal cell population. However, primary cells outnumber interneurons in most regions of the hippocampus (Amaral et al,1990).

The apical dendrites of the pyramidal cells are found in stratum radiatum which has an approximate width of 303 um +\- 7.8 um (Richardson et al.1987). This layer also contains the axonal projections from the pyramidal cells of CA3, referred to as the Schaffer collaterals. A second axonal projection from CA3 cells tracts out of the hippocampus via the fornix and fimbria. Recent evidence also points to some axonal projections extending from CA3 into the dentate hilar region (Pokorny, Schwartzkroin, 1991). The Schaffer collaterals differ from the axons of the CA1-CA2 pyramidal cells in that they synapse on the dendrites of all regions CA1-CA3, whereas the axons of CA1-CA2 do not directly synapse onto cells within these areas.

Stratum lacunosum moleculare (SLM) contains the most distal arborizations of the apical dendrites of the pyramidal cells and is the region within which the perforant path from the subiculum is located. Its approximate width is 102 um +\- 4.4 um (Richardson et al.1987). These

measurements give the apical dendrites of CA1 pyramidal cells a maximum length of just over 400 um.

The perforant path enters the subiculum from the entorhinal cortex and splits to cross the hippocampal fissure to synapse on the apical dendrites of the dentate granule cells in the molecular layer of the dentate gyrus. A second branch of the perforant path travels parallel to the Schaffer collaterals and then turns to innervate the dentate without crossing the fissure. This is accomplished as this path extends along the fissure towards CA3 and then changes direction towards the dentate gyrus, completely avoiding the fissure.

The dentate gyrus is made up of two blades. With an average diameter of 10um (Shepherd, 1990), the somata of the dentate granule cell is considerably smaller than that of the pyramidal cell. The dentate granule cells only have one set of dendrites which branch extensively and have average widths less than 2 um (Fricke, 1984; Shepherd, 1990). Within the granule cell layer the inhibitory basket cells synapse onto the granule cell somas. The dentate hilus is the region between the granule cell layers (blades). The axons from the granule cells course through the hilus towards CA3, where they synapse on the apical dendrites of the CA3 pyramidal cells. These axons are referred to as mossy fibers since they have varicosities along their length. These mossy fibers, leave the dentate gyrus to innervate the apical dendrites of CA3 with *en passent*

synapses. The presence of dentate mossy fibers is one of the main distinctions defining the border between CA3 and CA2. Mossy cells (spiny interneurons) within the hilus project to CA3 and the molecular layer of the dentate gyrus providing strong inhibition.

For further anatomical detail see Figure 2 and refer to Synaptic Organization of the Brain by Shepherd.

2.2 - Normal Population Discharge: the Population Spike

The anatomical structure of the hippocampal formation makes it possible to stimulate local populations of neurons in the hippocampal slice to fire synchronized action potentials. The resulting extra-somatic recordings are referred to as the population response or the population spike.

There are two forms of stimulation; antidromic and orthodromic. Antidromic stimulation refers to the direct stimulation of the axons of a cell population, whereas orthodromic stimulation requires that the population is driven to fire action potentials via synaptic transmission. The significant variation in the shape of the orthodromic responses between the two tissues illustrated in Figure 3.

The antidromic population response in both tissues are remarkably similar. These are biphasic, with a sharp, short latency negative spike occasionally followed by a small positive wave. No initial positive component (fEPSP\P1) is

Figure 3 **Orthodromic Population Responses in CA1 & the Dentate Gyrus**

Orthodromic population responses of the dentate granule cells (right) and the hippocampal CA1 pyramidal cells (left) are shown. The CA1 response has an initial positive component (P1/fEPSP) with a dominant negative spike (N1) and a second positive component (P2) which has a higher amplitude that the initial P1. In CA1, N1 extends well beyond baseline. The dentate gyrus response (right) has a predominant P1, and N1 extends below the baseline, but not to the degree of a CA1 response. The P2 of the dentate gyrus response is small in amplitude relative to its P1. These generalized response characteristics give CA1 the appearance of firing off of the rising edge of an underlying positive potential, while the dentate gyrus response appears to fire later, on the falling edge of an underlying positive potential.

Orthodromic Population Responses

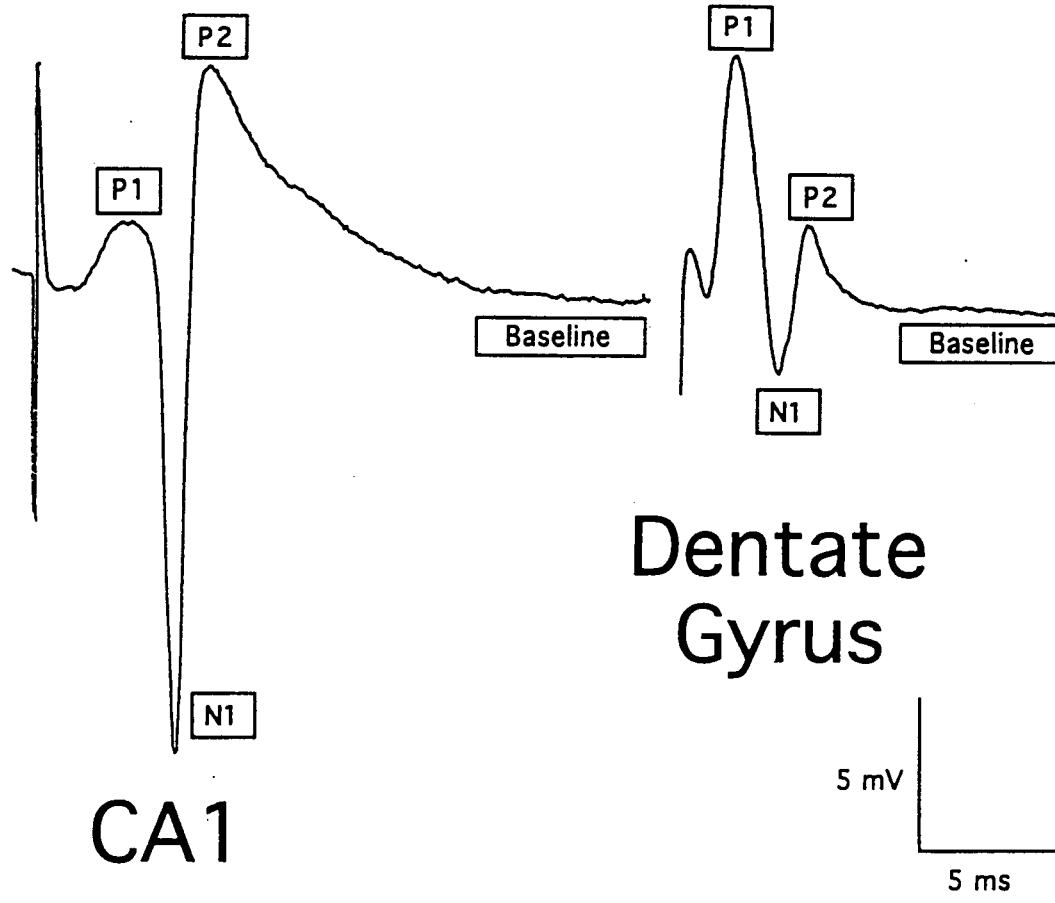

present. Usually this response has an extremely short latency from stimulation (1-2 milliseconds) and the negative population spike can have a substantial amplitude (in excess of 15 mV).

2.3 - Low $[Ca^{2+}]_o$ Treatment

It is well established that neurons bathed in solutions containing low concentrations of divalent cations are more excitable than neurons in standard mediums (Frankenhaeuser, 1957; Brismar, 1972). In 1978, Anderson et al described a model of cortical epilepsy in which the $[Ca^{2+}]_o$ was decreased. In this model, instead of a single antidromic stimulus resulting in a single biphasic response, a train of population spikes was observed. This train or burst of population spikes was thought to result from both an increased neuronal excitability and synchrony. A similar low $[Ca^{2+}]_o$ model of seizure activity was developed for experimentation with the *in vitro* hippocampal slice (Haas, Jefferys, 1984; Taylor, Dudek, 1982; Yaari et al.1983; Taylor, Dudek 1984; Schweitzer et al, 1992; Roper et al, 1992).

Lowering $[Ca^{2+}]_o$ has two major influences on the neuronal population of the hippocampal slice. Firstly, lowering the Ca^{2+} concentration results in the blockade of synaptic transmission by preventing Ca^{2+} dependent neurotransmitter release within the synaptic cleft

(Konnerth, 1983; Spray, 1985; Dudel, 1983; Katz, Miledi, 1970). Secondly, it removes the electric shielding normally afforded by Ca^{2+} and leads to an increased neuronal excitability. (See Frankenhauser, Hodgkin (1957) for background on low Ca^{2+} and excitability.)

Removing the $[Ca^{2+}]_o$ from the perfusate of the slice preparation is associated with a 20mV depolarization of CA1 pyramidal cell RMP (Haas, Jefferys, 1984). This was measured via an intracellular recording held throughout the change of perfusate. This generalized depolarization of the population should contribute to increased neuronal excitability and cellular discharge in the low $[Ca^{2+}]_o$ model of epilepsy.

Of some concern is the totality of synaptic blockade during perfusion with low $[Ca^{2+}]_o$ mediums. Some researchers (Schweitzer et al, 1992) have shown that prolonged repeated high frequency stimulation (10Hz for 4-10 seconds) in low $[Ca^{2+}]_o$ ACSF could evoke modest synaptic responses. For this reason, research groups studying low $[Ca^{2+}]_o$ bursting have added EGTA to sequester free Ca^{2+} (Roper et al 1992), as well as D,L-2-amino-5-phosphonopentanoate (AP-5), and 6-7-dinitroquinozaline-2,3-dione (DNQX) to block excitatory synapses (Schweitzer et al, 1992) (Also see Konnerth et al.1984; Haas, Jefferys, 1984; Yaari et al.1983). However, when low $[Ca^{2+}]_o$ ACSF was used alone and then in combination with these agents, antidromically stimulated results did not vary (Schweitzer et al, 1992).

The hyperexcitability that results from this treatment manifests itself in the CA1 pyramidal cell population of the hippocampus as what have come to be referred to as "low calcium bursts". These bursts are limited to area CA1, and are seldom observed in the dentate gyrus. The bursts manifest themselves after incubation in a low $[Ca^{2+}]_o$ perfusate for 1-2 hours. They are characterized by a negative DC shift in the extracellular potential in the stratum pyramidale and a positive potential in the basal distal dendrites (Albrecht et al 1989; Haas, Jefferys 1984; Richardson, O'Reilly 1993), with many superimposed negative going synchronized population spikes (Haas, Jefferys 1984; Taylor, Dudek 1984).

The low $[Ca^{2+}]_o$ burst resembles epileptic activity in several respects: 1) the burst is an intense event isolated in time, 2) it occurs spontaneously and is self-sustained, 3) it is comprised of repetitive neuronal firing, 4) bursts are accompanied by significant negative potential, and 5) bursts are accompanied by changes in the ionic micro-environment. A typical burst is demonstrated in Figure 4.

The evidence that low $[Ca^{2+}]_o$ bursts are the direct result of an increased neural excitability and an excessive neural discharge are that 1) single unit recordings in stratum pyramidale reveal bursts of activity in phase with the negative potential DC shift (O'Reilly, Richardson unpublished observation), 2) that this potential shift is accompanied by large transient decreases in $[Na^{+}]_o$ and

Figure 4 **Spontaneous Low $[Ca^{2+}]_o$ Bursts in CA1**

A typical low $[Ca^{2+}]_o$ burst in the CA1 is shown. These bursts occur spontaneously and regularly when the in vitro hippocampal slice is perfused with low $[Ca^{2+}]_o$ ACSF. The top trace is an extracellular recording in the stratum pyramidale, while the lower trace is an extracellular recording in the distal apical dendrites of this pyramidal cell population (stratum moleculare). Features of this event include: 1) a significant negative extra-somatic DC potential, 2) a positive extra-dendritic DC potential in the moleculare layer of CA1, and 3) superimposed on this shift, numerous synchronized population spikes. The difference in potential between these two sites reflects the extracellular field generated by this population of cells along its apical dendrites.

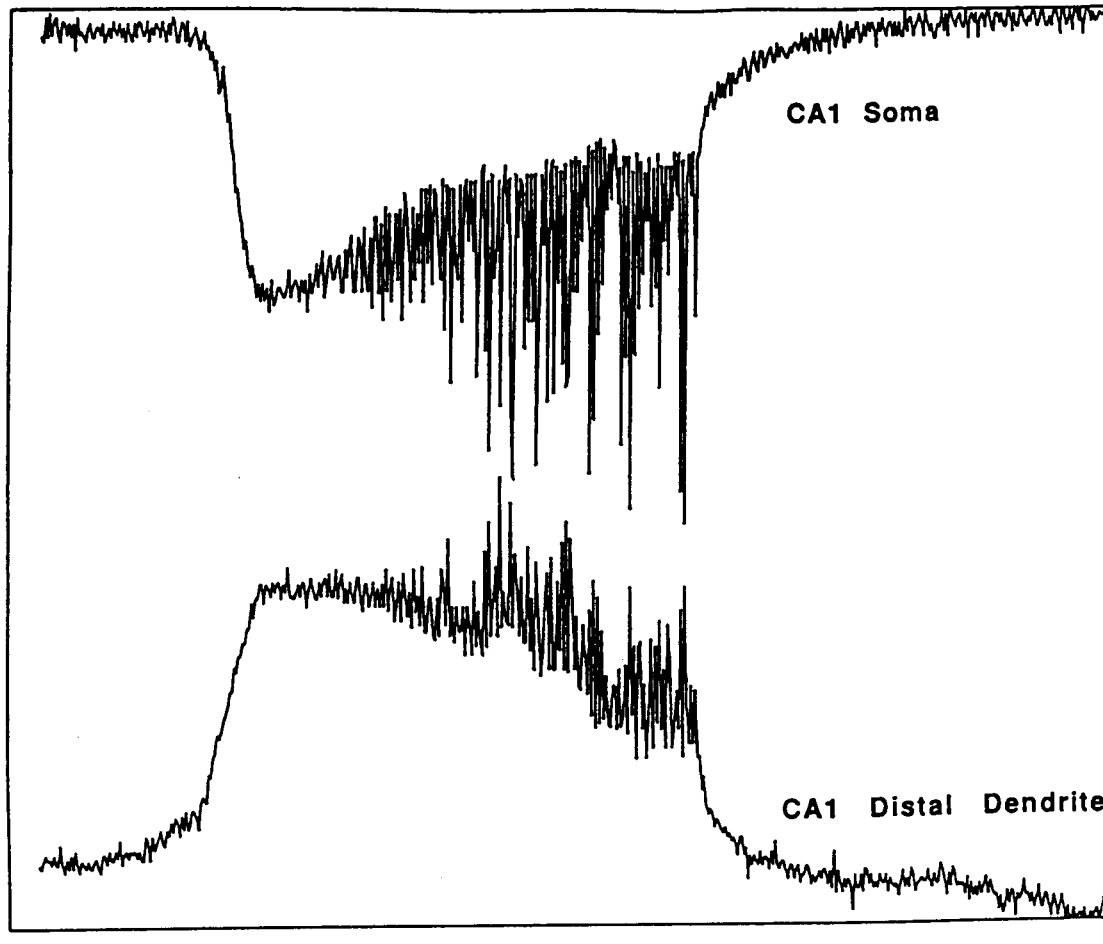
CA1 Soma
CA1 Distal Dendrite
1sec/div
Soma 2mV/div
Dendrites 1mV/div

increases in $[K^+]_o$ (Heinemann et al 1992; Heinemann et al 1985; Konnerth et al 1984; Yaari et al 1986; Konnerth et al 1986), 3) the potential shifts and the above changes in $[Na^+]_o$ and $[K^+]_o$ are abolished by the application of tetrodotoxin which blocks the Na^+ driven action potential (Yaari et al. 1983), and that 4) increasing the extracellular concentrations of divalent cations (Example: Mg^{2+}, Mn^{2+}) abolishes the bursts (Haas, Jefferys, 1984).

In other experimental models of epilepsy, seizure activity in the CNS is accompanied by a decrease in the $[Ca^{2+}]_o$ which indicates that active epileptogenesis can involve the movement of Ca^{2+} into cells (Heinemann et al.1977; Heinemann, 1982; Prince 1982). During the depolarization phase of action potentials in cells participating in a seizure, Ca^{2+} moves from the extracellular space into the cell via voltage dependent Ca^{2+} channels. The resulting decrease in $[Ca^{2+}]_o$ occurs simultaneously across all layers of the hippocampus (stratum oriens through stratum radiatum).

While Ca^{2+} may play a central role in some epilepsies (Heinemann, 1977), it is not believed to be a significant ion in the genesis of low $[Ca^{2+}]_o$ bursting. This conclusion is further supported by the presence of bursting even when EGTA is used to reduce the $[Ca^{2+}]_o$ to minimal levels (Konnerth et al.1984; Haas, Jefferys, 1984; Yaari et al.1983).

2.4 - Low $[Ca^{2+}]_o$ Bursts in CA1 verses the Dentate Gyrus

For almost a decade, low $[Ca^{2+}]_o$ bursting has been considered a phenomena exclusive to CA1. During perfusion with a low $[Ca^{2+}]_o$ and normal $[K^+]_o$ medium, virtually all slices will exhibit bursting in the CA1. In contrast, bursts in the dentate gyrus are rarely observed. Only one recent study reports bursting in the dentate gyrus and only in 7% of slices (Roper et al, 1992). It is not clear why CA1 has a greater propensity for low $[Ca^{2+}]_o$ bursting than the dentate gyrus.

However, functional differences in inhibitory interneurons, recurrent inhibition, or excitatory synaptic interconnections are not responsible for this difference as synaptic transmission is blocked in low $[Ca^{2+}]_o$. Perhaps the difference in propensity for bursting in low $[Ca^{2+}]_o$ is the result of local differences in the extracellular volume between CA1 and the dentate gyrus. The extracellular volume in CA1 is notably smaller than the dentate gyrus with a higher extracellular resistance than either CA3 or the dentate gyrus (McBain et al, 1990). These physical characteristics should, on theoretical grounds, enhance extracellular field effects in the CA1.

Since field effects are known to contribute to the recruitment and synchronization of cell discharge during low $[Ca^{2+}]_o$ bursts (Taylor, Dudek 1984), it is possible that the dentate gyrus fails to develop bursts in low $[Ca^{2+}]_o$ because

the sensitivity of granule cells to field effects is insufficient to support robust epileptiform activity. However, this hypothesis is inconsistent with the marked sensitivity of granule cells to experimentally generated fields (Jefferys 1981; O'Reilly, Richardson 1992; O'Reilly, Richardson 1993).

Alternatively, this difference in propensity for bursting in low $[Ca^{2+}]_o$ may result from differences in the basal levels of excitability in the two regions. It is often stated that dentate granule cells have a more negative resting membrane potential than pyramidal cell and, therefore, exist in a relatively hyperpolarized state (Schwartzkroin, 1990). As a result granule cells may be more resistant to spontaneous activity resulting from the membrane depolarization and enhanced excitability associated with low $[Ca^{2+}]_o$ treatment.

This hypothesis is supported by the finding that elevating $[K^+]$ in the low $[Ca^{2+}]_o$ medium to 7mMol, altered the antidromic response in the dentate gyrus from a single spike to a robust burst of spikes. The increase in $[K^+]_o$ may have resulted in an increment in neuronal excitability (Somjen et al,1981;Yaari et al, 1986) capable of overcoming the relative hyperpolarization of the granule cells.

2.5 - Non-Synaptic Mechanisms of Epileptiform Discharge

With epileptic events prevailing in the absence of synaptic drive, non-synaptic mechanisms for these events demand attention. The following sections review the relevant literature for three possible non-synaptic mechanisms.

A - $[K^+]_o$ During Epileptiform Bursts

Elevated $[K^+]_o$ associated with neuronal discharge should contribute to seizure discharge by shifting the K^+ equilibrium potential in the depolarizing direction. During spontaneous low $[Ca^{2+}]_o$ bursts the $[K^+]_o$ can rise from approximately 6 to 10 mMol in stratum pyramidal (Haas, Jefferys, 1984). This increase in $[K^+]_o$ corresponds to an estimated membrane depolarization of 13 mV calculated from the Nernst equation (Haas, Jefferys, 1984) and should contribute to the high rate of discharge present during each burst. Consistent with this hypothesis is the finding that increasing $[K^+]_o$ of the perfusing solution from 6.25 mMol to 9.25 mMol increases the frequency of bursts and the rate of population spike discharge within each burst, whereas decreasing $[K^+]_o$ from 6 mMol to 3 mMol, eliminates spontaneous bursting activity (Haas, Jefferys, 1984). For a review of spatial buffering by glia, refer to Appendix C.

Two types of low $[Ca^{2+}]_o$ bursts have been reported in CA1; slow and fast onset bursts (Haas, Jefferys, 1984). In the case of "slow onset" bursts, small increases in $[K^+]_o$ have been reported prior to onset of the electrical phenomena (Haas, Jefferys, 1984) and it has been postulated that this could move the population towards the threshold for bursting and therefore be responsible for the initiation and propagation of the slow burst (Konnerth et al.1984).

In contrast, the $[K^+]_o$ increase associated with fast onset bursts never precede the burst and is probably not responsible for burst initiation (Haas, Jefferys 1984).

Extracellular K^+ shifts in the alveus have also been postulated to contribute to the recruitment and synchronization of CA1 pyramidal cell discharge (Jefferys, Haas, 1982). However, when the alveus is lesioned, the CA1 burst pattern remains unaffected (Haas, Jefferys, 1984). Based on this observation it is now generally accepted that the alveus is not actively involved in the spread of the bursts.

Spreading depression is an abnormal population phenomenon whose propagation is believed to be dependent on $[K^+]_o$ (Leao, 1972; Bures et al.1974; Bures, 1984; Nicholson, 1981). In human subjects this phenomena is occasionally present during a seizure episode and it may be responsible for profound cortical dysfunction seen during some migraine attacks (Milner, 1958). Spreading depression is of some interest here since the buffering processes that allow high

$[K^+]_o$ concentrations to be distributed, may affect the threshold of onset of these events (Gardner-Medwin, 1983a).

Spreading depression has been reported in slices exposed to low $[Ca^{2+}]_o$ ACSF. This phenomena differs distinctly from low $[Ca^{2+}]_o$ bursts as these events are infrequent and no neuronal activity, spontaneous or evoked, is present during the event. The time course of a spreading depression episode is long (often several minutes), whereas low $[Ca^{2+}]_o$ bursts have a relatively fast onset (1-10 ms), brief durations (500ms -10s), and a higher frequency of repetition (several events per minute). Additionally, spreading depression involves extracellular potential shifts in the order of 30-50 mV, while low $[Ca^{2+}]_o$ bursts produce a significantly smaller potential shift in the order of 15 mV (example: Haas, Jefferys 1984; Richardson, O'Reilly 1993). All of these differences lead to the conclusion that, the bursting phenomena under study in low $[Ca^{2+}]_o$ ACSF is likely to have a different mechanism than spreading depression.

B - Electrotonic Coupling: Gap Junctions

Since electrotonic interactions through gap junctions have a time course of milliseconds (Snow, Dudek, 1986) they represent a good mechanism for neuronal synchronization and seizure initiation. The prevalence of functional gap junctions in the hippocampus and dentate gyrus under various conditions remains unclear. Part of the difficulty arises

from the debate as to whether the existence of dye couples verifies the existence of electrotonic coupling in the CNS. However, direct electrophysiological evidence that dye coupled cells are connected by electrical synapses has been reported (Barnes, 1987; McVicar, Dudek, 1981; OBeirne, 1987; Rao et al.1987).

Based on dye coupling studies, groups of approximately three cells are frequently coupled in both CA1 and the dentate gyrus (Barnes 1987; Baimbridge 1991). The degree of coupling is sensitive to various factors including pH (Church 1991; Baimbridge 1991) and $[Ca^{2+}]$ (Alverez-Leefmans, 1979). Tissue incubation in low concentrations of divalents cations, such as the low $[Ca^{2+}]_o$ treatments associated with bursting in CA1, tend to disrupt gap junctions (Alverez-Leefmans, 1979).

Taken as a whole, these findings suggest that the level of coupling necessary to support epileptic activity is probably not present during low $[Ca^{2+}]_o$ bursting (Dudek, Traub 1988).

C - Extracellular Field Effects

As outlined in the Introduction, field effects are known to contribute to the recruitment and synchronization of neuronal discharge during the individual populations spikes within a low $[Ca^{2+}]_o$ burst. This section reviews the characteristics of the hippocampus which are relevant to the

generation of field effects. Recall that the conditions which favor substantial field effects are 1) a high extracellular resistance, 2) a dense approximation of uninsulated neurons, and 3) the parallel alignment of the dendro-somatic axis of neurons within a population. Under these conditions extracellular voltage gradients can affect the firing patterns of neurons in the CNS and particularly in the hippocampal formation where all three criteria are dominant features.

Measurable extracellular voltage gradients in neural tissues have been observed in cortical structures by several research groups dating back to 1957. These observations are presented below in Table form. The ranges of physiologically generated gradients reported by these groups is 0.5 mV/mm up to 50mV/mm.

Table 1 Extracellular Voltage Gradients Recorded Under Various Physiological Conditions

Research Group	Region	Response	Gradient
Richardson & O'Reilly 1993	CA1 pyramid	Seizure	>100mV/mm
	Dentate GC	Evoked	
Lomo 1971	Dentate GC	Evoked	50mV/mm
Gardner-Medwin, 1976	Dentate GC	Evoked	50mV/mm
Green & Petsche, 1961b	Dentate GC	Seizure	20mV/mm
Green & Petsche, 1961a	Dentate GC	Slow wave	0.5-4mV/mm
Winson 1974	Dentate GC	Slow wave	0.5-4mV/mm
Gloor et al, 1961	Dentate GC	Physiol. Conditions	4mV/mm
Gloor et al, 1963	Dentate GC	Seizure	10mV/mm
Bures 1957	neocortex	Physiol. Conditions	10mV/mm

Extracellular voltage gradients of 50 mV/mm have been seen to modify the spontaneous firing rates of neocortical cells in the cat (Creutzfeldt et al.1962), and of 2.5 mV/mm in the rat (Bindman, 1964). Evoked population responses have been modified by fields of 20-30 mV/mm in the intact cortex (Purpura, Malliani, 1966; Purpura, 1969; Purpura, 1974) and fields of 5mV/mm can alter the amplitude of orthodromic population responses in the dentate gyrus (Jefferys, 1981; O'Reilly, Richardson, 1992)

The extracellular resistance should, on theoretical grounds, vary directly with the extracellular volume. Early studies of extracellular volume fraction (ECVF) reported a value of 7% for CA1 stratum pyramidal and 20% for other hippocampal regions including the dentate gyrus (Green, Maxwell, 1961). More recent studies by McBain, Traynelis and Dingledine (1990) using modern techniques produced the values presented in Table 2 below.

Table 2 Extracellular Volume Fraction in Various Regions of the Hippocampus

REGION	ECVF
CA1 stratum pyramidale	11.9%
stratum radiatum	13.2%
CA3 stratum pyramidale	17.7%
stratum radiatum	15.5%
Dentate Granule Layer	14.8%

These values are substantially lower than the brain's average ECVF of 20% (McBain et al,1990) and are particularly low in CA1 where low $[Ca^{2+}]_o$ bursting is most dominant. The original observation by Haas and Jefferys (1984) that a 10% dilution of low $[Ca^{2+}]_o$ perfusate enhances the synchronization of population spikes within low $[Ca^{2+}]_o$ bursts may be based on a lowering of the extracellular volume and, hence, an increased extracellular resistance. Similar dilutions, in standard ACSF, have enhanced evoked population responses in the CA1 of rat (Andrews,1991; Andrews et al,1989). The importance of a high extracellular resistance is also predicted by several theoretical models (Yim et al.1986a; Dudek, Traub 1988). See Korn and Faber (1989) for a review of this topic.

D - Influence of Externally Applied Fields on the Dentate Gyrus

Externally generated fields were used in the present study to transiently alter the membrane potential of the granule cell population. The application of an externally generated field across the dendro-somatic axis of the granule cell population (see Figure 5) can alter the excitability of granule cells (Jefferys, 1981; O'Reilly, Richardson, 1992; O'Reilly, Richardson 1993). These affects are often profound when the applied fields are similar in

Figure 5 Applied Field Apparatus

The experimental set-up for applying current across the hippocampal slice is illustrated. The top illustration depicts a hippocampal slice on the net of an interface chamber with the applied field apparatus and stimulator in place. The bottom illustration allows the details of current delivery to be examined. Current passing electrodes are aligned perpendicular to the dendro-somatic axis of the dentate granule cells and then lowered onto the net in the recording well such that these electrodes straddle the entire slice. An isolated constant current stimulator is used to apply a field across the experimental region. If the extracellular potential in the somatic region is positive with respect to the dendrites, then the field will hyperpolarize the granule cell population. When the current polarity is reversed, the somatic region negative with respect to the dendrites, the cells will be depolarized.

APPLIED FIELDS

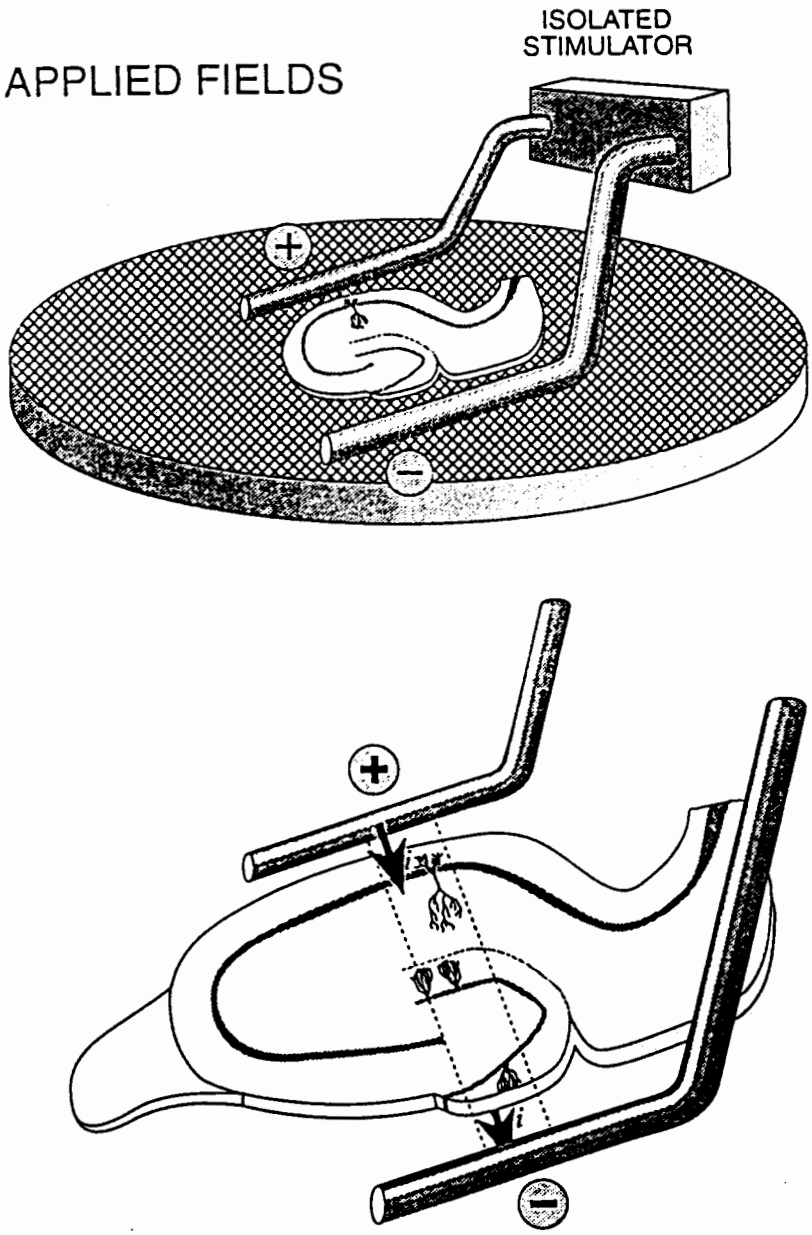

magnitude to those generated by the tissue during evoked potentials (20-100mV) (O'Reilly, Richardson 1992).

Applied fields influence neuronal excitability by altering the TMP of the neurons exposed to the field. The influence of applied fields on the TMP of granule cells has been confirmed by simultaneously recording the intra and extracellular potentials during application of fields with known magnitudes. The results indicate that there is a linear relationship between field strength and change in TMP and that 100mV/mm voltage gradients will induce a 6mV shift in TMP (see Figure 6) (O'Reilly, Richardson 1992).

Figure 6 Experimental Arrangement for TMP Measurements in Dentate Granule Cells

The experimental procedure for establishing the change in transmembrane potential (TMP) of a granule cell during the application of a field potential across the dentate gyrus is illustrated. At the top left note the experimental set-up with respect to the hippocampal slice as a whole. Current (I) passed between these electrodes establishes a voltage gradient along the dendrosomatic axis of the granule cell population. The change in TMP is calculated by subtracting the intracellular potential (A) from the extracellular potential (B). The extracellular recording electrode is positioned in the immediate vicinity of the cell penetrated by the intracellular electrode. Following TMP measures, the intracellular electrode is retracted from within the cell and is used to make the actual extracellular measures. The permanently placed extracellular electrode was used to confirm the accuracy of these extracellular recordings.

Intra & Extracellular Recording During Applied Fields Used to Measure TMP of Granule Cells

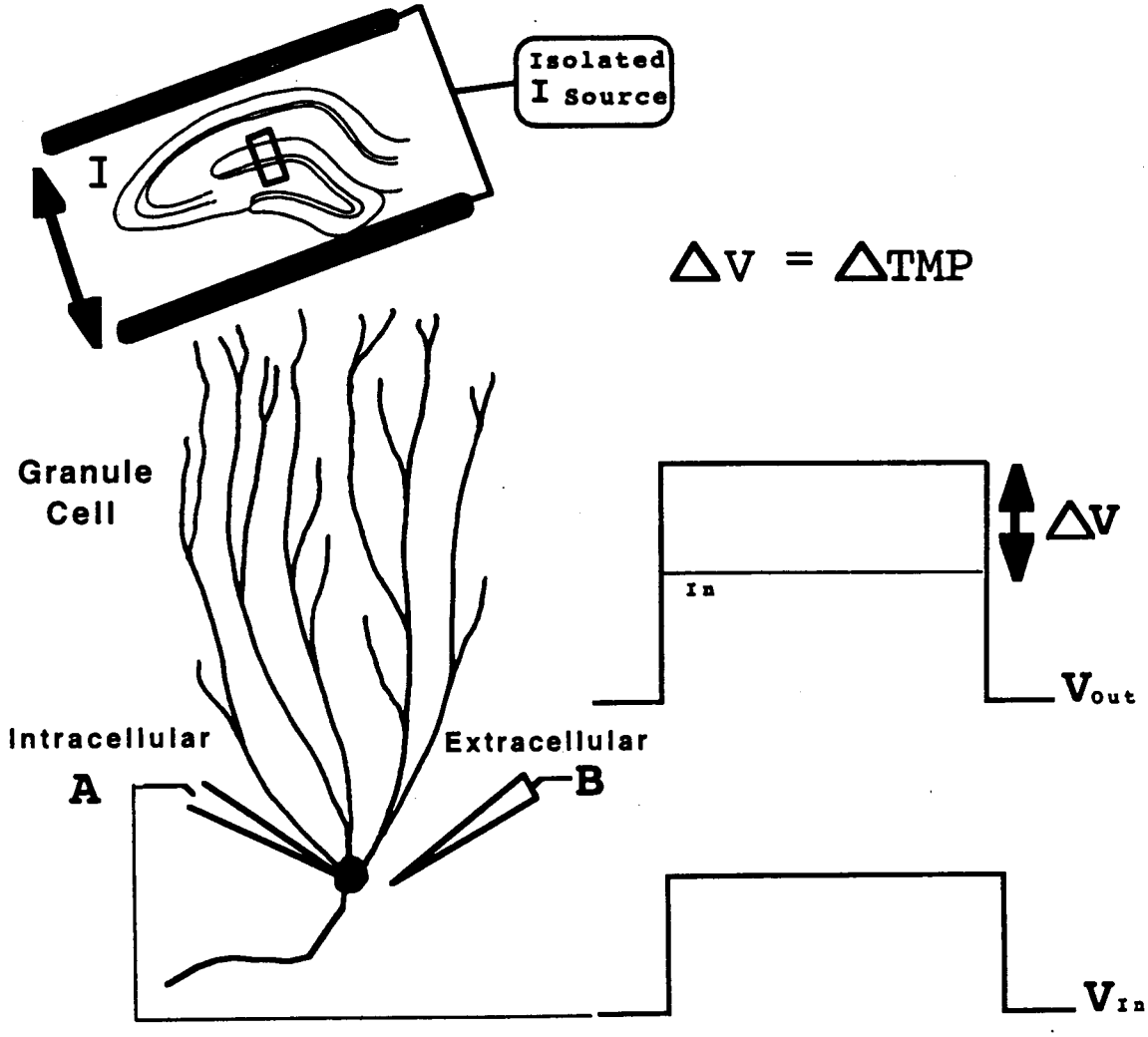

3.0 - THESIS PROJECT

Quantification and characterization of the influence of extracellular fields on epileptiform activity in the dentate gyrus

HYPOTHESIS

This thesis focuses on the excitability and synchronization of dentate gyrus granule cells in a low Ca^{2+} and standard K^+ perfusate. As epilepsy undoubtedly has many mechanisms, the motivation for this study is based on the need to experimentally isolate the contributing factors to epilepsy. The study of low $[Ca^{2+}]_o$ bursts, exclusive to CA1, have been productive in uncovering non-synaptic mechanisms. Previous work (Eg. Snow, Dudek,1984; Richardson et al,1984a; Jefferys, Haas, 1982) has established that extracellular field effects play a role in the synchronization of both spontaneous and evoked bursts observed in CA1. Despite the fact that granule cells of the dentate gyrus are sensitive to these field effects (Jefferys, 1981; O'Reilly, Richardson 1992) and are organized in a highly laminar manner similar to CA1 pyramidal cells, the dentate gyrus rarely demonstrates these epileptiform events. This thesis investigates the hypothesis that the difference in propensity for bursting in these two regions during low $[Ca^{2+}]_o$ perfusion may be based on the relative hyperpolarization of the granule cells

rather than other functional differences between granule cells and pyramidal cells.

The hypothesis is tested by applying a uniform voltage gradient across the dentate gyrus of the hippocampal slice, exposed to low $[Ca^{2+}]_o$ ACSF, to depolarize the population of granule cells. If the resistance to low $[Ca^{2+}]_o$ bursting in the dentate gyrus is based on a relative hyperpolarization of the granule cells then this treatment of the tissue should allow the dentate gyrus to develop epileptiform bursts similar to CA1.

Three experimental hypotheses were investigated.

#1: The dentate gyrus fails to develop low $[Ca^{2+}]_o$ antidromically stimulated bursts because the granule cell population is less excitable in the generation of bursts, not because the tissue lacks the intrinsic mechanisms necessary to burst under these conditions.

#2: The dentate gyrus can develop epileptiform activity during perfusion with low $[Ca^{2+}]_o$ ACSF in the absence of antidromic stimulation if the granule cell population is sufficiently depolarized.

#3: Antidromic bursts in the dentate gyrus and CA1 have similar characteristics with respect to spike amplitude, inter-spike interval, and pattern of discharge.

These hypotheses were tested by using field effects as a tool to increase the excitability of the granule cell population. The rational for this approach is based on the known influence of field effects on hippocampal neurons, as

reviewed in the Introduction and Background. Is is well established that applied extracellular fields can alter the TMP and evoked responses of granule cells.

4.0 - METHODS

The following section briefly describes the general experimental procedures required to complete the proposed study. A separate section entitled, "4.2 - Experimental Protocols" outlines specific experimental details for each hypothesis.

4.1 - Procedures

In Vitro Hippocampal Slice During Low $[Ca^{2+}]_o$ ACSF & Applied Fields

A) In Vitro Chamber Preparation

In the present experiments slices were maintained in a standard interface chamber (Fine Science Tools). The tissue was placed in the chamber on the interface between Artificial Cerebral Spinal Fluid (ACSF) and humidified oxygen. The ACSF was preoxygenated, buffered with 95% O_2\5% CO_2, and warmed. The flow rate through the chamber was regulated to 3-5 ml per minute using a constant flow valve (Dial-a-Flo). Temperature was maintained at 34 ^oC +\- 1 ^oC using thermistor feedback to a Temperature Control Unit (Fine Science Tools). Warm, humidified O_2 flowed across the top surface of the slice and a canopy of this O_2 was maintained by an enclosed lid with a small access port for

recording\stimulating electrodes. Chamber set-up is presented in Figure 7.

B) ACSF Preparation

STANDARD ACSF

The water source used to make the ACSF was filtered, de-ionized, 18 MOhms laboratory water. The constituents of the ACSF were NaCl 124mM, $NaHCO_3$ 24mM,D-glucose 10mM, KH_2PO_4 1.25mM, KCl 2mM, $MgCl_2$ 1.5 mM, and $CaCl_2$ 1.5mM. The ACSF was preoxygenated and pH balanced to 7.4 with 95% O_2\ 5% CO_2. In order to avoid precipitation, the $CaCl_2$ was added after the solution had been pH balanced.

LOW CALCIUM ACSF

The low $[Ca^{2+}]_o$ medium had the following ionic concentrations: NaCl 130mM, $NaHCO_3$ 24mM, KCl 5.0mM, NaH_2PO_4 1.25mM, $MgSO_4*7H_2O$ 1.5mM, d-glucose 10mM, $CaCl_2$ 0.0mM. Although no calcium salts were added to the media, the Ca^{2+} concentration due to impurities was estimated as 12uM.

Before exposure to low $[Ca^{2+}]_o$ media, the viability of the slices was confirmed by observing the presence of well formed orthodromic and antidromic responses in the standard ACSF media.

C) Dissection of the Cortex and Hippocampus

A male Wistar rat was anesthetized with halothane and then decapitated. Upon removing the dura and exposing the

Figure 7 **Tissue Chamber & Supporting Apparatus**

The supporting apparatus for the in vitro hippocampal slice preparation is illustrated. The tissue is maintained on the interface between ACSF and humidified oxygen. Gravity feeds ACSF (top left) to the chamber (middle) at a controlled flow rate. Oxygen is humidified and warmed by passing through an outer water bath and is continuously delivered to the slice through vents to an enclosed canopy. The ACSF is warmed by passing through the outer bath in fine tubing, flows into the recording well, and is removed vial a distant suction device (lower right). Using this set-up hippocampal slices remain viable in vitro for several hours and can be studied with a high degree of experimental control.

Interface Tissue Chamber & Supporting Apparatus

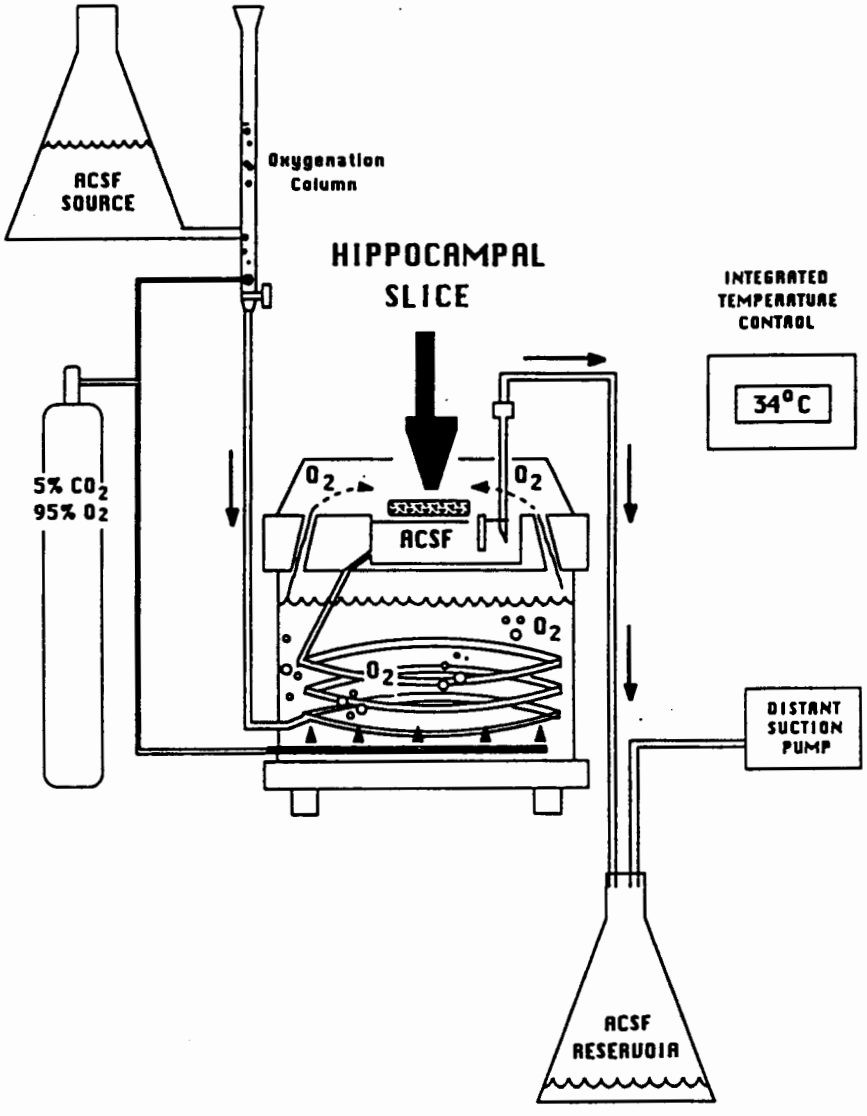

cortex, the brain was continually bathed in cold (0-10^{o}C) ACSF. This stage of the dissection did not exceed 1 to 2 minutes as recommended (Dingledine et al 1980; Dingledine, 1984; Schwartzkroin, 1981). The brain, posterior from bregma, was isolated and transported to a cold (0 - 10^{o}C) dissection stage.

The brain was transected along the sagittal fissure into two halves. One half of the brain was placed in cold, oxygenated ACSF while the hippocampus of the opposite half was dissected, sliced, and placed in the recording chamber. After slice transfer was complete for the first hippocampus, the second half of the brain underwent the same procedures.

The cortex and brain stem were retracted from the hippocampal formation in a blunt dissection. The isolated hippocampus was transferred to the slicing stage.

D) Slicing & Slice Transfer

The slice angle was parallel to the hippocampal striations\fibers seen on the anterior surface of the hippocampus. Slices 300-400 um thick were prepared from the anterior pole of the hippocampus using a Stoelting tissue slicer.

A fine sable brush was used to lift the hippocampal slice by the fimbria for transfer to the chamber without physically contacting the region of interest.

E) Stimulation \ Recording Techniques

The bipolar stimulating electrodes were constructed from a twisted pair of fine Teflon coated tungsten wires (50-75um). The end of the electrode was cut with a scalpel to bare the tips. The electrode tip was positioned on the surface of the slice using a micromanipulator. An isolated Isoflex constant voltage stimulus (0.1 ms duration) was used in all experiments. Stimulus rate and duration were controlled by a programmable timer (Master-8).

To achieve good quality extracellular field recordings, low resistance glass micropipettes, 3-5 Mega Ohms, backfilled with 4M NaCl were used. The electrodes were placed on the surface of the slice under visual control. The electrode depth was adjusted until a maximal response was recorded for a given stimulus. The microelectrodes were placed in the somatic layer of CA1 or the dentate gyrus, and\or along the dendro-somatic axis of these cells. See Figure 8 for details of the experimental recording electrode placements.

To evoke an orthodromic response in the dentate gyrus, the stimulating electrode was placed in the molecular layer. For an antidromic response the stimulus placement was in the hilus.

Figure 8 **Experimental Recording Locations**

The locations of the recording and stimulating electrodes during the data trials are illustrated. An extracellular recording electrode was positioned at the granule cell layer (bottom right) of the dentate gyrus and a second electrode at the dentate moleculare layer, approximately 150-200um apical (middle right). The granule cell population was activated antidromically by a bipolar stimulating electrode positioned at the dentate hilus and aligned with the mossy fibers as they tract to CA3 (bottom left). The voltage difference between these recording electrodes, and the measure of their physical separation was used in calculating the voltage gradient along the dendro-somatic axis of this cell population. In CA1 stratum pyramidale (top right) an extracellular recording electrode was used in assessing slice viability and to monitor the progression of the low $[Ca^{2+}]_o$ treatment.

Experimental Electrode Placements

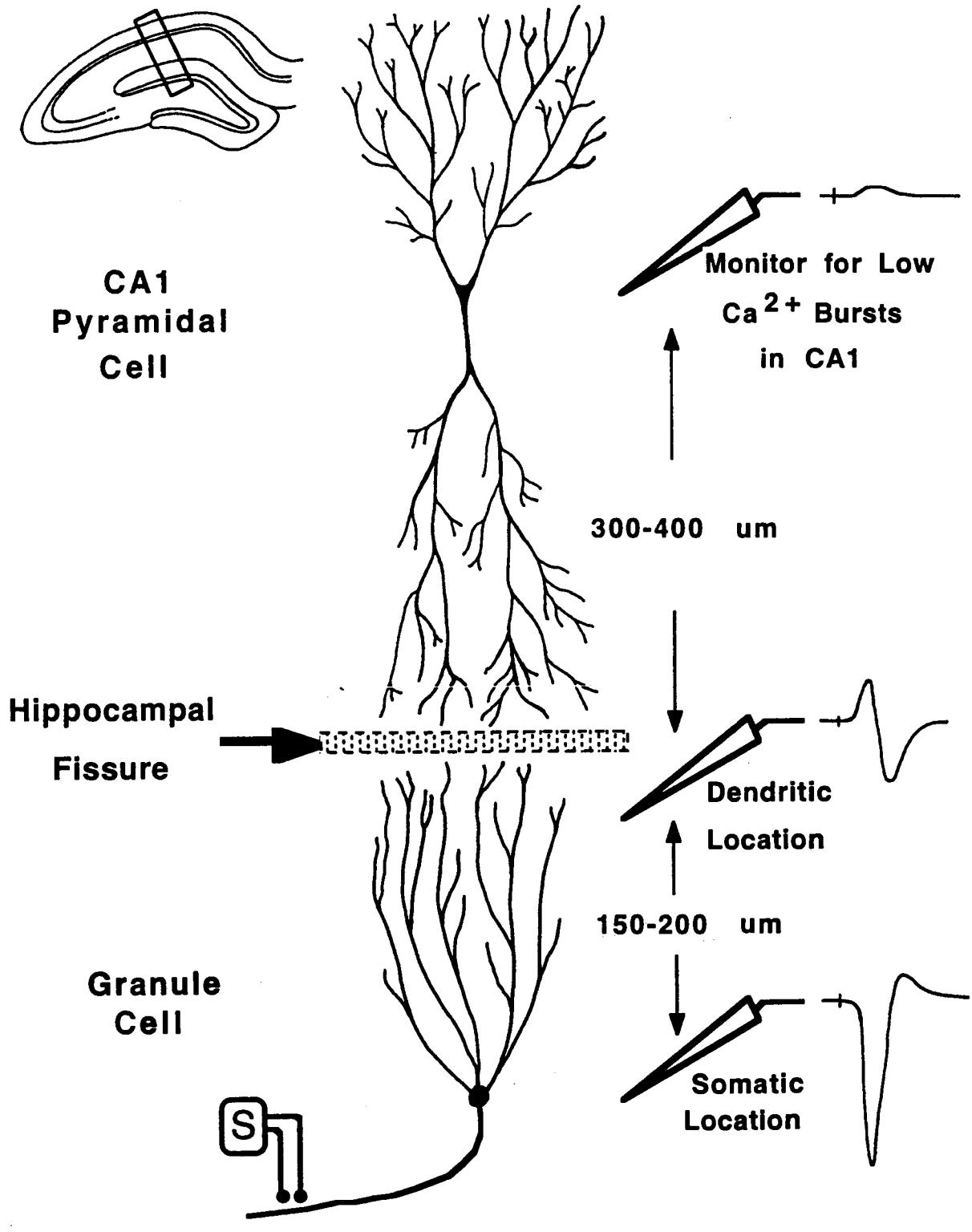

F) Field Application Protocol in the Dentate Gyrus

Electric fields were applied to the dentate gyrus by placing two silver chloride coated silver wires on either side of the hippocampal slice parallel to the dentate granule cell layer (see Figure 5).

Using these parallel electrodes, rather than applying current from point source electrodes, the entire hippocampal slice was exposed to a uniform voltage gradient. A constant isolated current source was used. For a discussion of other considerations given to the development of the applied field technique refer to Appendix E and B.

The applied voltage gradient was carefully aligned to produce current flow parallel to the dendro-somatic axis of the cells under study in the upper blade of the dentate gyrus. The gradient was assessed by measuring the voltage at two points along this axis. Measurements demonstrated that the gradient was approximately linear and uniform across this region.

Note that electric fields applied in this manner induce change to the TMP at ends of spatially distended cells and minimal change to the TMP at the center of these cells. Thus the somata of the dentate granule cell (with its single dendritic tree) is affected by these fields, while the CA1 somata (with opposing dendritic trees) is not dramatically affected.

4.2 - Experimental Protocols

The series of specific experimental protocols conducted during the present study are detailed in this section.

Step 1 Preparation of the slices

Hippocampal slices were prepared from male Wistar rats (150-250 grams) for each experimental run. These slices were perfused with standard ACSF. The slices were then left to incubate for a minimum of 45 minutes as they recovered from the surgical manipulations.

Step 2 Electrode placements

Two extracellular recording electrodes were used. In assessing the tissue viability and monitoring the progression of the low $[Ca^{2+}]_o$ treatment, one electrode was located within stratum pyramidale of CA1 and the second at the stratum granulosum of the dentate gyrus.

For subsequent data collection, the CA1 electrode was relocated 100-400 um apical of the granule cell layer in the dentate molecular layer. These electrodes were aligned along the dendro-somatic axis of the dentate granule cell population. The electrodes remained in position for the duration of the experiment.

A single stimulating electrode was used. Its location varied: the alveus for antidromic CA1 stimulation, the stratum radiatum for orthodromic CA1 stimulation, the molecular layer for dentate orthodromic stimulation, and the dentate hilus for antidromic dentate stimulation.

Step 3 Determination of slice viability

The antidromically and orthodromically evoked responses in CA1 and the dentate gyrus were used to assess slice viability. Slices with a maximal orthodromic population spike less than 3mV in the dentate gyrus and 7mV in CA1 were excluded from the study. These values were based on commonly reported spike amplitudes in the literature and on the findings in pilot studies.

Finally, the antidromically evoked response in the dentate gyrus was assessed. If the maximal response was less than 6mV the slice was rejected. Slices demonstrating secondary population spikes, or other signs of abnormally high levels of excitability, were excluded. Tissue that demonstrated spreading depression was excluded from the study. The majority of slices passed all of the tests for viability.

Step 4 Determining the range of applied field intensities

The range of applied field intensities used in each run was determined by orthodromically stimulating the dentate gyrus and ramping upward through a range of fields that had a notable impact on the amplitude of the population spike. When a suitable range of fields had been determined, the field increments were defined. No fewer than 5 intensities per run were investigated. However, an entire experimental run in low $[Ca^{2+}]_o$ ACSF was not extended beyond 2 hours. The experimental surgical preparation, tissue

recovery, low $[Ca^{2+}]_o$ treatment, condition protocols, and treatment recovery averaged 5-6 hours total.

The absolute applied field intensity was not known at the time of data collection. The range of applied field intensities used were known to influence the dentate gyrus, however the actual intensity in mV/mm was calculated after these data were collected. As a result, the field intensities applied during a given experimental run could vary considerably between experimental runs. The actual field intensities applied, ranged from 0 to 90 mV/mm in both polarities.

Electric fields were applied for 70 ms and the antidromic stimulus was delivered 35 ms after the onset of the field. The 35ms delay was used to allow the tissue to achieve a steady state response to the applied field before the stimulus was delivered. The remaining 35 ms of the applied field allowed the initial antidromic response and a train of up to 14 secondary responses to be recorded during the field application. Following these preliminary steps the stimulus intensity was adjusted to produce an antidromic population spike of 50-60% of maximal. If this was less than 3mV, the slice was rejected from the study.

Step 5 Incubation and re-assessment of slice viability in low $[Ca^{2+}]_o$ ACSF

Once the slice was accepted into the study, the perfusate was changed to low $[Ca^{2+}]_o$. The slices incubated for a minimum of one hour before data collection. At this

point, if antidromic stimulation failed to evoke the minimal response or evoked a burst response in the dentate gyrus, the slice was excluded from the study.

Step 6 Control and condition responses to applied fields

Data was collected under three conditions for each intensity of applied field: 1) a control stimulus with no applied field, 2) a stimulus during a hyperpolarizing field, and 3) a stimulus during a depolarizing field. The pulses were delivered to the tissue in the above order and at increasing steps in applied field intensity The delay between each stimulus was approximately 10-30 seconds.

The control response at each intensity served as a record of any changes in the data over time. This record was used to correct for small drifts in response amplitude during the experimental run.

Step 7 Recovery

Upon completion of data collection, the perfusing solution was changed back to standard ACSF. Recovery from the low $[Ca^{2+}]_o$ treatment confirmed that any significant differences between "standard" and "low $[Ca^{2+}]_o$" responses were not the result of diminished viability of the tissue. Recovery was extended up to 60 minutes post-low $[Ca^{2+}]_o$ and was confirmed when spontaneous low $[Ca^{2+}]_o$ bursts ceased and either orthodromic stimulation produces a population response, and\or antidromic stimulation produced a robust single population spike. Recovery was assessed with six slices and achieved in five.

Step 8 Data acquisition & analysis

A four channel Gould 1604 oscilloscope was equipped with the necessary hardware to interface with a Hewlett Packard Laser Jet III. This allowed the printer to serve as the output device for hard copy records of the evoked responses. The key points from each plot were digitized using a Summagraphics digitizing tablet and custom software.

Data analysis included:

1) Calculation of the extracellular field intensities externally applied to the tissue during the experimental conditions.

The extracellular potentials (mV) that resulted from the application of the external field were recorded in both the extra-somatic and extra-dendritic regions of the dentate granule cell population. These data were plotted. The distance separating these recording sites was measured with a Technival dissection microscope, equipped with 20x eyepieces and two measuring graticules. The voltage difference (mV) was digitized from the plots, divided by the separation (um) and then converted to mV/mm.

2) Calculation of the maximal extracellular voltage gradients generated during the control and condition responses.

The peak negative extra-somatic potential (mV) during a population spike, and the temporally concurrent extra-dendritic potential (mV) were measured. These voltages were

measured as the difference from the baseline 1-2ms prior to antidromic stimulation, to the corresponding point of each spike. This measure was independent of voltage deflections caused by externally applied fields. The voltage gradient was measured and calculated as above in (1).

3) Measures of the change in amplitude of the primary antidromic spike between the control and condition responses.

The peak negative extra-somatic potential (mV) during a population spike was measured relative to the pre-stimulus baseline for both the control spike and the two condition spikes (hyperpolarizing and depolarizing applied fields). The control spike amplitude was reported as 100% of itself. The condition spike amplitude was divided by the control spike amplitude and expressed as a % of the control spike amplitude. Condition spike amplitudes >100% denote a potentiation of the spike, and amplitudes <100% denote a habituation. These values were plotted against the intensity of the applied field under which they were recorded and regression analysis was conducted. Additional statistical tests included an ANOVA with repeated measures and calculation of Pearsons Correlation Coefficient (r) and r^2.

4) Measures of the change in amplitude of the second and third spikes within the burst to the amplitude of the control spike.

In this analysis the 2nd and 3rd spike amplitudes were assessed as a percent of the control spike. Details were the same as above.

5) Comparison of the applied field threshold intensities of the antidromic burst and the depolarizing field induced burst.

The applied field intensity was determined as in (1) above. The appearance of both bursts was resolved by using the following criteria: a burst contains a minimum of 3 successive population spikes, with the third spike having a minimum amplitude of 1mV. Means and standard error were calculated. A paired T-test was conducted.

6) The duration of the first inter-spike interval of bursts containing various number of spikes.

The duration of the first interval was calculated as the time difference (ms) between the initial antidromic population spike of a burst and the second spike. The measure was taken from the peak negative voltage deflection of the population spike recorded by the extra-somatic electrode. The number of spikes contained in a burst was counted as the number of population spikes that occurred during the 35 ms following the antidromic stimulus and the termination of the applied field. This count included the initial antidromic spike. Regression analysis was conducted and means with standard error were calculated.

7) The duration of the inter-spike interval as a burst of a given size progresses.

Burst size and inter-spike interval were calculated as above. The first interval is the duration (ms) between the 1st and 2nd spike of a burst. The second interval, the duration between the 2nd and 3rd, etc.. The last interval is the duration between the last recorded population spike and its previous population spike. For example, the last interval could be measured between the 4th and 5th spikes in small bursts, or the 11th and 12th spikes in large bursts. Means and standard errors were calculated. The pattern of inter-spike intervals as a burst progresses was compared between bursts of various sizes using ANOVA with repeated measures, and between antidromic bursts of the CA1 and dentate gyrus using ANOVA and T-tests.

8) Parameters of CA1 antidromic bursts

Spike amplitude, inter-spike interval, and burst size, were collected and calculated for CA1 in the same manner as for the dentate gyrus. Comparisons between the CA1 and dentate gyrus were made using unpaired T-tests and ANOVA.

Statistics Reported

Throughout this thesis regression analysis was used to describe relations between variables. Slopes of the regression lines and the standard error of the slope are reported along with the corresponding p value. In some instances r^2 was reported. The p value associated with these r^2 values is the same as for the corresponding

regression. Means are reported along with standard error. Unless explicitly stated, unpaired T-tests were used to compare means. In the comparison of inter-spike interval pattern within a tissue, and between tissues, repeated measures analysis of variance was used. Statistical analysis was conducted in consultation with Mr. F. Bellavance, Statistics Consultant, S.F.U..

5.0 - RESULTS

The data recorded in standard ACSF were collected from 34 *in vitro* hippocampal slices of 25 male Wistar rats. The data recorded in low $[Ca^{2+}]_o$ ACSF were collected of 27 *in vitro* hippocampal slices from 18 male Wistar rats. All slices included in the study met the criteria for viability described in the Methods section.

5.1 - Standard ACSF & the Incidence of Epileptiform Activity

It has been reported that the dentate gyrus fails to demonstrate antidromic bursting when *in vitro* slices are perfused with standard ACSF (Eg. Schweitzer et al 1992; O'Reilly, Richardson 1993;). The findings of the present study were consistent with these observations as the dentate gyrus did not demonstrate antidromic bursts in standard ACSF (n=34). Throughout the range of depolarizing applied fields in standard ACSF, the experimental incidence of antidromic bursts was 0% (n=8). Figure 9 illustrates and example of the dentate gyrus responding to applied fields under conditions of standard verses low $[Ca^{2+}]_o$ ACSF. This figure demonstrates the finding that no bursting activity occurred in standard ACSF even when high intensity (+85mV/mm) depolarizing fields were applied.

Figure 9 **Antidromic Responses of the Dentate Gyrus in Standard & Low $[Ca^{2+}]_o$ ACSF**

Extra-somatic and extra-dendritic antidromic potentials in the dentate gyrus during normal and low $[Ca^{2+}]_o$ ACSF are shown. Recording locations, stimulus intensity, and range of applied fields were kept constant. Data was first recorded in normal/standard ACSF (top 2 traces) and then in low $[Ca^{2+}]_o$ ACSF (bottom 2 traces). The applied field intensities ranged from no applied field (middle) to high intensity depolarizing fields (left) and high intensity hyperpolarizing fields (right). Note the similar change in antidromic spike amplitude with applied fields in both solutions. High intensity hyperpolarizing fields decreased this amplitude (far right), while high intensity depolarizing fields increased this amplitude (far left). The two graphs on the left indicate the % of control spike amplitude evoked by the antidromic stimulus at the various field intensities.

A striking difference between the responses in under these two conditions is the development of antidromic bursts in the dentate gyrus as the depolarizing applied field intensity was increased (bottom 2 traces left). Note: the time line between antidromic stimuli was not continuous, but has been depicted in this manner to aid in a visual comparison of spike amplitudes from baseline.

Normal [Ca] ACSF

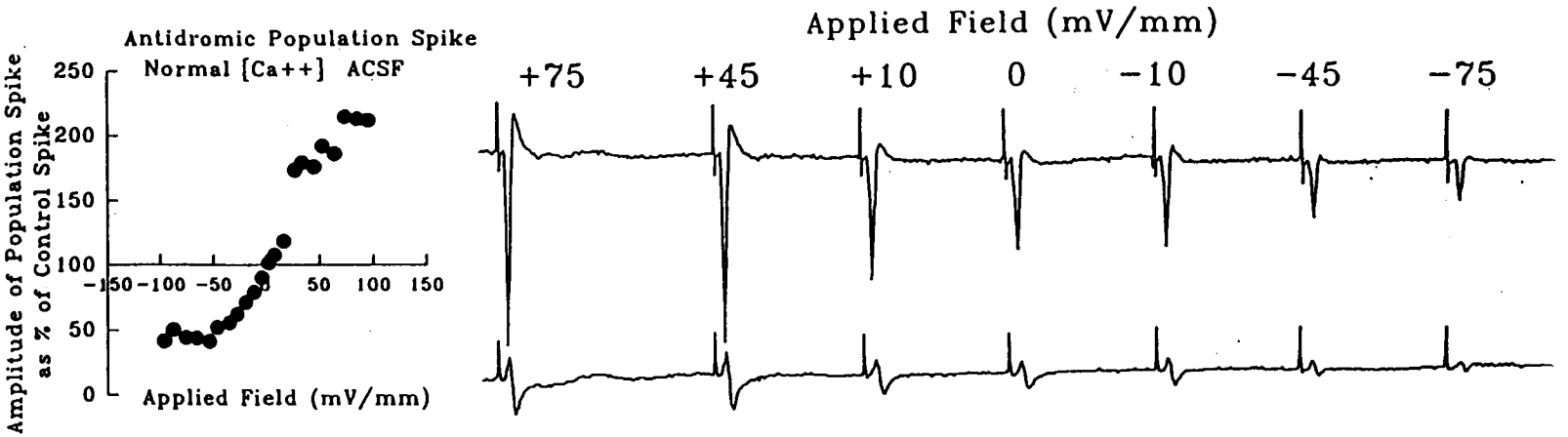

Low [Ca] ACSF

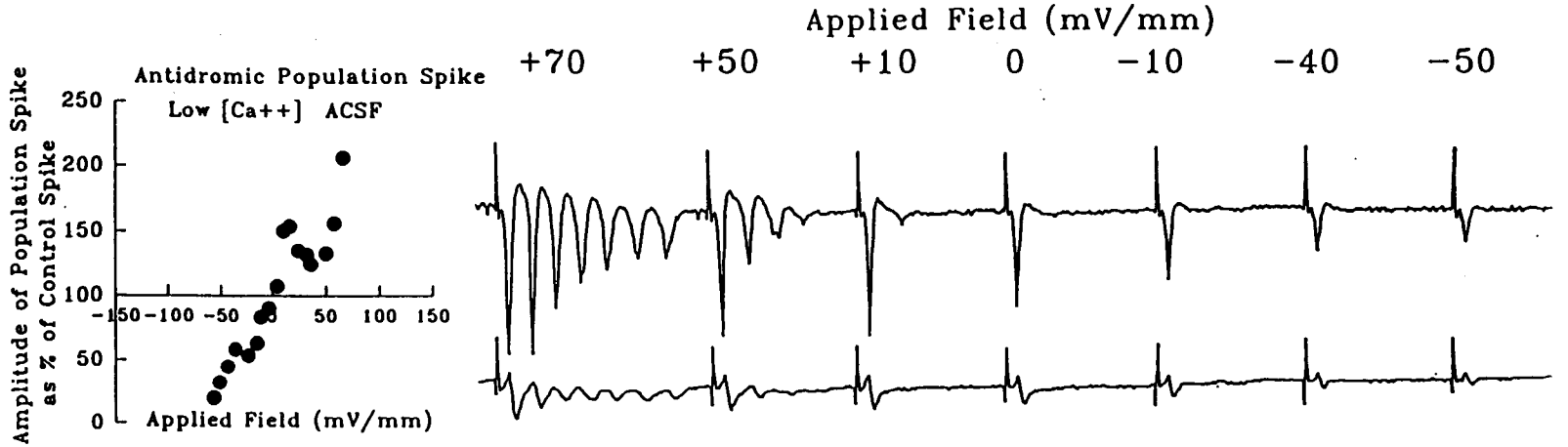

5.2 - Low $[Ca^{2+}]_o$ ACSF & the Incidence of Epileptiform Activity

Following the change to low $[Ca^{2+}]_o$ ACSF, orthodromic responses in CA1 and the dentate gyrus diminished and were undetectable after 20 minutes. The amplitudes of the antidromic responses in the dentate gyrus remained constant. Over this same period, the antidromic response in CA1 evolved from a single population spike to a burst of spikes. See Figure 10 for examples of various events recorded in CA1 during this study.

After one hour incubation, CA1 developed spontaneous seizures occurring on a regular basis (approximately 5-30s apart). This spontaneous epileptiform activity was consistent with published reports of CA1 activity under these same conditions (Eg. Haas, Jefferys, 1984; Taylor, Dudek, 1982; Yaari et al.1983; Taylor, Dudek 1984; Schweitzer et al, 1992; Roper et al, 1992). A few slices failed to develop epileptiform discharges and were rejected from the study. Similarly, slices which developed spreading depression were also rejected.

Under conditions of low $[Ca^{2+}]_o$ ACSF (and no applied fields) antidromic bursts were elicited from CA1 in 100% of slices accepted into the study. In contrast, the dentate gyrus was observed to burst under these conditions in only 3 of 27 slices for an incidence of 11%. In these 3

Figure 10 **CA1 Responses Used in Assessing Slice Viability**

The electrophysiological responses of CA1 used to assess slice viability for this study in normal and low $[Ca^{2+}]_o$ perfusions are illustrated. The orthodromic response in standard ACSF (upper left) typically consists of an initial positive potential (P1 or fEPSP) interrupted on its rising edge by a robust negative population spike (N1) that is followed by a second potential (P2) more positive than P1. In standard ACSF, the antidromic response (upper right) is typically biphasic with an equally robust negative population spike as the orthodromic response. In low $[Ca^{2+}]_o$ this response evolves (lower right) from a single spike to multiple spikes evoked by a single antidromic stimulus. Occasionally in low $[Ca^{2+}]_o$, spreading depression (bottom) develops. This is characterized by an abrupt, large amplitude sustained negative potential at the somatic layer, and can last for long periods (in the order of minutes.). Slices demonstrating spreading depression were not accepted into this study. Not shown are the spontaneous low $[Ca^{2+}]_o$ bursts of CA1. See Figure 4 for the details of these events.

Various CA1 Responses Observed Under Experimental Conditions

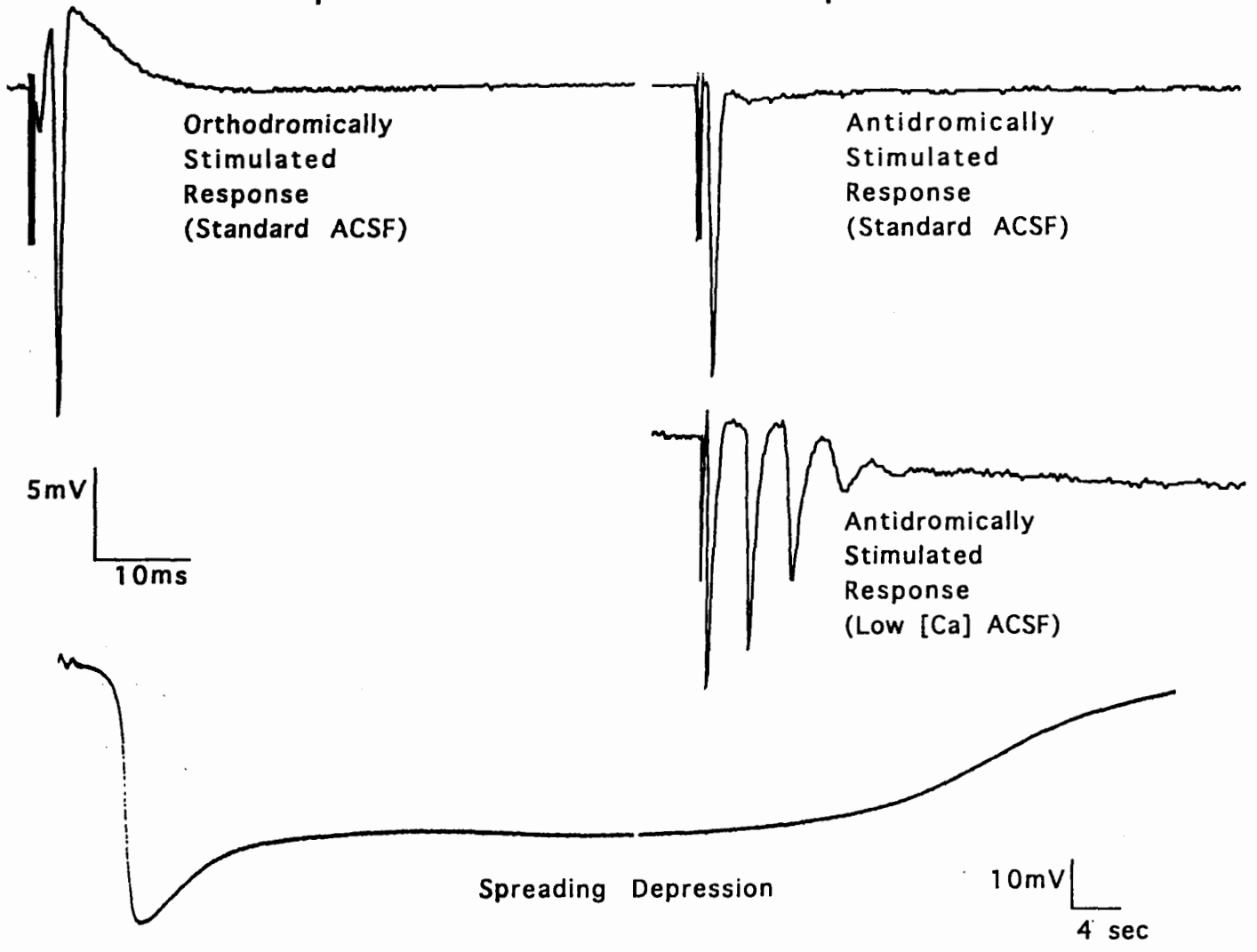

experiments the bursts were generally less robust than those similarly evoked in CA1. In the remaining 24 of 27 slices, antidromic stimulation of the dentate gyrus produced a single population spike. These events are depicted in Figure 11.

In 24 of 24 runs the onset of epileptiform events in the dentate gyrus demonstrated threshold behavior that was related to the intensity of the depolarizing applied field imposed upon the tissue. There exist two separate threshold events with respect to these field intensities: 1) the applied field required to evoke an antidromically stimulated burst and, in the same tissue, 2) applied field induced bursting, during which the applied field evoked a burst in the absence of any direct axonal stimulation. See Figure 12 for samples of these two events.

For the first threshold event, the antidromic burst, the intensity of depolarizing applied field at which a single antidromic population response potentiated into a burst response was 22.86 +\- 2.46 mV/mm (n=24).

The second threshold event, applied field induced bursting in the absence of antidromic stimulation, was measured in the same tissue. On average, this event was evoked 25-35 ms after the onset of the uniform applied field. The depolarizing applied field intensity required to elicit this event was 84.56 +\- 3.56 mV/mm (n=24). These data are summarized in Figure 13.

Figure 11 **Incidence of Various Antidromic Responses in the Dentate Gyrus**

Examples of antidromically stimulated responses in the dentate gyrus recorded in this study are depicted. In low $[Ca^{2+}]_o$, the dentate gyrus evoked a single population spike in response to antidromic stimulation without the application of depolarizing fields in 89% of trials (A top). During 3 trials (11%), these conditions resulted in multiple spikes following the single antidromic stimulus (A middle). In all 27 trials in low $[Ca^{2+}]_o$, where an antidromic stimulus was delivered during a depolarizing applied field, a burst of multiple spikes was evoked (B bottom). The antidromic burst in the dentate gyrus during low $[Ca^{2+}]_o$ perfusion and applied fields was the event examined in this study.

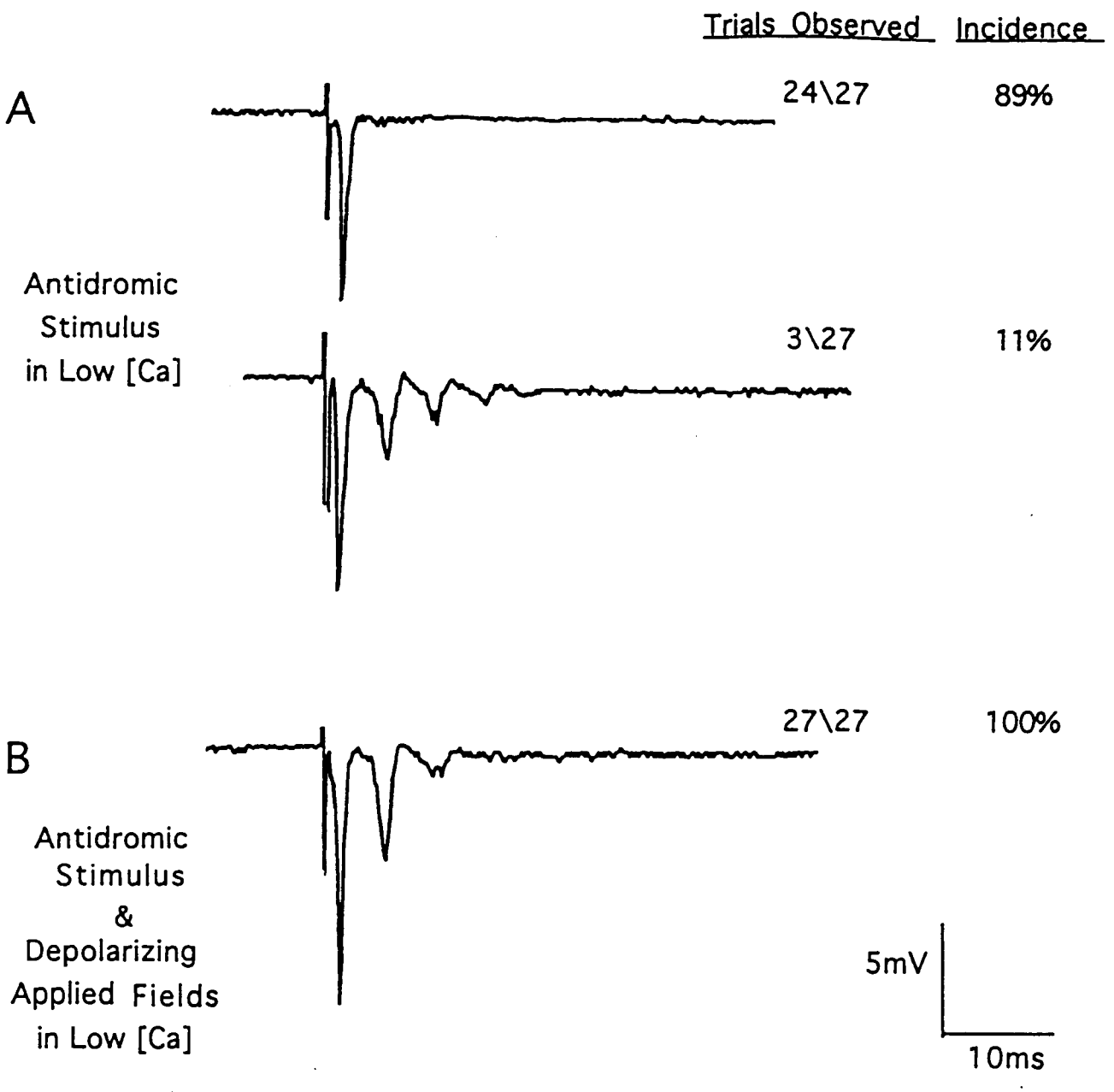
Trials Observed
Incidence
A
24\27
89%
Antidromic
Stimulus
in Low [Ca]
3\27
11%
27\27
100%
B
Antidromic
Stimulus
&
Depolarizing
Applied Fields
in Low [Ca]
5mV
10ms

Figure 12 **Two Distinct Epileptiform Responses of the Dentate Gyrus to Depolarizing Applied Fields**

Extra-somatic and extra-dendritic potentials in the dentate gyrus during threshold events in low $[Ca^{2+}]_o$ and applied depolarizing fields are shown. Two distinct events observed to have clear thresholds, occur in the dentate gyrus during low $[Ca^{2+}]_o$ perfusion and the application of depolarizing fields. The first (bottom 2 traces) is the antidromically evoked burst. This threshold is defined as the field intensity at which the first appearance of 3 successive population spikes following a single antidromic stimulus in which the third spike has a minimum amplitude of 1 mV. With increases to the applied field intensity, the features of this event increase in a graded manner. The second threshold event (Top 2 traces) is the development of a burst shortly after the onset of an externally applied field in the absence of any direct antidromic stimulation. The delay to this event from the onset of the applied field is approximately 25-35 ms. This event is distinguished from antidromic bursts in the text by referring to it as an applied field induced burst.

Threshold Events of Bursting Activity in the Dentate Gyrus

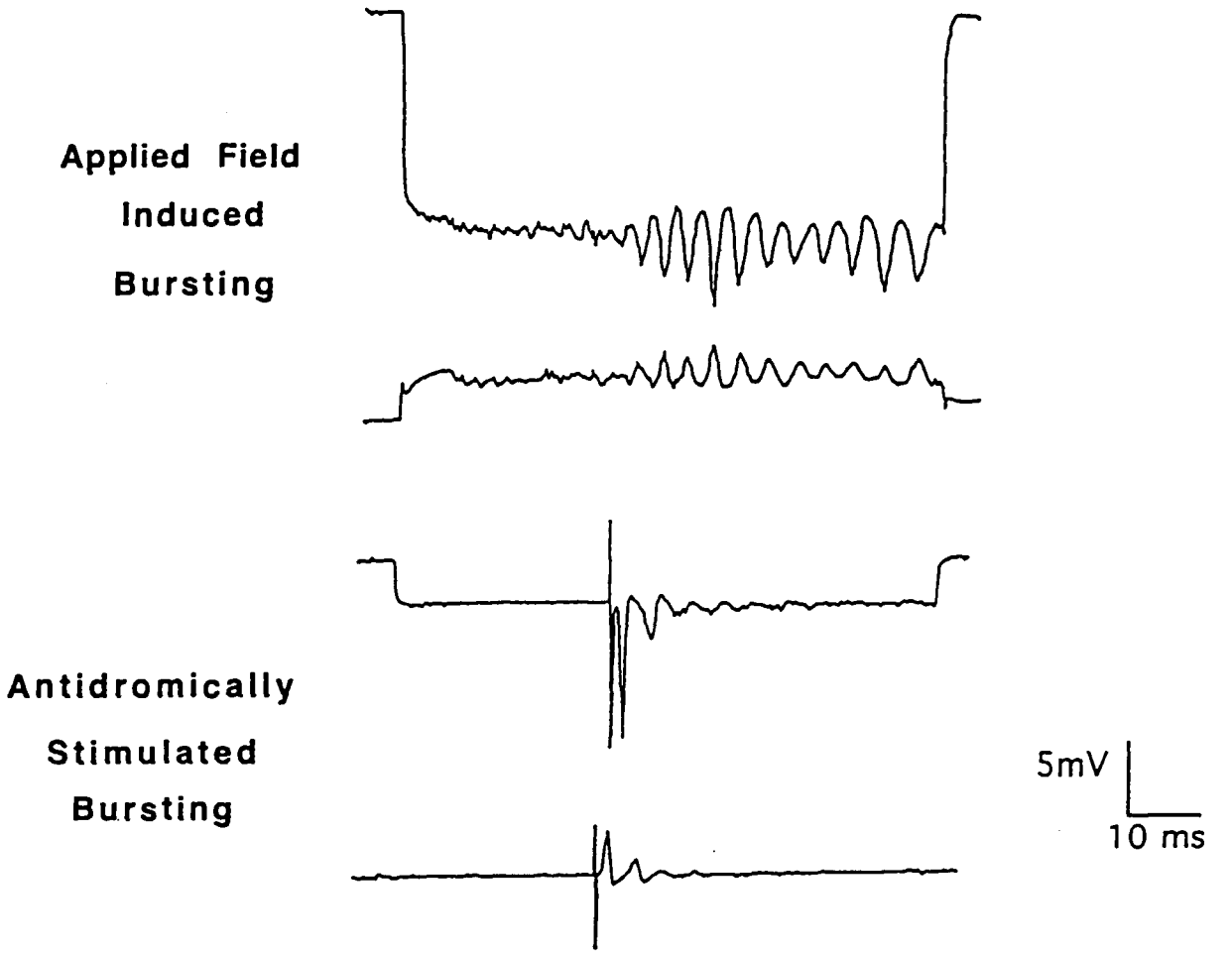

Figure 13 **Threshold Events in low $[Ca^{2+}]_o$ with Applied Depolarizing Fields**

In low $[Ca^{2+}]_o$, two distinct events can be induced in the dentate gyrus during the application of depolarizing fields. Examples of these events are shown on the right, while a histogram of the field intensities required to induce them is shown on the left. The first event is the antidromically evoked burst (right bottom 2 traces; described in previous Figure). The antidromically evoked burst has a threshold of 22.86 +/- 2.46 mV/mm and can be enhanced in a graded manner by increasing the magnitude of the applied field. The second event is characterized by the development of a burst shortly after the onset of an externally applied field in the absence of any direct stimulation (right top 2 traces). This applied field induced burst has a threshold of 84.56 +/- 3.56 mV/mm, and is also enhanced with the application of larger fields.

Average Applied Field Thresholds to Antidromic and Non-Stimulated Bursting

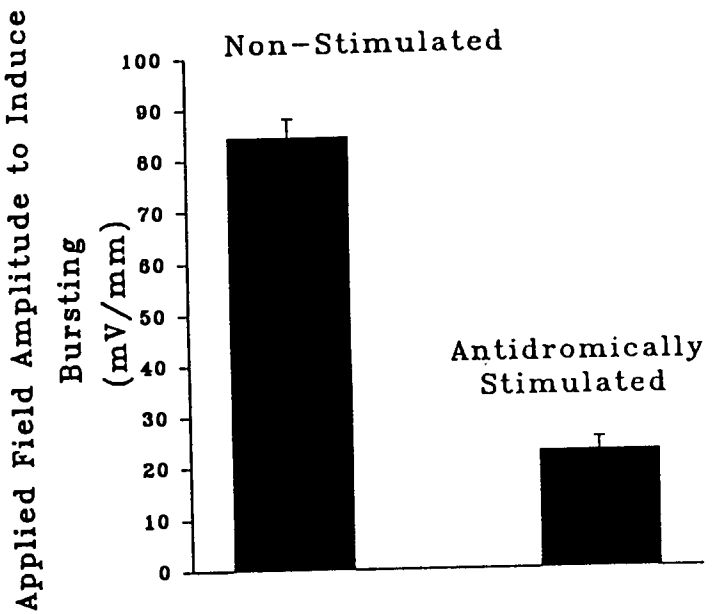

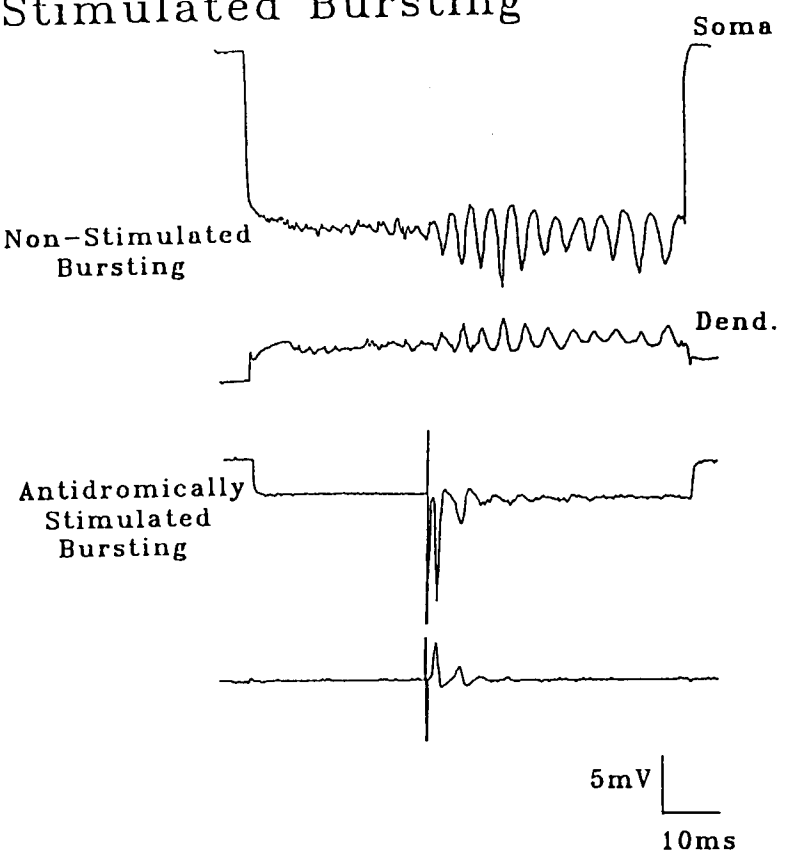

To test the hypothesis that these two events occurred at distinct field intensities a paired T-test was conducted on the two threshold values. The depolarizing applied field intensities required to evoke these two separate events are significantly different ($p<0.0001$).

Hyperpolarizing applied fields of 0 to -85mV/mm never elicited either the antidromic burst response or the applied field induced bursting without direct axonal stimulation ($n=24$).

In the 3 runs in which the dentate gyrus demonstrated antidromic bursts without fields, the subsequent application of depolarizing applied fields potentiated the antidromic burst responses by increasing the number and amplitude of the spikes within the burst. Conversely, hyperpolarizing applied fields diminished the number and amplitude of the spikes within the bursts. See Figure 14.

5.3 - Comparison of Low $[Ca^{2+}]_o$ Events in the Dentate Gyrus & the Low Ca^{2+} Events of Ammon's Horn (CA1)

The obvious qualitative similarities between the antidromic bursts in CA1 and the dentate gyrus initially prompted the questions posed within this thesis. While extracellular events of CA1 and the dentate gyrus during low $[Ca^{2+}]_o$ perfusion are markedly different (See Overview for details), the application of depolarizing fields across the dentate gyrus can reduce these differences. Can

Figure 14 **Antidromically Stimulated Bursts in Dentate in Low $[Ca^{2+}]_o$ with Applied Fields**

An example of an antidromic burst in the dentate gyrus that occurred in low $[Ca^{2+}]_o$ without the application of depolarizing fields is shown. This response could be manipulated with a application of external fields. Antidromic stimulation of the dentate gyrus in low $[Ca^{2+}]_o$ without the application of fields could evoke a burst response (top trace). When this response was exposed to depolarizing applied fields (middle trace) it was enhanced, and when exposed to hyperpolarizing applied fields it was diminished (bottom). The incidence of these events was low (11%).

Antidromically Stimulated Bursts of the Dentate Gyrus During Low [Ca] ACSF Perfusion

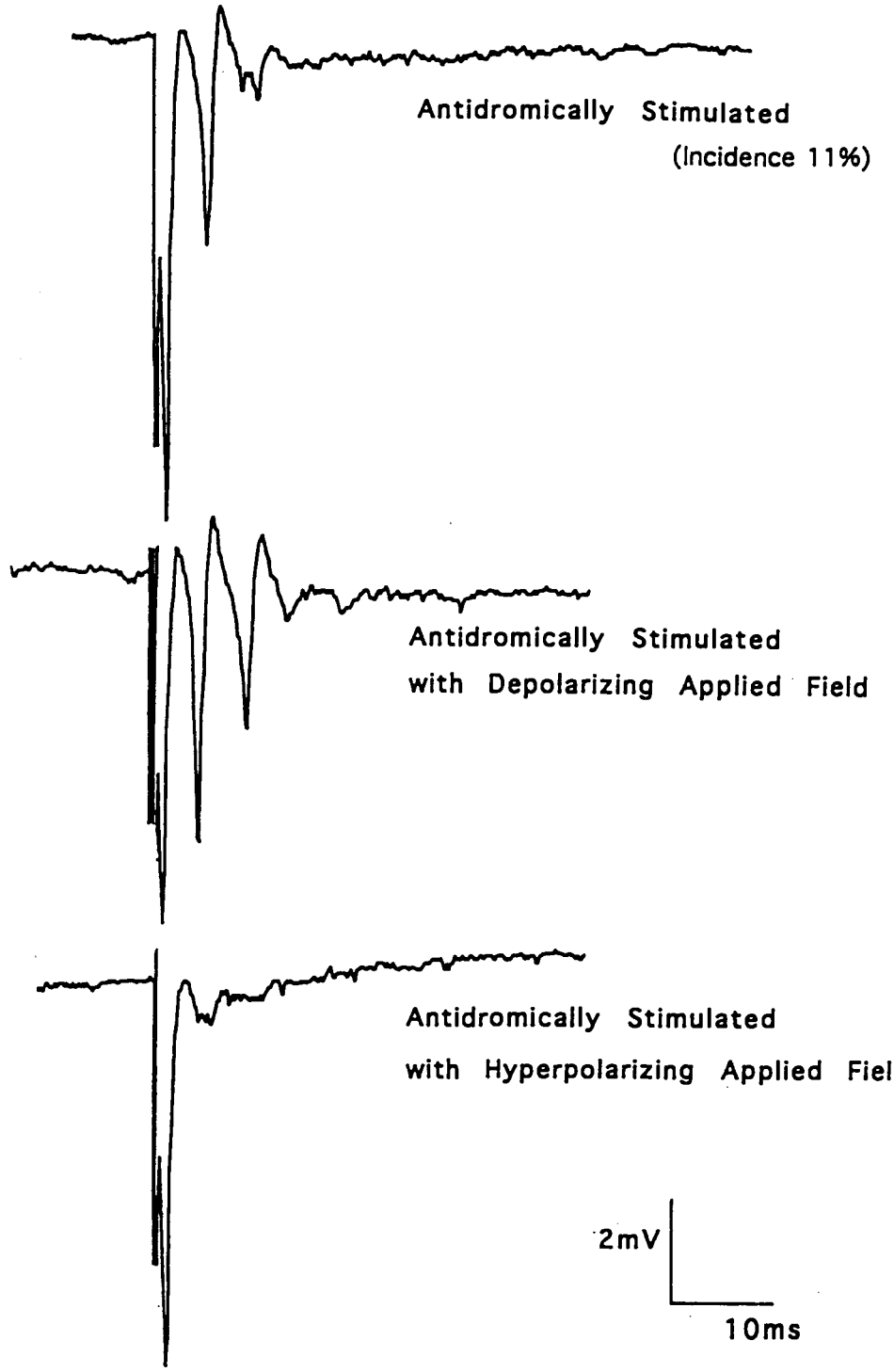

depolarizing applied fields eliminate these differences such that the antidromic responses can be considered similar?

The responses under comparison in the CA1 and the dentate gyrus were evoked by the same stimulus; an electric impulse (volts) to the axons of the primary neurons. The responses differ in that the dentate gyrus required external depolarization for the burst response to be revealed in 89% of slices.

Antidromic Population Spike Amplitudes

In quantifying the similarities and differences of antidromic bursts in the CA1 (low $[Ca^{2+}]_o$ only) to those reported in the dentate gyrus (low $[Ca^{2+}]_o$ and applied fields), the absolute amplitudes of the first antidromic population spike of bursts from both tissues were measured. The absolute spike amplitudes of the two tissues varied over large ranges. The dentate gyrus demonstrated antidromic population spikes of 4.39 mV to 18.48 mV, while the CA1 demonstrated spike amplitudes over a similar range from 5.46 mV to 25.39 mV. Despite these wide ranges, the mean amplitudes of antidromic spikes in the dentate gyrus and CA1 respectively were 10.18 mV +\- 0.19 mV and 12.74 mV +\- 1.68 mV. A comparison between tissues of these absolute amplitudes failed to show a significant difference ($p>0.15$). These data indicate that both tissues exhibit equally robust

population responses when presented with an antidromic stimulus.

One of the most distinct features of antidromic bursts recorded in both regions was that the initial antidromic spike (first spike) was equal or larger than all other spikes within the burst. In CA1 this was demonstrated in 87.5% of the antidromic bursts recorded, whereas in the dentate gyrus this was the case for 99.3% of all bursts recorded. The responses shown in Figure 15 are typical of those recorded throughout this study and clearly illustrate this feature.

Irrespective of which tissue was examined, the amplitudes of the population discharges within the antidromic bursts demonstrated a distinctive decreasing pattern as the burst progressed. In general spike amplitudes over the course of the bursts decreased monotonically (see Appendix A). This pattern was observed in 72.6% of CA1 bursts recorded, and in 59.4% of dentate bursts. An additional 27.8% of the dentate bursts deviated from the monotonic pattern by virtue of a single spike. Refer to Figure 15 for a representative extracellular trace.

These data indicate that: 1) the extrasomatic population responses in both regions were similar in amplitude, 2) the amplitude of the first spike of each burst in both regions was the largest recorded within the burst, and 3) the amplitudes of the population responses within the

Figure 15 Antidromic Burst Characteristics in CA1 and the Dentate Gyrus

Antidromic burst characteristics in the CA1 and the dentate gyrus are compared with sample traces and histograms. The upper left shows a CA1 antidromic burst in low $[Ca^{2+}]_o$. The upper right shows an equivalent burst in the dentate gyrus under the influence of depolarizing fields. Upon initial examination, the similarities of these responses appear to outweigh the differences. Below these traces (lower histograms), responses are grouped into small and large bursts. Each bar represents an inter-spike interval as a % of the first interval of the burst. The inter-spike interval differs between small bursts and large bursts in both the dentate gyrus and the CA1. The pattern of change over the duration of the burst does not differ between small and large bursts of the same tissue. In addition this pattern is similar between small bursts in the CA1 and the small bursts of the dentate gyrus or between large bursts in CA1 and the large bursts of the dentate gyrus.

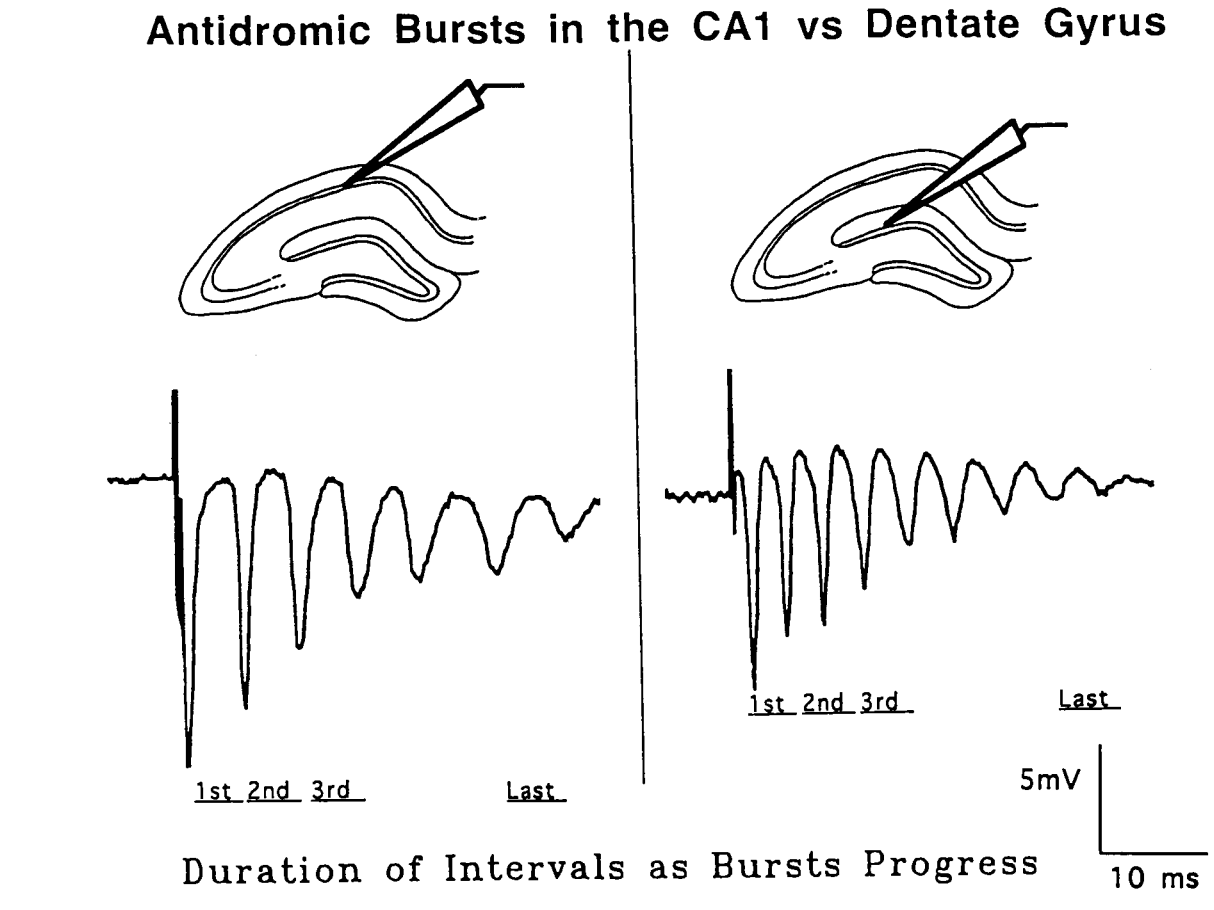
Antidromic Bursts in the CA1 vs Dentate Gyrus
1st 2nd 3rd
Last
1st 2nd 3rd
Last
5mV
10 ms

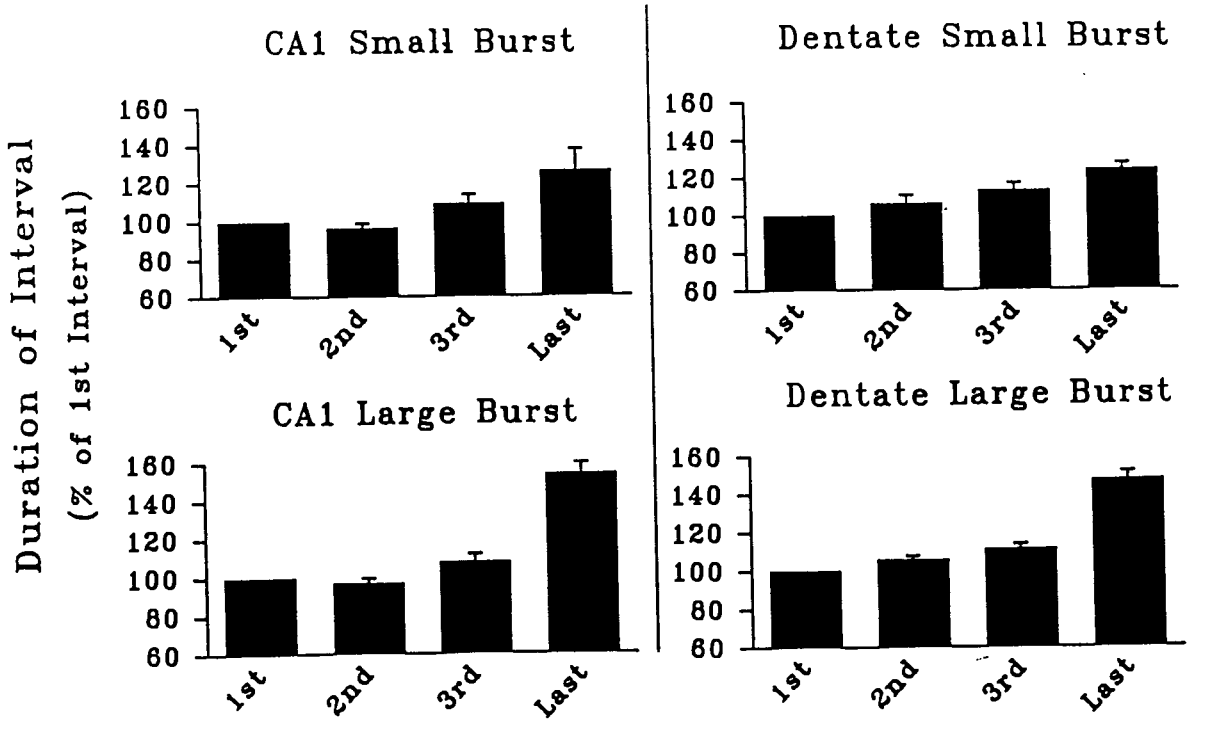
Duration of Intervals as Bursts Progress
CA1 Small Burst
Dentate Small Burst
CA1 Large Burst
Dentate Large Burst
Duration of Interval
(% of 1st Interval)
160
140
120
100
80
60
1st
2nd
3rd
Last

bursts decreased monotonically as the burst progressed in both tissues.

Duration of Inter-Spike Interval of Antidromic Bursts in the CA1 vs Dentate

The time intervals between successive spikes, or the instantaneous rate, within antidromic bursts of both the CA1 and the dentate gyrus were compared to assess response similarities. The duration of the inter-spike interval was defined as the time between the peak negative amplitude of one population spike to the peak negative amplitude of the following spike. In this parameter, antidromic bursts of the two tissues varied considerably. However, in general the inter-spike interval of both tissues increased as the burst progressed.

When mean inter-spike intervals within bursts of the dentate gyrus were examined, the interval increased in a monotonic fashion for bursts containing 3 - 11 spikes (see Figure 16), but in larger bursts consisting of 12 - 14 spikes this monotonic pattern deteriorated. The inter-spike intervals of CA1 bursts increased monotonically during only 23.5% of all bursts. Overall, inter-spike intervals increased in both tissues.

As inter-spike intervals changed with the size of the bursts, it was difficult to compare this parameter between the tissues. The purpose of this analysis was to convey

Figure 16 **Monotonic Increases in the Inter-Spike Interval of Dentate Bursts**

A sample antidromic burst in the dentate gyrus during low $[Ca^{2+}]_o$ perfusion and applied depolarizing fields is depicted and the inter-spike intervals are numbered. One striking feature of these events in the dentate gyrus is the monotonic increase of the inter-spike interval as the burst progresses. Each successive interval is equal, or longer, in duration than the previous interval. To visualize this increase, examine the 1st, 5th and 10th intervals and note the progression. This pattern of increase was generally seen in bursts consisting of 3-11 spikes, however it deteriorated in larger bursts of 12-14 spikes.

Monotonic Increase in Inter-Spike Interval During Antidromic Bursts of the Dentate Gyrus

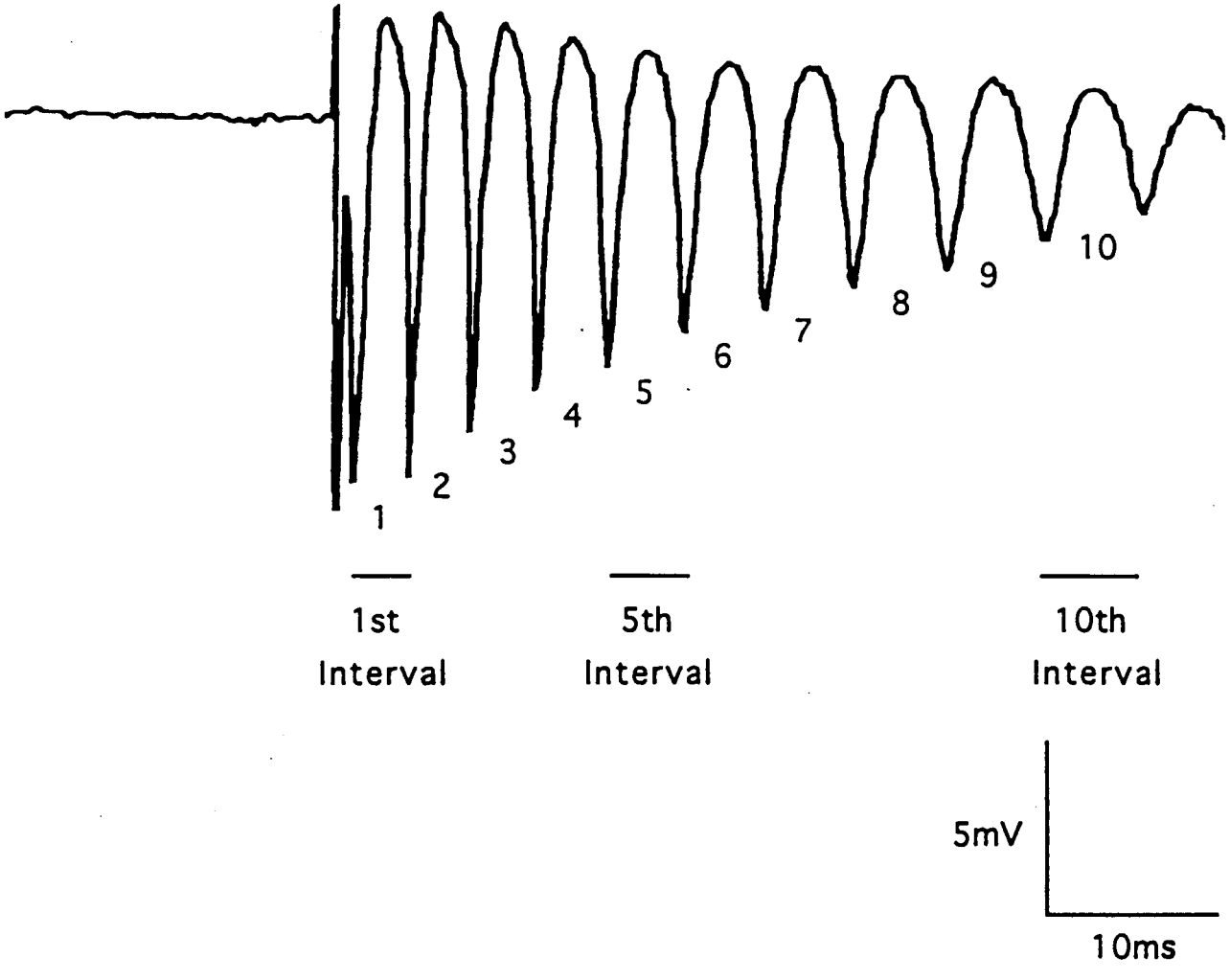

similarities and differences in the pattern of the antidromic burst. In assessing the low $[Ca^{2+}]_o$ antidromic burst in the dentate gyrus verses the corresponding event in CA1, the data were pooled arbitrarily for each tissue into "small" (5-6 spikes) and "large" bursts (8-12 spikes) and the inter-spike intervals were expressed as a percent of the first interval. These groupings were verified as being unique using statistical analysis of variance ($p<0.05$). The first, second, third and last inter-spike intervals were used in this analysis.

Interval patterns of small bursts verses large bursts for the respective tissues were significantly different ($p<0.0001$)(Figure 15). However, when the interval pattern of small bursts in dentate gyrus were compared to small bursts in CA1 and large bursts in dentate gyrus were compared to large bursts in CA1, no differences in the interval patterns were found ($p>0.925$).

The first intervals for short bursts in the dentate gyrus had a mean duration of 3.93 +\- 0.05ms, while short bursts in the CA1 had a mean duration of 4.95 +\- 0.29ms. In these same tissues, large bursts had mean first intervals of 3.2 +\- 0.04ms and 5.43 +\- 0.31ms respectively. When the mean of the first intervals were compared between the bursts of the dentate gyrus and CA1 they were found to be significantly different ($p<0.05$).

This analysis underscores the following points: 1) irrespective of the tissue examined, the mean inter-spike

intervals increased as the burst progressed ($p<0.0001$), 2) the pattern of this increase in inter-spike interval did not vary between the anatomical regions (Figure 15), and 3) overall the mean first inter-spike interval durations were longer in CA1 than the dentate gyrus.

5.4- Additional Findings

A - Applied Fields & The Antidromic Response

In low $[Ca^{2+}]_o$ ACSF, when a depolarizing applied field was imposed across the dentate gyrus, a single antidromic population spike could be potentiated in terms of three parameters: 1) the total number of spikes that comprised the response increased 2) the amplitude of the initial antidromic response increased, and 3) the amplitude of the spikes present within the burst are weakly related to the applied field intensity, but strongly related to the amplitude of the preceding spike.

Finding #1) The number of spikes contained within an antidromic burst was related to the intensity of the depolarizing field applied.

To quantify the influence of depolarizing applied fields on the number of spikes within a response, an incremental change was made to the intensity of the applied fields imposed upon the tissue over a range of 0-90mV/mm. This range of depolarizing field intensities has been

documented to represent the extracellular gradients produced within the hippocampal formation during physiologically generated population events.

When the number of spikes within a burst was plotted against the depolarizing applied field intensity, a linear relationship was established with a slope of 0.147 +\- 0.007 ($p<0.0001$). These data are shown in Figure 17. This relation demonstrates that as the depolarizing applied field intensity was increased, the number of population spikes produced in response to a single antidromic stimulus also increased.

Hyperpolarizing applied fields never (n=24) elicited antidromic bursts or multiple population spikes in the dentate gyrus of slices accepted into this study.

Finding #2) The antidromic population spike amplitude was influenced by artificially applied fields.

To quantify the influence of applied fields on the amplitude of the initial antidromic population spike, an incremental change was made to the intensity and polarity of the applied fields imposed across the tissue. The applied fields varied in intensity from -85 mV/mm (hyperpolarizing) to +85mV/mm (depolarizing).

The absolute amplitude of a population spike varied between different experimental runs on independent hippocampal slices. Therefore, in order to compare data across slices, spike amplitudes were expressed as a percent of their control spike amplitudes. See Methods Section for

Figure 17 **Number of Population Spikes Within a Burst versus the Applied Field Intensity**

The number of population spikes within an antidromic burst of the dentate gyrus is plotted against the applied field intensity used to induce the burst. The total number of population spikes within an antidromic burst of the dentate gyrus increases with the increasing intensity of depolarizing field applied. This plot shows a linear relation with a slope of 0.147 +/- 0.007 ($p<0.0001$). This relation assists in quantifying the graded nature of antidromic burst development with the application of fields.

Total Number of Spikes in a Burst vs Applied Field Intensity

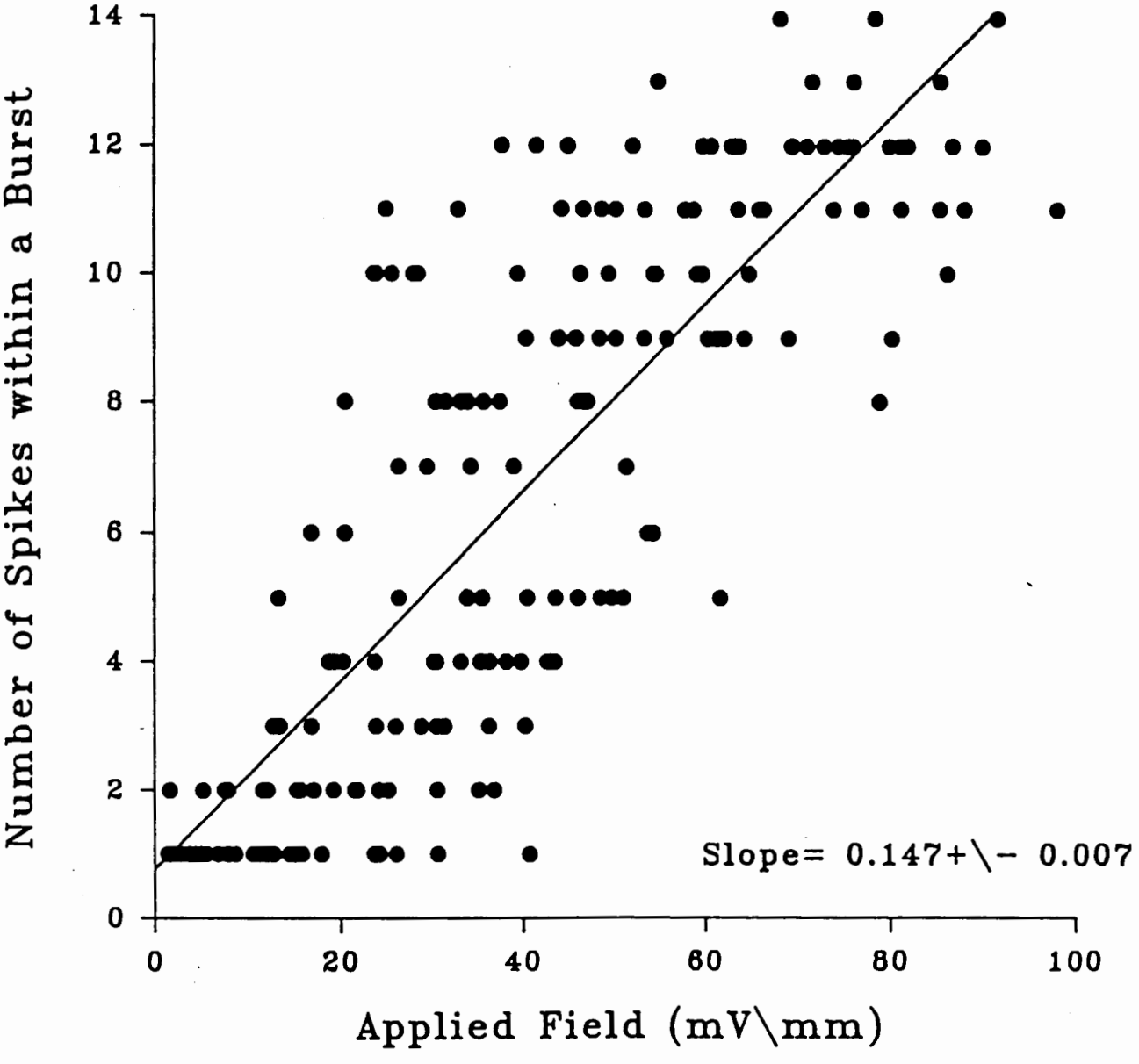

details pertaining to control spike measurement. This allowed changes in spike amplitude during a given experimental run to be standardized and comparisons between runs to be made.

With an increase in the intensity of the depolarizing applied fields, the amplitude of the initial antidromic population spike increased (n=24). At high intensity fields (+85mV/mm) the average increase was 33.21 +\- 12.09 %. With an increase in the amplitude of the hyperpolarizing applied fields, the amplitude of the initial antidromic population spike decreased (n=24). At high intensity fields (-85mV/mm) the average decrease was 52.89 +\- 7.94 %.

Figure 18 depicts data of antidromic population spike amplitude, as a percent of its control amplitude, verses the applied field intensities (-85mV/mm to +85mV/mm) and illustrates a linear relation with a slope of 0.494 +\- 0.026 ($p<0.0001$). This relationship supports the experimental observations that depolarizing applied fields increase the amplitude of the antidromic population spike and hyperpolarizing fields decrease the amplitude of the antidromic population spike.

Finding #3) The amplitudes of the spikes within an antidromic burst, subsequent to the initial antidromic response, are related to the intensity of the depolarizing applied field.

As the spikes within a burst are part of an epileptiform event, further analysis was conducted to reveal

Figure 18 Alteration of the Antidromic Response in the Dentate Gyrus During Applied Fields

A plot of the antidromic population spike amplitude vs applied field is shown. The change in antidromic population spike amplitude during low $[Ca^{2+}]_o$ perfusion was examined over a range of field strengths (0 - 85 mV/mm) noted during physiological events. The influence the applied field had on the population spike amplitude was revealed by examining the change in population spike amplitude relative to a control spike amplitude. To the right of the graph are the spike amplitudes that were evoked during depolarizing applied fields and to the left are these values for hyperpolarizing fields. Hyperpolarizing fields depressed and depolarizing fields enhanced spike amplitude in a linear fashion. The slope of the line describing this relation was 0.496 +/- 0.026 ($p<0.0001$). The control spike was delivered seconds prior to the field application (see Methods).

Amplitude of Antidromically Stimulated Population Spikes As a % of Control Amplitude

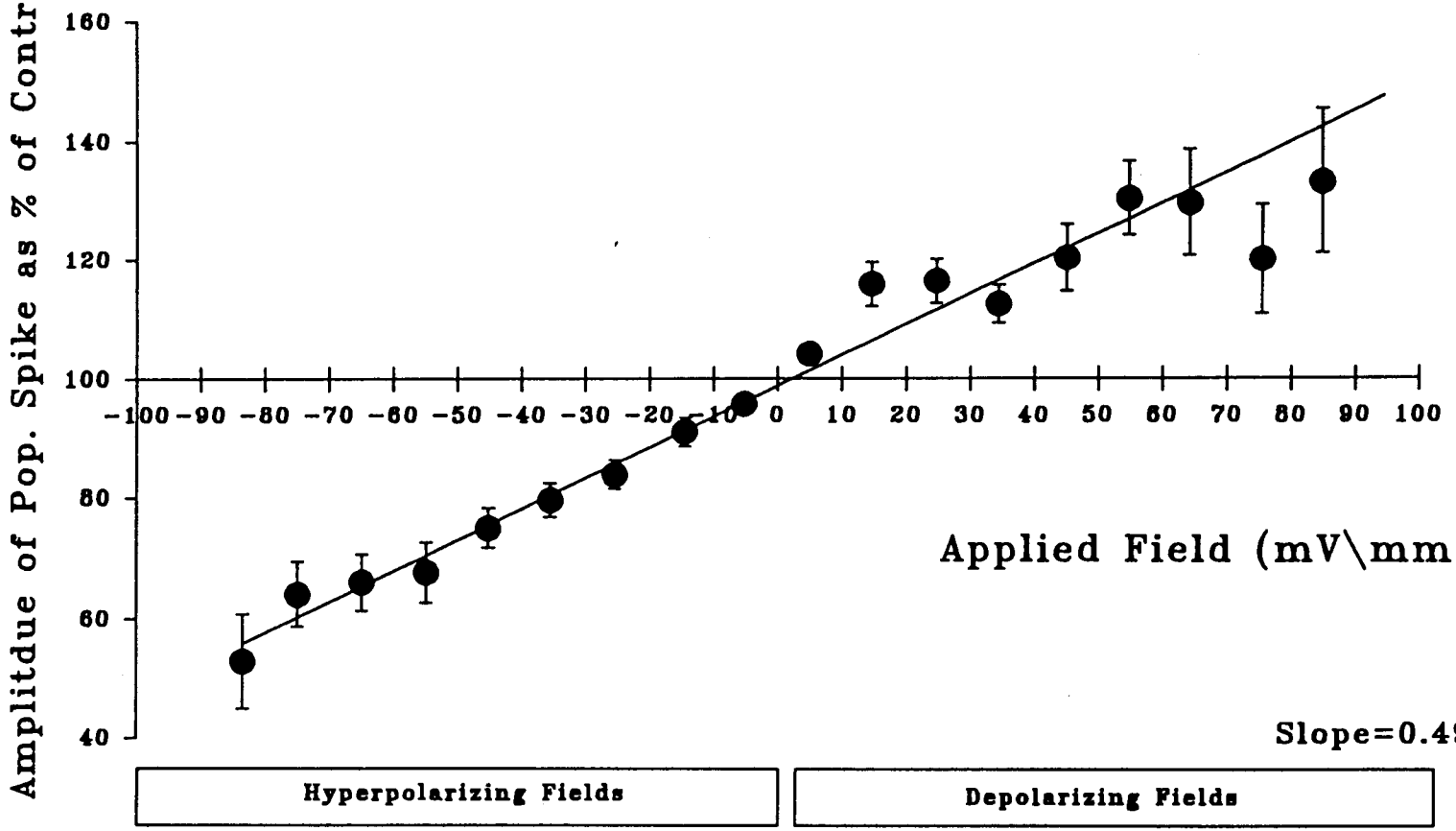

whether the second and third population spikes of a given burst would also demonstrate a relationship to the intensity of depolarizing field imposed.

Examination of the percent of control spike amplitude of the second spike within an antidromic burst versus the intensity of depolarizing field applied across the tissue, revealed a linear relationship with a slope of 0.977 +\- 0.137 ($p<0.0001$) and $r^2=0.23$. The same analysis of the third spike also revealed a linear relationship with a slope of 0.760 +\- 0.154 ($p<0.0001$) and $r^2=0.14$ (Figure 19).

While the first, second and third spike amplitudes of an antidromic burst have statistically verified relationships to the depolarizing applied field intensity, with each successive spike of a burst, the relationship between spike amplitude and depolarizing applied field intensity weakens as reflected in the r^2 values. As the r^2 values decrease, smaller percentages of the variance in amplitudes are explained by changes in the field intensity. It is, therefore, reasonable to question whether the amplitudes of these subsequent spikes were influenced by the amplitude of each preceding spike more than by the applied field intensity. This question was intuitively supported by an examination of raw data, in which a burst containing 3 spikes did not develop a 4th spike until the 3rd spike was a significant amplitude.

To investigate this possibility, the amplitude of the 3rd spike was compared to the amplitude of the 2nd spike.

Figure 19 **Population Spike Amplitude versus Applied Field Intensity For Various Spikes Within a Burst**

The relations of the population spike amplitude on the intensity of the applied depolarizing field is examined. Population spike amplitude is presented as a % of a given event's control spike amplitude. As reported in the previous figure, and reproduced here for comparison, the antidromic spike amplitude increases with an increasing intensity of applied field in a linear fashion (A). The other spikes within a burst do not result from antidromic invasion and it is of interest to observe whether they too demonstrate a relation to applied field intensity. B is a plot of the 2nd spike amplitude verses applied field intensity, while C is a plot of the 3rd spike amplitude verses applied field intensity. As the burst proceeds, the relation of each successive spike to applied field intensity weakens. This is revealed by the decreasing r^2 values.

% of Control Spike Amplitude
For the Antidromic, 2nd, and 3rd Spikes of a Burst
Versus Depolarizing Applied Field Intensity

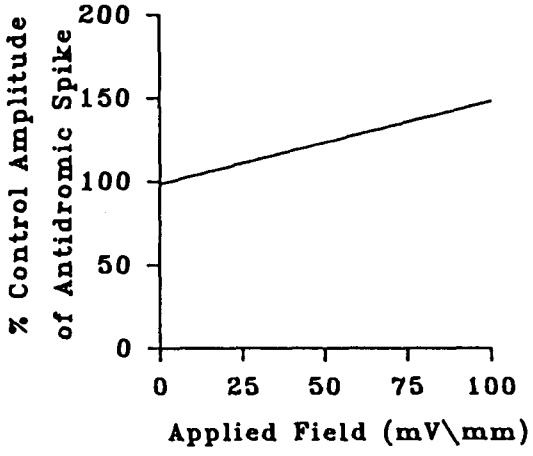

A Antidromic Spike

Slope = 0.496 +\- 0.026
R-squared = 0.46

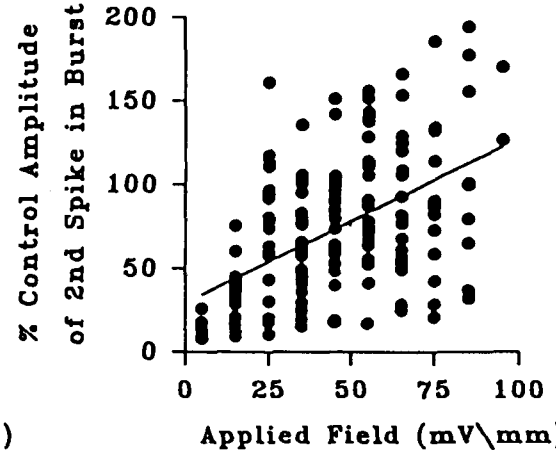

B 2nd Spike

Slope = 0.977 =\- 0.137
R-squared = 0.23

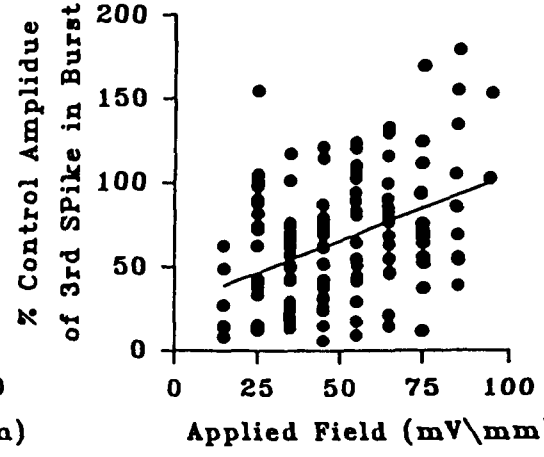

C 3rd Spike

Slope = 0.76 =\- 0.154
R-squared = 0.14

The resulting relationship was strongly linear with a slope of 0.906 +\- 0.024 ($p<0.0001$) and $r^2= 0.91$ (Figure 20). This relation predicts that 91% of the variance in the third spike amplitude is accounted for by the amplitude of the second spike and statistically confirmed the intuitive observation that the amplitude of a burst spike is related to the amplitude of its preceding spike.

In addition, the amplitude of the second spike to that of the initial antidromic spike was also more strongly correlated to the preceding spike amplitude than it had been to the intensity of applied field. This line had a slope of 0.944 +\- 0.081 ($p<0.0001$). The $r^2= 0.44$ for this relation compared to 0.23 for the relationship of second spike amplitude to applied field intensity.

In summary, these data indicate that as the population events of an antidromic burst progress in time, the individual population spikes demonstrate a decreasing relationship to the applied field intensity and an increasing relationship to the amplitude of the immediately previous spike.

B - Duration of the First Interval for Bursts of Different Sizes

The inter-spike intervals within a burst contain information regarding the physiology underlying the burst.

Figure 20 **Population Spike Amplitudes as Related to Other Population Spike Amplitudes within a Burst**

The relationships of individual spike amplitudes to the 1st and preceding spike amplitudes, within an antidromic burst, are depicted for the first 3 spikes. Amplitudes are expressed as a % of the control spike amplitude. On the left, A is a plot of the 2nd spike amplitude verses the 1st, while B is a plot of 3rd spike amplitude verses the 1st. C is a plot of the 3rd spike amplitude verses its preceding spike, the 2nd spike. Note a similar and weak relation exists between the 2nd spike amplitude to the 1st spike (A) and the 3rd spike amplitude to the 1st spike amplitude (B). However, the graded or evolving nature of the burst as an event is revealed by the strong linear relation of the 3rd spike amplitude to its preceding spike amplitude (C). This strong relation suggests that the variability in amplitude of a spike intrinsic to a burst is related to the immediately preceding burst spike amplitude.

% of Control Spike Amplitude of Various Spikes Related to Other Spike Amplitudes Within the Burst

A

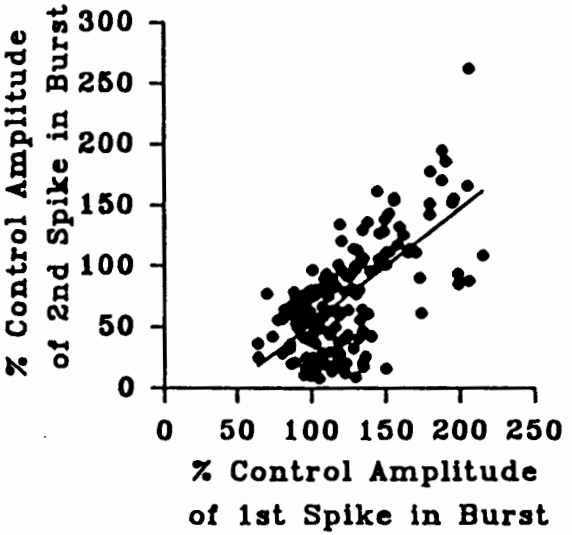

B

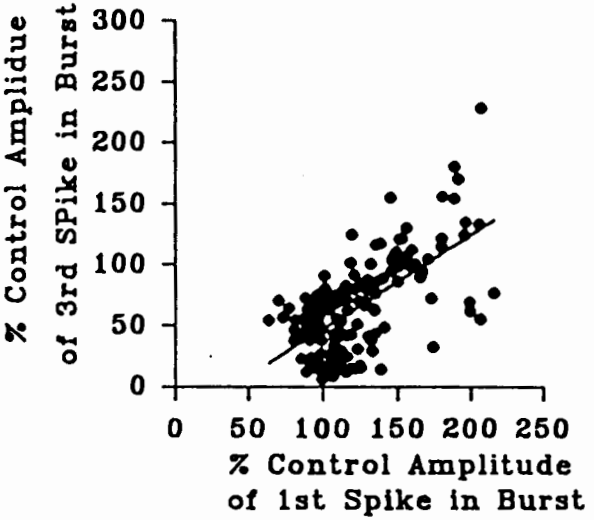

C

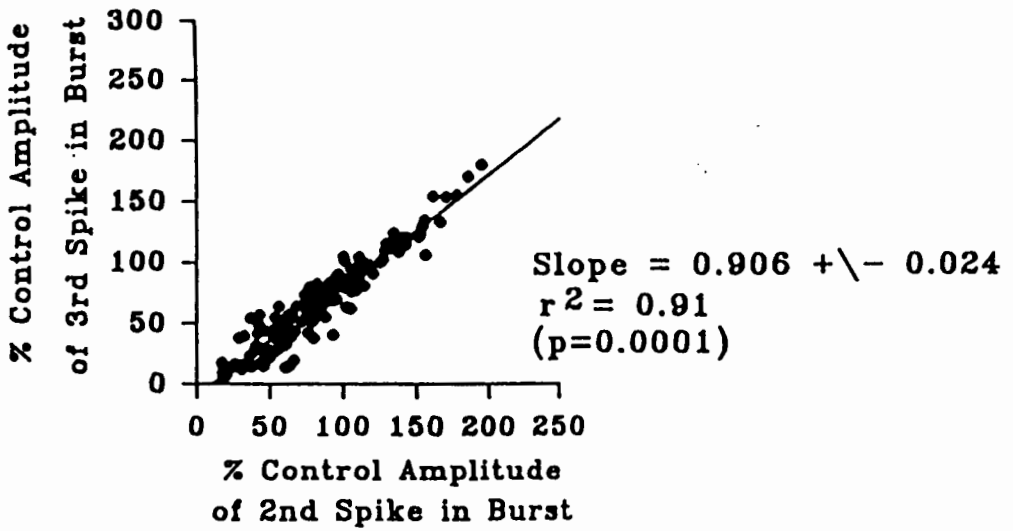

Of particular interest was the duration of the first interval.

Finding: The duration of the first inter-spike interval was related to the number of spikes within a burst.

The first interval duration varied over a range of 4.18 to 2.87 milliseconds. However, it was observed that within this range a relationship existed between the number of spikes within a burst and the duration of its first interval.

Regression analysis revealed a negative linear relationship with a slope of -0.136 +\- 0.007 ($p<0.0001$). These data indicate that, as the total number of spikes which make up a burst increased, the duration of the first interval decreased. These data are shown in Figure 21.

Overall, the interval data presented in this thesis can be summarized as follows: 1) the inter-spike intervals within a burst increased as the burst progresses (section 5.3) and 2) the first interval of a burst decreased as the number of spikes within the burst increased.

C - Physiologically Generated Extracellular Gradients in the Dentate Gyrus During Synchronized Population Events

A population of spatially extended granule cells with a negative extra-somatic potential and a positive extra-dendritic potential establishes an extracellular voltage gradient for the brief period of time over which these

Figure 21 **Duration of the 1st Inter-spike Interval Versus the Number of Spikes Intrinsic to a Burst**

The durations (milliseconds) of the 1st inter-spike interval from bursts of various sizes are plotted. The duration of the first interval decreases as the number of the spikes within a given burst increases. The slope of the regression line describing this is -0.136 +/- 0.007 ($p<0.0001$). This decrease in the first interval duration with an increase in the size of the burst implies that a higher initial rate of discharge may result in a sustained burst, while a lower initial rate of firing may produce a limited number of responses.

Number of Spikes Within a Burst

vs

Duration of the First Interval

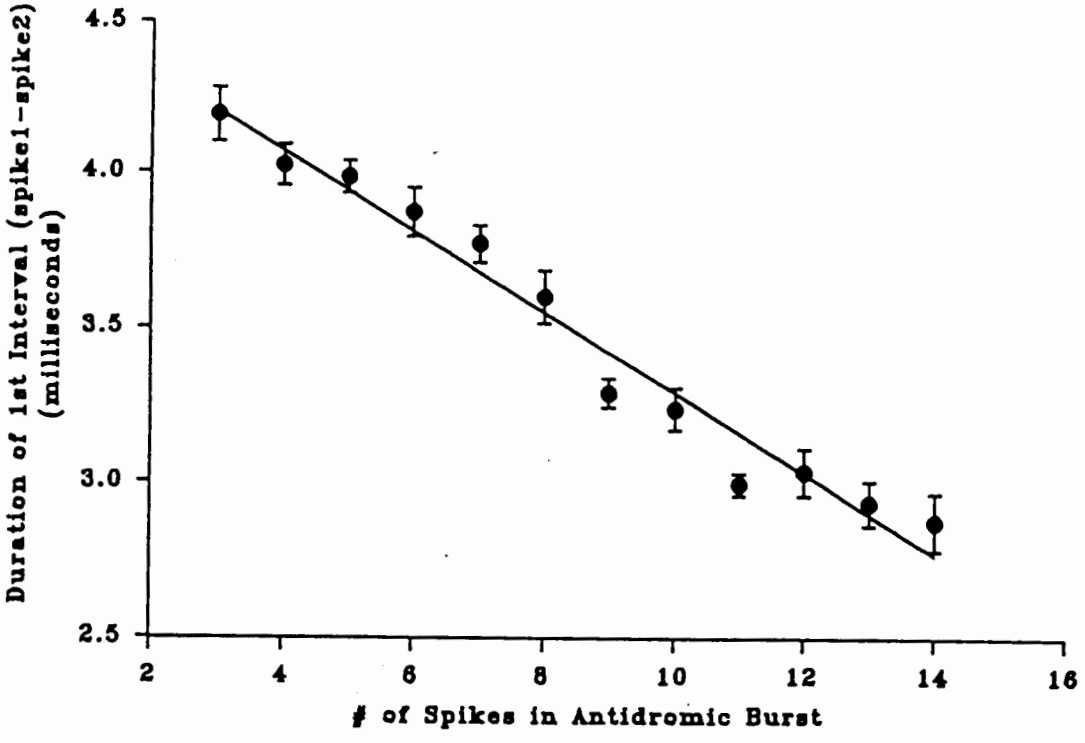

Sample Burst

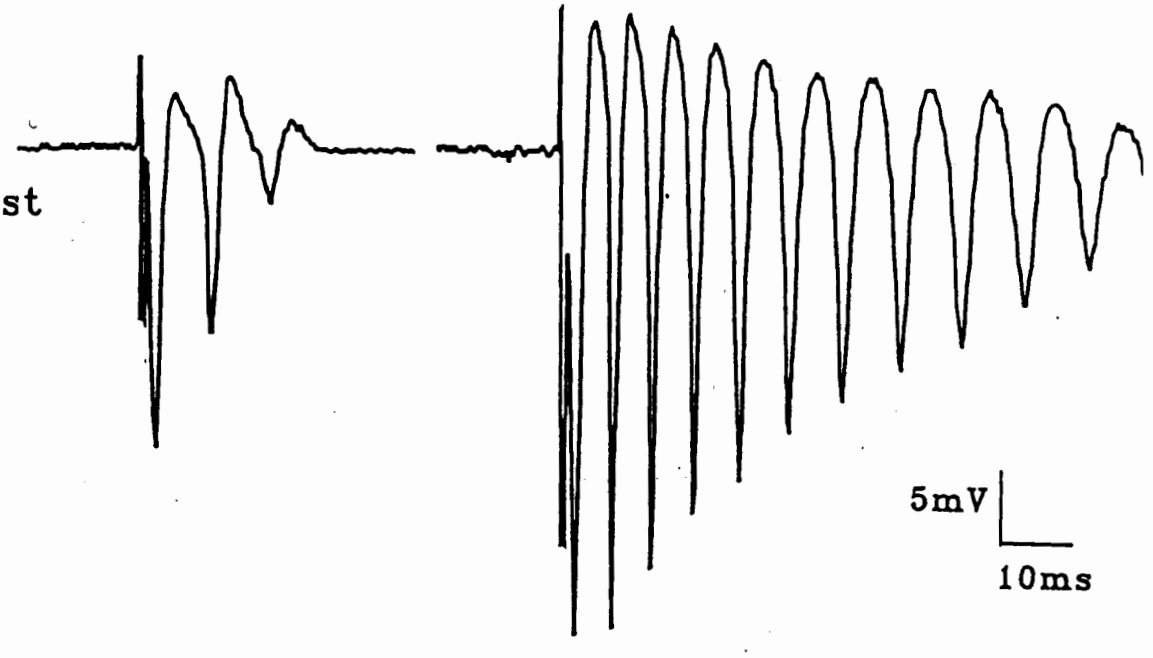

1st Interval

1st Interval

* A Burst is defined as having a minimum of 3 spikes

potentials exist (Taylor, Dudek 1984; Chan, Nicholson 1986; Richardson et al 1984a,b; Richardson et al 1987; O'Reilly, Richardson 1992).

It is critical to recognize that the presence of an extracellular potential at one location does not constitute an extracellular voltage gradient, but a spatially separated voltage difference does. For example, if a population of granule cells was to fire synchronously and the potential of the extracellular space in both the region of the soma and the dendrites was recorded at -5mV, then no current would flow between these two points and no extracellular gradient would exist.

Having underscored this point, the relationship between the robust negative extra-somatic potentials recorded in the granule cell layer and the physiologically generated voltage gradient present during these spikes was analyzed.

Finding: A linear relationship was revealed between the amplitude of the extra-somatic population spike of dentate granule cells and the physiologically generated voltage gradient along the dendro-somatic axis of this population.

All available data was pooled (n=1,495) and plotted (Figure 22). As no measurable background gradient exists when the population is at rest, the Y intercept of the regression line was forced to 0.0. The slope of the regression line was 0.133 +\- 0.001 ($p<0.0001$) and $r^2= 0.94$. Figure 22 illustrates both the raw data and these same data

Figure 22 Physiologically Generated Fields During Burst Spikes

The extracellular voltage gradients produced by the synchronous discharge of large populations of granule cells during antidromic bursts in low $[Ca^{2+}]_o$ are plotted against the amplitude of the extra-somatic population spike recorded during the gradient. The raw data with the regression is reported graphically (top) in addition to data grouped according to field intensity (bottom). This data represents the pooling of all antidromic population responses collected in this study (n=1,495). Regression analysis revealed a linear relation (slope= 0.133 +/- 0.001, p=0.0001). This relationship may provide a useful means of predicting the approximate extracellular voltage gradient that exists during an extrasomatic population spike in the dentate gyrus.

Magnitude of Field Generated By Population Spikes of Various Amplitudes

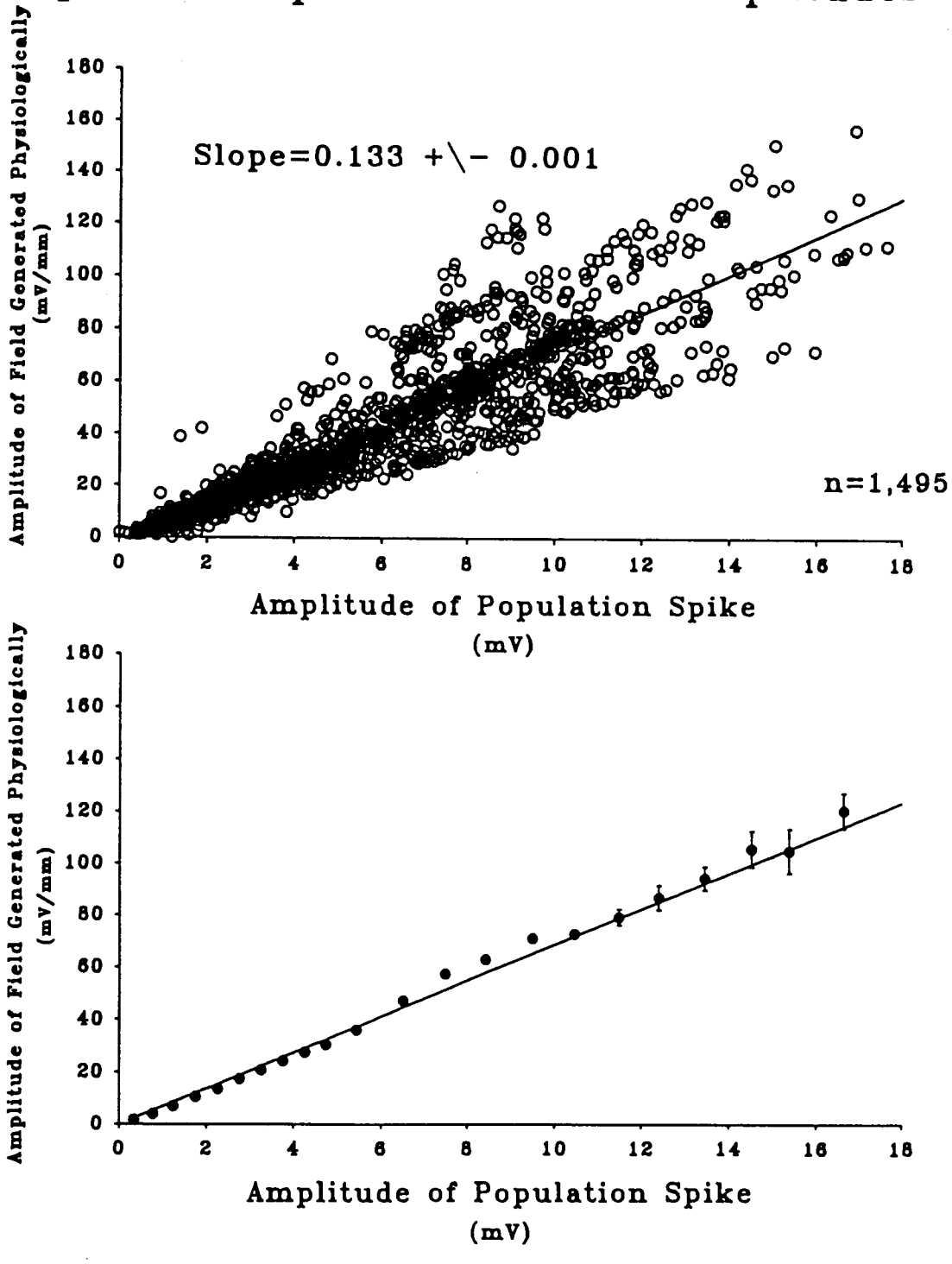

are grouped according to field intensities. These data indicate that as the population spike amplitude increased the extracellular gradient associated with the event also increased and that these gradients were always depolarizing in polarity.

The above analysis combined data from a variety of population events, including direct antidromic responses without applied fields, with depolarizing fields, and with hyperpolarizing fields. In addition, this data pool included indirect population spikes generated within a burst evoked with depolarizing applied fields. The relationships of the above grouped spikes to the gradients they generated were compared. The slopes and errors for these linear relations are reported in Figure 23. These data and their regressions do not indicate that varying the condition under which a spike occurred, significantly impacts the relation of the spike's amplitude to the gradient it generates.

Figure 23 A Comparison of Regressions of Gradients verses Spike Amplitude from Population Spikes of Various Forms

The slopes of the regression lines describing gradients generated during Population spikes of various forms are shown in this histogram. The error bars are the standard error of the slopes. The relationship of voltage gradient generated by a given population spike to the amplitude of that spike for all antidromic data collected in this study is described in the previous figure. The slope of this relation is represented here as the average slope of all spikes (far left). These data are distinguishable by the condition under which the responses were evoked. The slopes of the relations describing these same data separated in this fashion are reported graphically. From left to right, these categories are 1) the average of all evoked spikes, 2) antidromically evoked spikes without the application of fields, 3) antidromically evoked spikes during depolarizing applied fields, 4) antidromically evoked spikes during hyperpolarizing fields, and 5) non-antidromic, evoked spikes of the burst during depolarizing fields (far right). No physiologically significant difference can be attributed to the differences in these slopes.

Slope of PopulationSpike Amplitude vs Physiological Gradient Generated For Various Population Events

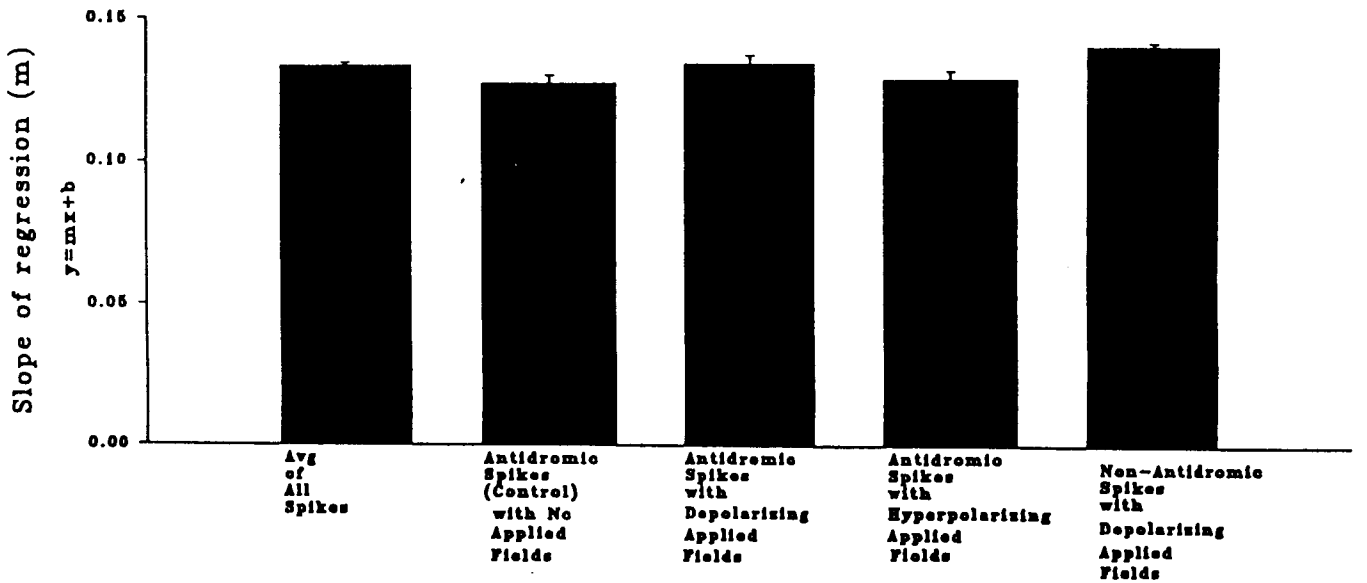

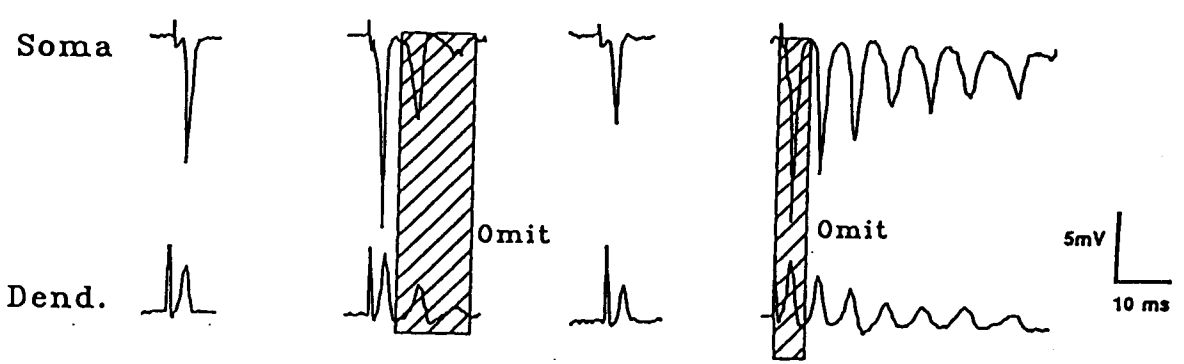

6.0 - DISCUSSION

In this study applied electric fields were used as a tool with which to induce epileptiform activity in the absence of synaptic interactions in order to further our knowledge of hippocampal seizures as they pertain to human temporal lobe epilepsy. Antidromic bursts during low $[Ca^{2+}]_o$ perfusion are common epileptiform events in CA1. These events are rare in the dentate gyrus. However, through manipulation of the conditions within the dentate gyrus, replication of these events may add to our understanding of this tissue's apparent seizure resistance in the epileptic brain.

Antidromic Dentate Bursts in the Presence of Fields

Under control conditions, with perfusion of standard $[Ca^{2+}]_o$ ACSF and no applied fields, even maximal antidromic stimulation failed to produce epileptiform activity in either CA1 or the dentate gyrus. When the same tissue was exposed to a low $[Ca^{2+}]_o$ medium, antidromic stimulation evoked a robust, multi-spike burst of CA1 from all slices studied. Under these same conditions, maximal antidromic stimulation of the hilus evoked only 11% of the slices to respond with bursts in the dentate gyrus. Furthermore, on these occasions the antidromic bursts of the dentate gyrus consisted of a limited number of population spikes and did

not develop into the prolonged, self-sustaining bursts observed in CA1. Additionally, spontaneous bursts were always recorded in the CA1, but were very rare in the dentate gyrus. In this study, the incidences of antidromic bursts in CA1 and the dentate gyrus, during perfusion with standard and low $[Ca^{2+}]_o$ mediums, were similar to those previously reported (Example: Haas, Jefferys 1982; Haas et al 1984; Konnerth et al 1984; Albrecht et al 1989; Schweitzer et al 1992) and support the general hypothesis that the dentate gyrus is relatively resistant to developing seizure activity (Heinemann et al 1992; Albrecht et al 1989).

Granule cells and pyramidal cells have many morphological and physiological differences. Cellular organization within the tissues, the dentate gyrus and CA1 respectively, also differs. It is likely that one or more of these differences accounts for the clearly greater propensity of CA1 for seizure activity relative to the dentate gyrus when slices are perfused with low $[Ca^{2+}]_o$ ACSF. This thesis attempts to determine whether the difference in propensity for low $[Ca^{2+}]_o$ bursts in these tissues is the result of a quantitative difference in the excitability of these regions. If so, then depolarizing the granule cell population may overcome the relatively low level of excitability within this tissue and result in robust epileptiform activity in low $[Ca^{2+}]_o$ ACSF.

In the present study, an antidromic stimulus was delivered during the application of an externally applied electric field which was used to transiently depolarize the granule cell population. Under these conditions 100% of the slices examined generated robust bursts of population spikes similar in appearance to those evoked without the application of fields in CA1. On average, the minimum amplitude of applied field necessary to observe this effect was 22.86 +\- 2.46 mV/mm.

During the application of higher magnitude fields the dentate gyrus developed bursts of epileptiform activity in the absence of antidromic stimulation. These applied field induced bursts occurred in 100% of slices examined, but only when the magnitude of applied field was increased beyond the threshold which contributed to antidromic bursts. The field intensity that resulted in these applied field induced bursts was 84.56 +\- 3.56 mV/mm. This field intensity was significantly greater than the minimum field required to induce antidromic bursting ($p<0.0001$). These responses may be analogous to the spontaneous bursts of CA1. The high intensity applied field may replicate the fields present during the DC shift of spontaneous low $[Ca^{2+}]_o$ bursts. Pilot data collected for future studies demonstrated that when applied fields capable of evoking field induced bursts (>84mV/mm) were applied for prolonged periods to the dentate gyrus, this tissue experienced robust seizure-like discharges not unlike the low $[Ca^{2+}]_o$ bursts of CA1. Figure

24 illustrates an example of the response to these prolonged field exposures.

Previous studies have shown that applied fields greater than 5mV/mm (Jefferys 1981; O'Reilly, Richardson 1992) can influence orthodromically evoked population spikes in the dentate gyrus. Intracellular studies (O'Reilly, Richardson 1992) have confirmed that the somatic transmembrane potential of granule cells is altered in a graded and linear fashion during the application of external fields along the dendro-somatic axis of the neuronal population. The sensitivity values reported within these other studies predict that a 20mV/mm gradient should depolarize the granule cell somata by 1 to 2 mV (O'Reilly, Richardson 1992). The fact that, in every slice studied, the dentate gyrus developed epileptiform activity in low $[Ca^{2+}]_o$ ACSF when exposed to depolarizing applied field, supports the conclusion that non-synaptic mechanisms can evoke epileptiform activity in this region by raising the level of excitability of the neuronal population. This is an important conclusion because from these findings it is evident that non-synaptic mechanisms contribute to epileptiform discharge in two very different regions of the CNS.

Figure 24 Prolonged Depolarizing Fields (High Intensity) & the Dentate Burst Response

An example of bursting in the dentate gyrus during prolonged depolarizing applied fields is shown. When the dentate gyrus was exposed to prolonged (seconds) depolarizing applied fields, of sufficient intensity to result in applied field induced bursts (+84mV/mm), the tissue participated in a robust epileptiform discharge (top). The discharge began with the onset of the field (top left) and its appearance suggests it may be analogous to the spontaneous low $[Ca^{2+}]_o$ bursts of CA1. Note the spikes intrinsic to the bursts (middle & bottom) and the transient depolarizing extracellular gradients that exist during these spikes. Also note that the expansion is not from the same burst shown in the top trace, but is an example of these events captured during a separate burst.

Prolonged Epileptiform Bursts in the Dentate Gyrus in low [Ca] Media During Applied Depolarizing Fields

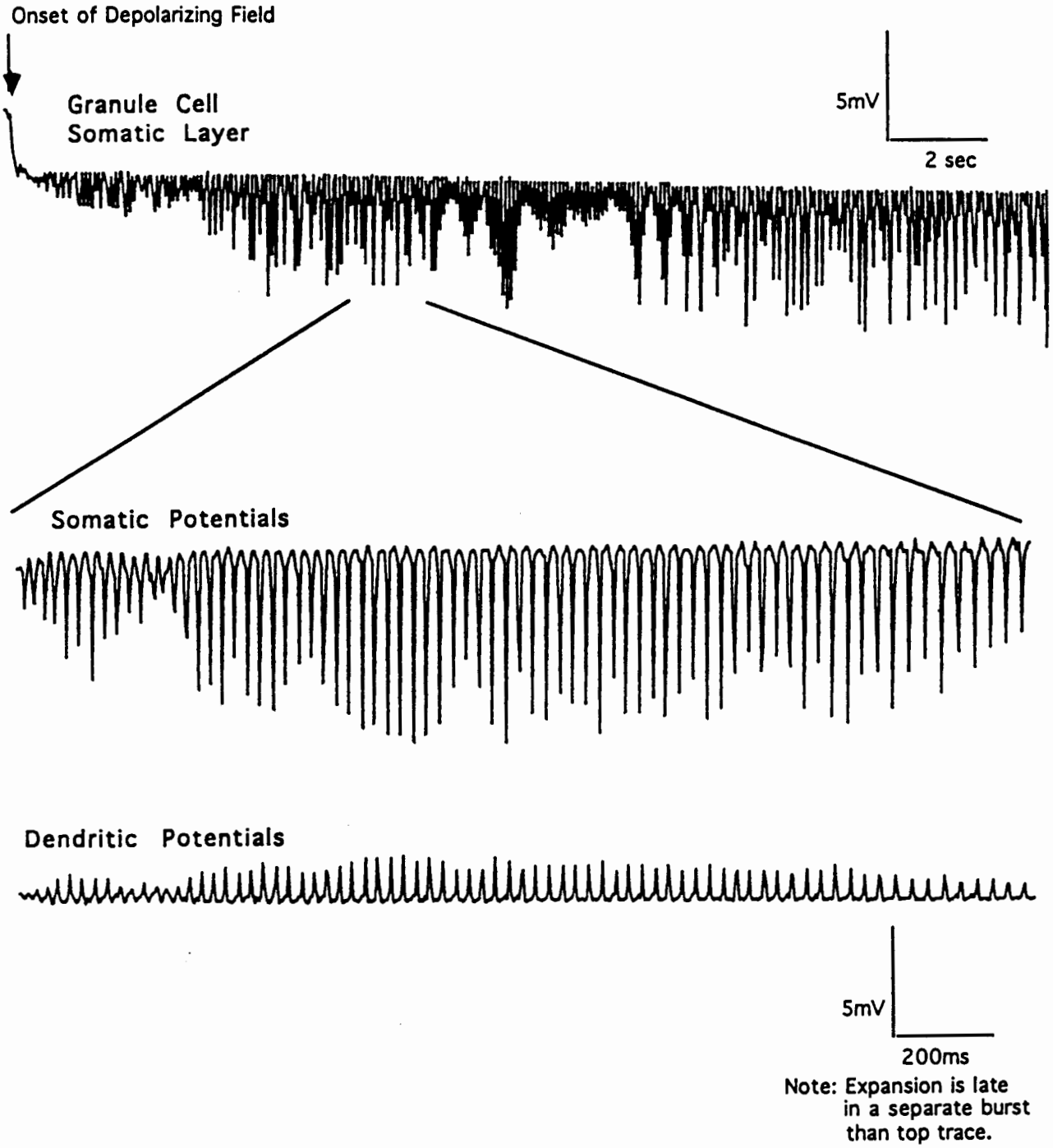

Note: Expansion is late in a separate burst than top trace.

Comparison of Bursts in CA1 and the Dentate Gyrus

An underlying hypothesis of this thesis is that antidromic bursts in CA1 and the dentate gyrus during low $[Ca^{2+}]_o$ perfusions are the same phenomena occurring in two distinct regions of the hippocampal formation. In fact, the obvious qualitative similarities between these events initially prompted the questions posed within this thesis. If these antidromic bursts were the same phenomena, then their basic characteristics (amplitude, interval, pattern) should be more similar than different.

During a quantitative examination, the extrasomatic antidromic bursts in both regions were found to possess several similar characteristics. In CA1 and the dentate gyrus, the absolute amplitudes of the antidromic spikes were not significantly different ($p>0.1$) indicating robust population responses in both regions. In both CA1 and dentate gyrus antidromic bursts: 1) the first spike of the burst had the largest amplitude, 2) the spikes within the burst decreased in amplitude as the burst progressed, and 3) the time interval between the spikes increased as the burst progressed. The rate of discharge within the bursts of the two regions differed, however these differences may reflect simple physiological differences between the participating neurons (pyramidal and granule) of the two regions.

Examination of this extracellular data revealed no marked differences in the antidromic bursts in the CA1

versus the dentate gyrus. As these events were recorded in both regions during perfusion with low $[Ca^{2+}]_o$ ACSF, it is clear that non-synaptic mechanisms underlie the discharges. Field effects are one possible non-synaptic mechanism that may underlie these events. During low $[Ca^{2+}]_o$ bursts in CA1, field effects have been implicated as the mechanism responsible for synchronizing population discharges during individual burst spikes (Taylor, Dudek 1984).

With the burst similarities quantified here, it is reasonable to speculate that both CA1 bursts and the dentate gyrus bursts occur as the result of common mechanisms and that these mechanisms are non-synaptic. While field effects are an example of a non-synaptic mechanism that contribute to population synchrony in CA1, and field effects were used in this study as a means of depolarizing the granule cell population, field effects are not necessarily the only non-synaptic mechanism contributing to synchrony in CA1 or the dentate gyrus. Future intracellular studies may help elucidate the specific mechanisms underlying prolonged synchronous discharge of neuronal populations.

The general characteristics of antidromic bursts in low $[Ca^{2+}]_o$ media reported here are consistent with those observed in the CA1 by other investigators (Taylor, Dudek,1984; Snow, Dudek,1984; Jefferys, Haas, 1982; Schweitzer et al 1992). While the features of the bursts were not quantified, examination of the published data revealed no obvious differences between the antidromic CA1

bursts reported here and those reported elsewhere. Very little data exists on antidromic bursts of the dentate gyrus during low $[Ca^{2+}]_o$ perfusions. Recently, antidromic bursts were observed in the dentate gyrus during perfusion with raised $[K^+]_o$ and lowered $[Ca^{2+}]_o$ (Schweitzer et al, 1992). These bursts were remarkably similar to those reported here. Despite this notable exception, the dentate gyrus continues to be considered resistant to participate in epileptiform discharge and is speculated to be a restrictive gate or brake to the spread of such activity from the enthorinal cortex into the hippocampus.

Applied Fields and the Antidromic Population Spike Amplitude

One unforeseen finding of this study was that applied fields influence the amplitude of the direct antidromic spike. The antidromic spikes in the dentate gyrus reported here under conditions of standard and low $[Ca^{2+}]_o$ perfusions were similar to those observed by other investigators (Haas, Jefferys 1984; Haas et al 1984; Konnerth et al 1984; Schweitzer et al 1992;).

With appropriate voltages, antidromic stimulation of hippocampal cell populations reliably results in somatic invasion and action potential discharge of individual cells within a population (Kandel et al 1961; Anderson, Lomo 1966; Anderson et al 1973; Sperti et al 1966; Leung 1979; Taylor, Dudek 1984). Irrespective of the perfusing solution,

antidromic stimulation of an associated bundle of axons, such as the mossy fibers in the dentate hilus, results in the synchronous discharge of the cells from which the axons originated. In the classic picture, only these cells, in which antidromic invasion of the soma produced an action potential, contribute to the population response. In this study, the classic view of an antidromic response is supported by the lack of change seen in the antidromic spike as the perfusing mediums were changed between standard and low $[Ca^{2+}]_o$, indicating little to no contamination of this response by synaptic interactions.

However, for CA3 neurons field effects have been suggested to result in an 8-38% enhancement of the antidromic spike amplitude "...by raising their excitability..." and this "...facilitates the excitation of non-invaded pyramidal cells by antidromic field potentials."(p. 361 Dalkara et al 1986; Taylor et al 1984). Similar contributions to the antidromic population spike were suggested for CA1 pyramidal cells (Yim et al 1986). This non-traditional description of the antidromic response finds further support in the relationship of applied field to spike amplitude reported here.

As stimulus intensity was kept constant throughout data collection, it was somewhat unexpected to reveal a positive linear relation (0.494 +\- 0.026, $p<0.0001$) between the antidromic spike amplitude and the magnitude of the field externally applied (refer to Figure 18). These data

indicate that an antidromic spike stimulated to 50-60% of the tissue's maximal response amplitude, can have its amplitude increased by 33.2 +\- 12.1 % with applied depolarizing fields or decreased by 52.9 +\- 7.9 % with applied hyperpolarizing fields. These observations dispute assumptions that the field potential of the population spike is representative of only those neurons whose axons were directly activated by the stimulus.

This finding compliments the findings of Snow and Dudek (1986) in which the amplitude of antidromic population responses from the dentate granule cell population was found to be sensitive to field effects (Snow, Dudek 1986).

In the absence of synaptic communication, extracellular field effects have been strongly implicated in contributing to recruitment during individual spikes of CA1 low $[Ca^{2+}]_o$ bursts (Taylor, Dudek 1984) and antidromic population spikes (Richardson et al 1984). Could field effects influence the amplitude of the antidromic population spike in the dentate gyrus during low $[Ca^{2+}]_o$ perfusion? For this influence to exist, extracellular fields of appropriate size and polarity must be generated during the dentate antidromic population spike.

There are two sources of extracellular fields that must be considered in the present study. Firstly, externally applied fields were used as an experimental tool with which the granule cell population was depolarized (see Methods section). These externally applied fields were purposeful

and, therefore, experimental manipulation ensured that they were appropriate in magnitude and polarity to either depolarize or hyperpolarize the population of granule cells under study.

A second physiological source of extracellular fields is generated during synchronous population discharge (see Figure 22) and was measured during these experiments. Transient extracellular voltage gradients, along the dendro-somatic axis of the granule cells, were generated by the active granule cell population during each population response. The relation of peak population spike amplitude to magnitude of voltage gradient generated was linear (0.133 +\- 0.001, $p<0.0001$). The relation describing these data may serve as a useful predictive tool during future studies.

According to this relation, even a moderate antidromic spike of 5 mV could generate a transient extracellular gradient of +30 mV/mm. This gradient is six times larger than the minimal field required to influence granule cell TMP (Jefferys 1981; O'Reilly Richardson 1992). Note that gradients generated by discharge of a granule cell population have the appropriate polarity to depolarize the somata of adjacent granule cells. Therefore, the gradients recorded in these experiments were of sufficient amplitude and correct polarity to have a depolarizing influence on the granule cell population under study. Based on these observations, field effects could recruit granule cells and

result in an increase in antidromic population spike amplitude.

A description of how the above mentioned recruitment could be achieved is presented here. Figure 25 assists in summarizing the synchronizing and recruiting factors involved in the antidromic population response. The fact that data was recorded during low $[Ca^{2+}]_o$ perfusions simplifies any synaptic influences that may confound this description. The cells contributing to a given antidromic response in this study can be segregated for the purpose of discussion into three populations: 1) directly antidromically stimulated (Figure 25 B), 2) recruited by tissue generated fields during antidromically stimulated spikes (Figure 25 C), and 3) depolarized below threshold by applied fields and transient tissue generated fields, therefore not discharging (Figure 25 A).

The findings presented here suggest that during antidromic stimulation, approximately 50% of the spike amplitude may result from directly activated axons causing somatic invasion and action potential discharge (Figure 25 B). The voltage gradients generated by the response of these cells are depolarizing to neighboring cells and may recruit a percentage of the neighboring inactive population to the response (Figure 25 C). The amplitude of the resultant extracellular population response would be contributed to by both populations (Figure 25 B and C).

Figure 25 **Recruitment During Antidromic Stimulation of Hippocampal Populations**

This figure is stylized illustration of the three populations involved in the production of the extracellular population spike during antidromic stimulation (low $[Ca^{2+}]_o$). There are 3 populations of granule cell shown (A,B,C). Population B (middle) receives direct antidromic activation of its axons from the stimulus. This stimulus results in antidromic invasion of the soma and cell discharge. Data from this study suggests that approximately 50% of the extracellular population spike amplitude may be attributed to the discharge of this population. This population (B) produces a transient depolarizing field that may influence the surrounding populations (C, A). A second population of cells (population C bottom), whose axons were not directly stimulated, is depolarized by the tissue generated transient of population B. In fact, Population C is depolarized to threshold and can contribute to the overall response recorded extracellularly. Population C was ephaptically recruited into the response by the extracellular fields generated by population B. A third population of cells (population A top), also did not have its axons directly stimulated, and was also depolarized by the transient depolarization produced by the active cells. However, this population (A) was not depolarized sufficiently to reach threshold and discharge. As a result it is not recruited and cannot add to the extracellular currents measured during the antidromic population response. The combined discharge of populations B and C contribute to the extracellular population response. This combined response differs from the classic definition of an antidromic response, but more precisely describes this population event.

Recruitment During Antidromic Stimulation

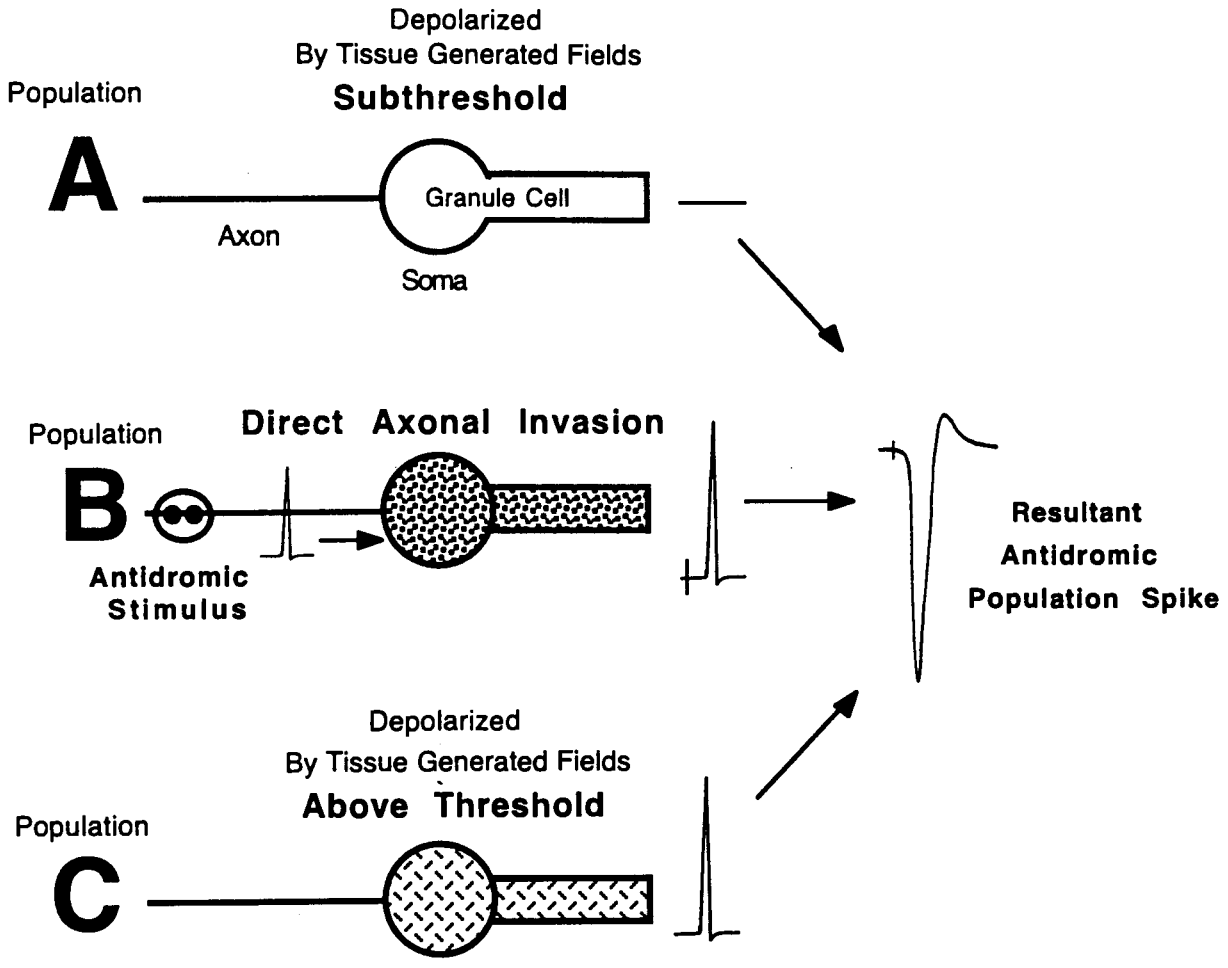

Applying a depolarizing field allows the third population of cells (Figure 26 A middle) to be drawn into the response. The axons of these cells were not directly activated by the stimulus (Figure 26 B), and their membrane potential had previously remained subthreshold during the transient depolarization generated by the population response (Figure 26 B,C left). However, a general field imposed depolarization brings this population of cells closer to its threshold. With this additional depolarization the tissue generated depolarization can be sufficient to bring this third population to threshold. The discharge of these cells contributes to the overall population response and is responsible for an increase in the antidromic spike amplitude during the applied depolarizing field.

Conversely, a hyperpolarizing applied field causes a general movement of all somatic potentials away from threshold. This is predicted to have a minimal effect on the directly stimulated population (Figure 26 B right). However, this additional hyperpolarization removes any opportunity for the third population (Figure 26 A right) to reach threshold, discharge, and contribute to the response. Perhaps, the greatest impact of applying hyperpolarizing fields results from a decrease in the excitability of the population (Figure 26 C right) that was recruited by the spike generated gradient. The hyperpolarization provided via the applied fields is similar in magnitude, but opposite

Figure 26 Recruitment During Antidromic Stimulation & Applied Fields

This figure illustrates the impact of applied fields on the antidromic response (see previous figure). The population contributions to the antidromic responses without applied fields are shown on the left. The activities of the 3 populations during applied depolarizing fields are shown in the middle and during hyperpolarizing fields are shown on the right.

Consider population B. This population receives direct antidromic stimulation of its axons and reliably discharges under no applied field, a depolarizing applied field or a hyperpolarizing applied field. This population reliably generates a depolarizing field during this discharge.

Now consider Population A. While this population was depolarized by the tissue generated fields, in the absence of a depolarizing applied field (left) this population remained subthreshold. However, with the application of an additional depolarizing field, this population is depolarized towards its threshold. The tissue generated transient is now sufficiently depolarizing to recruit this population to discharge. The result is an increase in the extracellular population response recorded. This increased response is contributed to by populations A,B, and C. Under hyperpolarizing applied fields population B is hyperpolarized away from its threshold. As a result the depolarizing tissue transient is insufficient to recruit it into the extracellular population response.

Finally, consider population C. Under depolarizing applied fields (middle) both the tissue generated transient and the applied field result in this population discharging. Under hyperpolarizing applied fields this population is moved away from its threshold. This hyperpolarization may be sufficient to cancel the depolarization gained from the tissue generated transient. The result is that this population (C) may fail to reach threshold. Under hyperpolarizing fields, it is conceivable that the only population contributing to the extracellular population response is population B, the directly activated population.

Recruitment During Antidromic Stimulation & Applied Fields

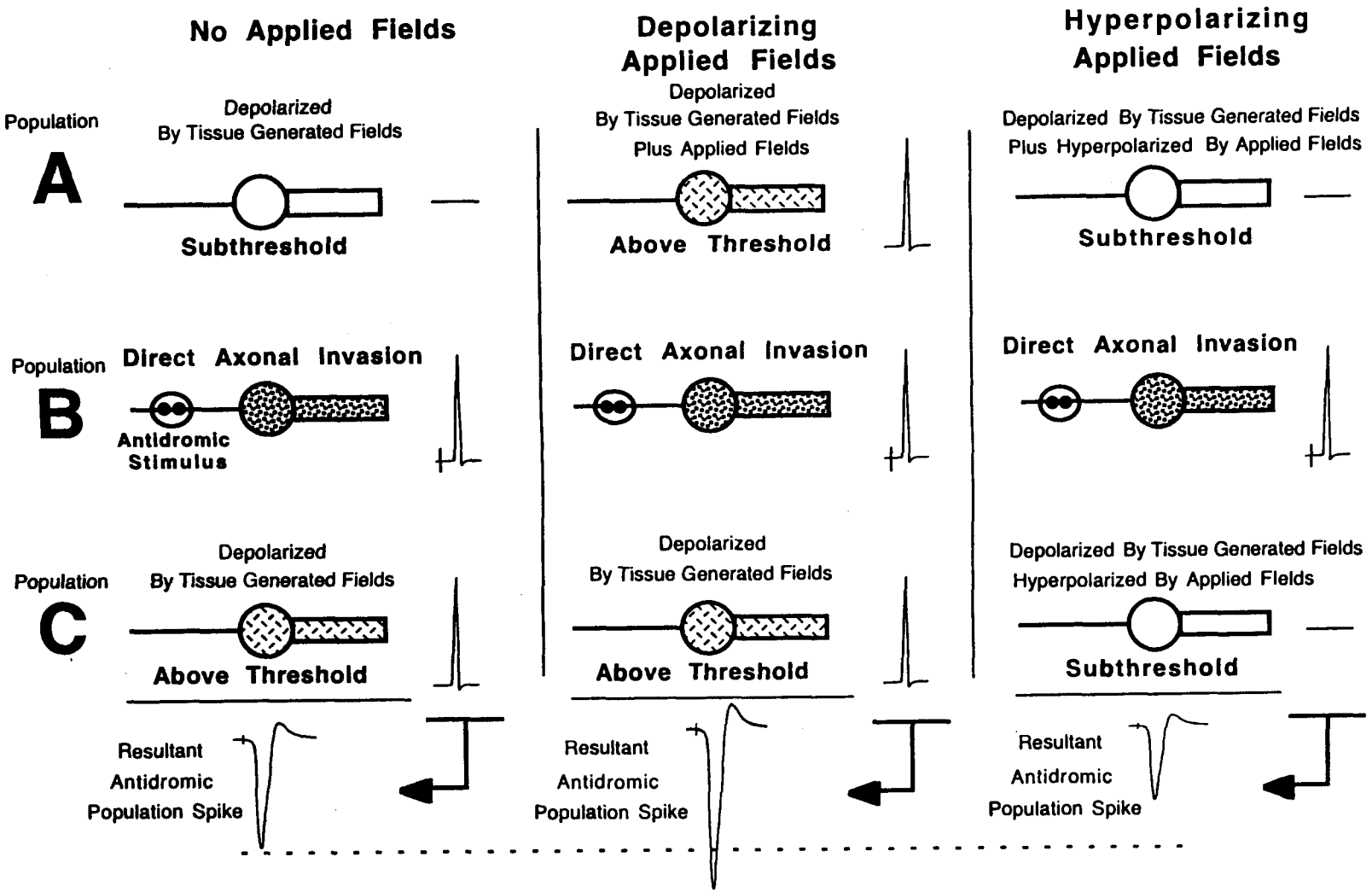

in polarity, to the tissue generated gradients. As a result, the applied hyperpolarization cancels the recruiting depolarization created by the active cells. Ultimately this effect is recorded as a decrease in the antidromic population spike amplitude.

At high intensity hyperpolarizing fields (-85mV/mm) the amplitude of the spike was diminished to 52.9 +\- 7.9 %. This percentage is striking, as it may indicate that only 50% of an antidromic population spike is the result of direct antidromic stimulation of axons leading to somatic invasion and synchronous action potential discharge. Data reported in this thesis suggest that the other 50% results from non-synaptic mechanisms transiently depolarizing a non-invaded population. These data support the hypothesis that field effects contribute to this process.

Antidromic Bursts Appear as a Graded Phenomena

Epilepsy is characterized as the abnormal, intense, synchronous, and self sustained discharge of large populations of cortical neurons (Jackson, 1870; Yaari, 1988). Many epileptic discharges are triggered or occur spontaneously as explosive, all-or-none events. In the hippocampus, examples of such events would include the elevated $[K^+]_o$ induced interictal in CA3 (Traynelis, Dingledine 1988), the observed disinhibition of pyramidal cells (Prince 1985; Hablitz 1983; Matsumoto, Ajmone Marsan,

1964), and the repeating, spontaneous low $[Ca^{2+}]_o$ induced bursts in CA1 (Anderson et al,1978; Taylor, Dudek,1982; Albrecht et al, 1989; Schweitzer et al, 1992).

In contrast, the epileptiform events reported in this thesis are graded in nature. With an increase in the applied field the number of spikes within the event and the amplitude of those spikes increases (see Figures 17 and 18). Conversely, the time between spikes of a given burst decrease (Figure 15,16, & 21). Recognition of the graded quality of antidromic bursts in the dentate gyrus is important because it allows research to focus on those mechanisms that could underlie such a graded response. These mechanisms could fundamentally differ from those that would result in an explosive, all-or-none seizure. The mechanisms underlying these events require investigation at the cellular level.

7.0 - CONCLUSIONS AND FUTURE RESEARCH

The hippocampal CA1 readily demonstrates robust epileptiform activity in human temporal lobe epilepsy as well as animal models of epilepsy. The dentate gyrus has only recently been reported to have the capacity to express the abnormal, robust, synchronous neuronal discharges that characterize epileptiform events. Multiple synchronous epileptiform discharges of the dentate gyrus have been demonstrated here in 11% of slices exposed to low $[Ca^{2+}]_o$ ACSF only, in 100% of slices exposed to low $[Ca^{2+}]_o$ ACSF and depolarizing applied fields, and elsewhere in 100% of slices exposed to low $[Ca^{2+}]_o$ and high $[K^+]_o$ ACSF (Schweitzer et al 1992). This study has added to the growing body of evidence that the dentate gyrus can actively participate in seizure activity.

At the most basic level, antidromic bursts in CA1 and the dentate gyrus during low $[Ca^{2+}]_o$ perfusion are considered epileptiform by virtue of the robust, multiple spikes that arise from a single antidromic stimulus. These bursts have been evoked, characterized, enhanced and diminished, all without directly investigating the most technically demanding, but fundamental question: **What is the mechanism responsible for the second and subsequent spikes of an epileptiform discharge?**

The presence of a second population response is profoundly significant in evoked seizure activity. A single

antidromic invasion typically brings the granule cells of the dentate gyrus to threshold once, in either standard or low $[Ca^{2+}]_o$ mediums. What results in the synchronous multiple discharge of this population of neurons? Has an intrinsic cellular alteration transformed the individual neurons into bursting or "epileptic" cells? Is the population more electrically coupled during certain experimental manipulations? Does a significant depolarizing after-potential exist only under specific circumstances? Can dendritic spikes reverberate back to the soma? These and other possible mechanisms can be postulated, but as yet, little or no data exists in direct support of these speculations. In order to reveal the mechanisms underlying low $[Ca^{2+}]_o$ bursts, or any evoked epileptiform discharge, future research should be aimed at resolving the mechanisms responsible for the 2nd spike.

It has been suggested that, "...the dentate gyrus serves as a gateway restricting the flow of epileptic activity into the hippocampus." (Stringer, Lothman, 1992. p309.) (also see Heinemann et al, 1990; Stringer, Lothman 1989; Stringer et al 1991). As the dentate gyrus rarely demonstrates epileptiform activity in experimental models and human epilepsies, its role as a gate or brake to the spread of seizure activity into the hippocampus continues to be investigated. From this perspective, identifying the conditions under which the dentate gyrus does exhibit epileptiform behavior could shed light on how this tissue

normally achieves this critical restrictive or braking function.

APPENDIX A

TERMINOLOGY & DEFINITIONS

As no convention in terminology exists between the leading research groups in either low $[Ca^{2+}]_o$ epileptogenesis or extracellular field studies, it is recommended that the reader familiarize themselves with the terms defined below as they will be used throughout this text. By adhering to these terms\phrases\definitions the author hopes to present the findings and interpretations with clarity.

A population spike or negative compound action potential, is an extracellular event that corresponds to an intracellular action potentials of a population of individual cells that have reached threshold.

The field EPSP (fEPSP or P1), is a compound extracellular event that corresponds to the intracellular EPSP's of individual cells within the stimulated population.

The active population refers to any locally dispersed neurons within a stimulated region that have received antidromic stimulation and have been depolarized sufficiently to reach their action potential threshold.

The passive population refers to any locally dispersed neurons that have: 1) received antidromic stimulation, but have not been depolarized sufficiently to reach their action potential threshold, or 2) not received antidromic invasion, but are local to the stimulated region.

Stimulus intensity refers to the voltage delivered locally to the tissue via the stimulating electrode. The pole separation of the stimulating electrode is 75 um. This electrode delivers a 0.1 ms square pulse in a voltage range of 1-15 Volts.

An antidromic burst is defined within this study as a complex response to a single antidromic stimulus that contains a minimum of 3 distinct and successive population spikes, where the 3rd spike has a minimal amplitude of 1mV. Using this definition, only robust transformations from single antidromic population spikes to antidromic bursts are recorded as epileptiform activity. Within an antidromic burst the first population spike to follow the stimulus will be referred to as the initial antidromic spike. This spike will be followed by the second spike of the burst and then the third, etc.

The size of an antidromic burst refers to the total number of spikes that follow a single antidromic stimulus. With the minimum number of 3, antidromic bursts with 3-5 spikes could be considered "small" with respect to bursts containing 8-12 spikes which could be considered "large". This subjective classification of burst size appears in the text only as is appropriate in a descriptive capacity and is not intended to infer any physiological assumptions.

A spontaneous burst or a low $[Ca^{2+}]_o$ burst is a population event commonly reported in the CA1 region. During this event a prolonged negative D.C. shift is

recorded in the extra-somatic layer (stratum pyramidale in CA1) and during this period synchronized population spikes are superimposed upon the D.C. shift. Low $[Ca^{2+}]_o$ bursts have recently been recorded in the dentate gyrus and a major premiss of the present study is that they are not considered exclusive to the CA1 region.

An extracellular field, applied field or extracellular voltage gradient refers to current flow in the extracellular space. A direct measure of this current flow is not readily available, and therefore spatially separated voltage measurements are used to best quantify this current. These field potentials are individual voltage measurements at isolated locations within the tissue. A minimum of two aligned field potential measurements and an accurate separation in microns of the recording positions is required to calculate fields from field potentials.

These fields differ dramatically from that which is described as a field effect. Field effects describe an active process by which extracellular current "impacts" the intracellular activities of individual cells or an entire population of cells.

An extracellular voltage gradient refers to a physiologically generated voltage difference along a spatially distended population of cells between the extra-somatic and extra-dendritic voltage recordings. These extracellular gradients are produced by synchronized population events such as stimulus evoked responses

(examples: orthodromically or antidromically stimulated population spikes) or spontaneous population discharges (examples: low $[Ca^{2+}]_o$ bursts in CA1, seizure discharge in temporal lobe epilepsy). Artificially applied fields similar in magnitude to the extracellular voltage gradients of these events will be experimentally imposed upon the tissue.

Both the physiologically generated gradients and the applied fields describe extracellular current flow, and could both correctly be referred to as extracellular fields. However, as the methods of the described experiments require using artificially applied extracellular fields it is useful to formally distinguish them within the text. The physiologically generated extracellular current will be referred to as "extracellular voltage gradients" and the applied extracellular current will be referred to as "applied fields". As a direct measure of the extracellular current is unavailable, both the gradients and the applied fields have an intensity\magnitude that is reported in mV/mm.

Applied field intensity refers to the voltage delivered between two spatially separated (1-2mm) current passing electrodes. Applied field intensities are reported in mV/mm and have polarity. See the Methods Section for details on the current passing apparatus.

Polarity of the applied fields refers to the direction in which current will flow between the electrodes of the

fixed extracellular field apparatus. The polarity is described with respect to the field's "predicted" impact on the dentate granule cells of the superior (upper) blade of the dentate gyrus. Depolarizing applied fields are those fields whose polarity would be predicted to produce a depolarizing or excitatory effect on these cells (positive field extra-somatic relative to a negative field extra-dendritic). A hyperpolarizing applied field is one in which the polarity would be predicted to produce a hyperpolarizing or inhibitory effect on the granule cells of the superior blade of the dentate gyrus (negative field extra-somatic relative to a positive field extra-dendritic).

The inter-spike interval describes the duration in milliseconds between the peak negative point of one population spike of a burst to the peak negative point of its successive population spike. Four inter-spike intervals are described in the present study; first, second, third and last. The first interval is, therefore, the time duration between the antidromically stimulated population spike (initial antidromic spike) and the second spike of the antidromic burst. The second interval is the time duration of the second population spike to the third population spike, while the third interval is measured between the third and fourth spikes. The last interval is the duration between population spike X and the last recorded population spike within a burst, whether that burst contains a total of 5 spikes or as many as 15 spikes.

A monotonic change is used to describe spike amplitude and inter-spike interval. This term refers to the relative change between two successive events in a series. It is used here to means that the second event was equal to, or larger than its preceding event. Using amplitude as an example, the first spike of the burst is always equal to or greater than the second spike, and the second spike is always equal to or greater than the third spike. This describes a monotonic decrease in amplitude.

Just as population spike amplitudes can vary between tissue preparations, so too can the absolute duration of a given inter-spike interval. To allow the comparison of the 2nd, 3rd, and last intervals between tissues to be made, successive interval values may be expressed as a percent of the first interval of the burst. In this manner, the first interval is always be expressed as 100%. Should the interval increase, its value would be expressed as a percentage >100%, and a decrease as a percentage <100%. When intervals are to be expressed as a percent of the first interval, this distinction will be explicitly stated in the text.

Spreading depression is a prolonged period of massive hyperpolarization. These episodes can last from 30 seconds up to several minutes with extra-somatic potentials recorded between 20 to 40 mV. Tissue demonstrating spreading depression is assessed to be "unhealthy" and the evoked

responses following a period of spreading depression are commonly inconsistent with those prior to the event.

APPENDIX B

HISTORY OF EPHAPTIC INTERACTIONS

"Ephapse" is derived from the Greek language meaning "to touch", distinct from the term "synapse" whose Greek derivation implies a strong linkage or union. The term "ephaptic interaction" refers to the direct influence of extracellular current on neuronal excitability (Haas, Jefferys, 1984). "Ephapse" was first used in 1942 by Arvanitaki, and later by Granit and Skoglund in 1945, to describe an artificial synapse. It was intended to imply a discrete electrical connection. In this case, the observed ephapse existed in the periphery and was accomplished by imposing contact between two axons. From this starting point the term "ephaptic" has evolved over the next few decades to describe the generalized influence of extracellular current on neuronal activity.

As early as the 1930's electrical interactions were postulated as an explanation for the connectivity and impulse speed observable within the nervous system. But these theories received limited physical support. With rare exception, these theories fell by the wayside with the discovery of the chemical synapse, accredited to Brock, Coombs and Eccles in 1952 for their ground breaking recording of intracellular potentials.

The earliest quantification of physiological field effects was reported by Libet and Gerard in 1940. In

studies of the frog olfactory bulb, they observed that oscillatory potentials would continue to propagate from one section of the tissue to another despite having physically cut the connecting neural pathways. The oscillations were obliterated only when the two tissue sections were separated in a physical manner. With these limited observations and the later discovery of the chemical synapse, the concept that extracellular current could have a depolarizing or hyperpolarizing effect on active neurons would remain virtually dormant for the next twenty years.

Further insight would not come until the 1960's when Furshpan and Furukawa discovered that an antidromic impulse in the Mauthner cell (M-cell) resulted in extracellular potentials of between -20 and -50 mV. Connecting this information with observations of suspiciously low intracellular action potential amplitudes, these researchers corrected for their extracellular reference and determined the true transmembrane potential (TMP) of the M-cell. In this manner they had confirmed that the extracellular field influenced the TMP under physiological conditions.

The extracellular space within the axon cap of the M-cell was found to have a resistance of up to 5 times that of the extracellular space in surrounding tissues. This observation of a high extracellular resistance would be repeated in future studies on a variety of tissues and is now accepted as an important factor contributing to the generation of strong field effects (Korn, Faber,1980). Over

the ensuing years, studies on the large and easily accessible M-cell flourished in mainstream neurophysiology making currents in the extracellular axon cap more difficult to pass over as insignificant observations.

In the 1980's medical researchers began to entertain the possibility that abnormal sensations associated with human neuromas were the direct result of field effects (see Korn & Faber (1989) review). Anatomical and physiological investigations of the neuromas revealed a dense, high resistance extracellular space, with unconnected and un-insulated neurons firing spontaneously, leading to discomfort in the patients. These conditions concur with the physical tissue properties observed in other regions where strong extracellular field effects can be demonstrated.

However, modern researchers use the term "ephaptics"* sparingly and preference is given to describing this phenomena as "extracellular field effects". While the terminology in this area continues to vacillate, for the purposes of this document, "ephaptic interactions", "ephaptics", "extracellular field effects", and "field effects" will be used interchangeably.

*Note: It is recommended that the reader familiarize themselves with the terms listed in Appendix A, as the various research groups have yet to standardize the terms used in extracellular current or low $[Ca^{2+}]_o$ research. The

author will abide by the terminology outlined in the Appendix A.

APPENDIX C

GLIAL-NEURONAL INTERACTIONS & SPATIAL BUFFERING

Glial buffering of K^+ and recent calcium currents observed in the glia (Smith, 1991.lecture) make these cells a very possible contributor to epileptiform activity. The membrane potentials of glial cells are very sensitive to $[K^+]_o$ (Kuffler et al, 1966) and during neuronal activity accumulation of K^+ in the intercellular clefts causes depolarization of the membranes of nearby glial cells (Orkand, 1966; Bortoff, 1964).

Much attention has been paid to Gardner-Medwin's 1983 work describing "spatial buffering" of K^+ by glial cells (Gardner-Medwin, Nicholson, 1983). However, this concept, was originally conveyed in an air of controversy, by the Kuffler group back in 1966:

> "The current flow which accompanies glial depolarization when circumscribed groups of cells are activated, suggests that such currents might distribute the accumulated K^+ in the clefts, without significantly altering the internal K^+ of glial cells. If a glial cell becomes depolarized by K^+ which has accumulated in the clefts, the resulting current carries K^+ inward, in the high $[K^+]_o$ regions, and out again, through electrically coupled glial cells in low $[K^+]_o$ regions. Under such conditions glial cells might serve as "spatial buffers" in the distribution of K^+ in the cleft system."(Orkand, Kuffler, Nicholls 1966 pp 804-805)

The relatively limited advances over the ensuing two decades underscores the lack of emphasis given to glial cells and their possible contribution to neural function.

Listed here are several summarized observations which were recorded during this interim and which support a theory of $[K^+]_o$ buffering by glia. 1) The honey bee drone was used to identify glial cells as a pathway for current mediated K^+ flux (Gardner-Medwin et al.1981). 2) The possibility that the buffering of $[K^+]_o$ in neural tissues involved neuroglia was considered (Varon, Somjen, 1979; Treherne, 1981). 3) Scar tissue containing glial cells, but devoid of neurones, was shown to demonstrate K^+ transport (Dietzel et al.1980) quantitatively similar to that reported by Gardner-Medwin & Nicholson 1983 (see below). 4) In reviews by Somjen (1973, 1981) evidence suggests that glial may be responsible for the extracellular currents and negative potentials in regions of high $[K^+]_o$ in the CNS. And finally, 5) evidence obtained from studies of the cerebellum suggest that the glial cell syncytium may contribute to K^+ buffering (Palay, Chan-Palay, 1974). Models of the cerebellar cortex indicate that the dendrites of Purkinje cells carry the majority of current that flows perpendicular to the surface of this structure. These neuronal dendrites terminate well below the surface (Palay, Chan-Palay, 1974) and the effect of this arrangement and the implications of glial cell mediation is captured in the following statement:

> "...the effects on $[K^+]_o$ of current flow through these cells {glial cells} should be in opposite directions at the two ends of these finite terminated cables. The lack of such a reversal suggests longer cables are involved, or a syncytium of electrically coupled cells such as is

postulated for glial cells in mammalian brain (Kuffler, Nicholls, 1976)."

The work of Gardner-Medwin group (Gardner-Medwin, 1983a; Gardner-Medwin, Nicholson, 1983b; Gardner-Medwin, 1983c) represents a significant summation of these advances and is consistent with passive glial cell involvement in spatial buffering described previously. Gardner-Medwin (1983) draw two important conclusions relevant to this thesis:

> 1) "..there is a selective mechanism for passive K^+ transport in an electrochemical gradient within brain tissue that results in higher K^+ fluxes than could be supported by ionic mobility in the extracellular fluid."(Gardner-Medwin, Nicholson 1983 p375)
>
> 2) "...approximately 5 times as much K^+ flux passes through cells (probably largely glial cells) as through extracellular space, with fluxes driven by either extracellular voltage or concentration gradients."(Gardner-Medwin 1983 p 353)

The characteristics of K^+ buffering by glial cells suggest that the following sequence of events may occur: 1) $[K^+]_o$ increases during neural activity, 2) an unequal distribution of $[K^+]_o$ causes K^+ currents to flow through the glial syncitium, 3) if the extracellular component of this current is large enough it will be associated with a measurable extracellular voltage gradient and could generate significant field effects. This suggests that the glial cell's response to K^+ can create an environment in which neuronal excitability is affected. Extracellular currents associated with the local build up of K^+ in the pyramidal

layer during low $[Ca^{2+}]_o$ bursts may be responsible for the DC shift in the extracellular potential and for a field-induced depolarization of the neuronal population. Thus glial buffering of K^+ may actually contribute to initiation and maintenance of low $[Ca^{2+}]_o$ bursts, particularly in slow onset bursts.

APPENDIX D

SEIZURE INITIATION & TERMINATION

INITIATION

The process of seizure initiation is a poorly understood area with many possible mechanisms. Some mechanisms that have received attention include: 1) synaptic excitation from distal and sensory inputs as seen in optically induced epilepsy, 2) spontaneous interictal bursts (extracellular reflections of paroxysmal depolarization shifts (PDS's)) which have been observed to precede both seizures and spreading depression, and 3) gap junction modulations possibly in response to ACSF pH changes.

At one point the synchronization and spread of epileptiform bursts was mainly attributed to synaptic mechanisms (Gjerstad, 1981). Several experimental models report a loss of inhibitory neural processes accompanying the onset of the seizure activity (Ayala, 1970; Ben-Ari et al.1979; Kandel, 1961; Matsumoto, 1964). This suggested that synaptic inhibition may modulate epileptic phenomena and that its loss could lead to seizure activity. While synaptic transmission may contribute to seizures, the discovery that epileptiform events persist in the absence on synaptic transmission in slices, as seen in low $[Ca^{2+}]_o$ bursts (Taylor, Dudek, 1982; Jefferys, Haas, 1982), emphasizes the importance of also considering non-synaptic mechanisms for epileptiform phenomena *in vivo*.

Additionally, it could be argued that, if synaptic mechanisms were as dominant in synchronizing the population as has been suggested, then the cross excitation (recurrent excitation) of CA3 by its Schaffer Collaterals should predispose this population to synchronized discharges. However, while CA3 pyramidale cells can fire trains of action potentials, the CA3 is not as strongly epileptic as CA1.

The view that chemical synapses represent the main initiating mechanism of epileptogenesis was further challenged by the study of paroxysmal depolarization shifts (PDS's). PDS's are epileptiform events which are the intracellular correlate to the extracellular interictal spike (Ayala et al.1973; Hablitz, 1983; Snow, Dudek, 1984). It is hypothesized that most convulsant-induced bursting is generated by the PDS or excitatory synaptic currents (Johnston, 1984; Hablitz, 1984) that are Ca^{2+} dependent. Spontaneous, repetitive PDS's can be induced by exposing tissue to convulsant drugs such as the GABA blocker picrotoxin (Hablitz, 1983). PDS's have been observed in CA1, CA2 and CA3, but not in the dentate gyrus (Snow, Dudek, 1984). Decreasing $[Ca^{2+}]_o$ abolishes PDS's and the interictal burst (Yaari, 1988). Once thought to be precursors to seizure activity (Ajmone Marsan, 1969), after these experiments an epileptic model existed in the absence of the PDS.

TERMINATION OF BURSTS

Two possible mechanisms for the termination of bursts have received considerable attention; Ca^{2+} activated K^+ conductance, and the electrogenic pump (Haas, Jefferys, 1984).

It is argued that if hyperpolarization caused by Ca^{2+} activated K^+ conductance was the mechanism behind the termination of low $[Ca^{2+}]_o$ bursts, then the addition of EGTA (strong Ca^{2+} buffer) to the perfusing solution should prolong the burst. However, when such studies were conducted (Haas, Jefferys, 1984) burst durations were not prolonged. Although intracellular stores of Ca2+ have not been excluded as a possible source of Ca2+ in low [Ca2+]o solutions, EGTA would sequester any free Ca^{2+} liberated to the extracellular space. Additionally, pharmaceutical treatments (dopamine, histamine, noradrenalin) known to modify the Ca2+ activated K+ conductances (Bernardo, 1982; Madison, 1982; Haas, 1983; Haas, Jefferys, 1984) affected the frequency of bursts, but not the duration.

The electrogenic pump hypothesis suggests that the activity of the pump is increased by the elevation of $[K^+]_o$ and the depression of $[Na^+]_o$ during a burst (Baker et al.1969). However, if the electrogenic pump were responsible for termination of the burst it would be expected that agents which block the pump, such as ouabain, would prolong the burst duration. When this was tested by Haas (1984) ouabain did not prolong the burst. Additionally,

the spatial buffering of K^+ originally described by Orkand et al (1966), and expanded by Gardner-Medwin et al (1983a,b), would tend to limit the local build-up of $[K^+]_o$.

Given less attention is the finding that inducing a hypoxic state greatly prolonged the duration of the bursts (Haas, Jefferys, 1984). This finding is interesting in light of observations made by Church and Baimbridge (1991) regarding the modulation of gap junctions by pH. Their findings suggest that the alkalosis of a hypoxic state could act to interconnect pyramidal cells by gap junction and allow for the maintenance of bursting. Alternatively, depolarization of the membrane potential associated with hypoxia may be responsible for the prolongation of bursts. Further work is required to differentiate between these possibilities.

APPENDIX E

APPLIED FIELD APPARATUS

In developing the applied field technique used in this thesis many considerations were made as to the possible inherent technical flaws. Initially, there was some concern that this technique might produce alterations in cellular and population responses by virtue of acting as a direct stimulus to the tissue, rather than providing a low intensity sustained extracellular fields. Of particular concern was the nature of the onset and offset of the current pulse. This concern was first raised during pilot studies as extracellular population spikes and intracellular action potentials could be observed to occur at this onset. Was there an error in the technique that resulted in a short duration, high amplitude voltage spike at this onset that could acted as a direct stimulus? To address this issue two approaches were taken.

The first line of evidence that suggested that this was not the case, came when an appropriate capacitor was added in-line to the isolated stimulus delivered to the current passing electrodes. With a capacitor in place, a sharp high amplitude voltage deflection at the transition points of the pulse could not exist, instead the field came on with a time constant of approximately 5 ms. Despite this fundamental change in the onset of the pulse, its effects on the tissue remained constant to those observed before the capacitor was added.

The second observation that supported the successful use of the current passing electrodes in field generation came as a result of intracellular recordings in granule cells. It was reasoned that if the onset of the current pulse was acting as a stimulus to the cells, then shortening the duration of the current pulse to 100 us should result in similar responses. This was not observed, in fact, both intracellular and extracellular recordings reflected no response to this altered current pulse duration.

Confirming the nature of the applied field allowed this technique to be used in studies of the transmembrane potential (TMP). By concurrently recording intracellularly and extracellularly (local) it was possible to directly measure the influence the applied fields were having on the TMP, by subtracting the extracellular voltage recording from the intracellular voltage recording (O'Reilly, Richardson, 1992a,b). This difference represents the change in TMP during the applied field. See Figure 6.

8.0 - REFERENCES

1. Ajmone Marsan C (1969) Acute effects of topical agents. In: Jasper HH; Ward,A.A.; Pope A. (ed) Basic mechanisms of the epilepsies. Little Brown, Boston, pp 229-328

2. Albrecht, D; Rausche, G; Heinemann, U; (1989) Reflections of low Ca^{2+} epileptiform activity from CA1 into dentate gyrus in the rat hippocampal slice. Brain Res. 480:393-396

3. Alverez-Leefmans FJ; de Santis,A.; Miledi,R. (1979) Effect of some divalent cations on synaptic transmission in frog spinal neurones. J Physiol (Lond) 294: 387-406

4. Amaral DG, Ishizuka N, Claiborne B (1990) Neurons, numbers and the hippocampal network. In: Storm-Mathisen J, Zimmer J, Ottersen OP (eds) Progress in brain research vol 83. Elsevier Science Publishing, New York, pp 1-9

5. Anderson P; Bland BH; Dudar JD (1973) Organization of the hippocampal output. Exp Brain res 17:152-168

6. Anderson P, Bliss TVP, Skrede KK (1971) Unit analysis of hippocampal population spikes. Exp Brain Res 13: 208-221

7. Anderson P; Lomo T (1966) Mode of activation of hippocampal pyramidal cells by excitatory synapses on dendrites. Exp Brain Res. 2:247-260

8. Anderson P, Gjerstad L, Langmoen IA (1978) A cortical epilepsy model in vitro. In: Chalazonitis N, Voisson M (eds) Abnormal Neuronal Discharges. Raven, New York, pp 29-36

9. Andrew RD (1991) Seizure and acute osmotic change: clinical and neurophysiological aspects. J Neurol Sci 101: 7-18

10. Andrew RD, Fagan M, Ballyk BA, Rosen AS (1989) Seizure susceptibility and the osmotic state. Brain Res 498: 175-180

11. Andrew RD; Taylor,C.P.; Snow,R.W.; Dudek,F.E. (1982) Coupling in rat hippocampal slices: dye transfer between CA1 pyramidal cells. Brain Res Bull 8: 211-222

12. Aram JA; Lodge,D. (1987) Epileptiform activity induced by alkalosis in rat neocortical slices: block by antagonists of NMDA. Neurosci Lett 83: 345-350

13. Arvanitaki A (1942) Effects evoked in an axon by the activity of a contiguous one. J Neurophysiol 5: 89-108

14. Ayala G; Matsumoto,H.; Gumnit,R. (1970) Excitability changes and inhibitory mechanisms in neocortical neurons during seizures. J Neurophysiol 33: 73-85

15. Ayala GF, Dichter M, Gumnit RJ, Matsumoto H, Spencer WA (1973) Genesis of epileptic interictal spikes. New knowledge of cortical feedback systems suggests a neurophysiological explanation of brief paroxysms. Brain Res 52: 1-17

16. Babb, TL; Brown, WJ; (1987) Pathological findings in epilepsy. In: Surgical treatment of the epilepsies. Engel, J. (Jr.) (ed.), New York, Raven, pp.511-540.

17. Babb, TL; Kupfer, WR; Pretorius, J; Davenport, C; Lieb, JP; Crandall, PH (1984) Temporal lobe volumetric cell densities in temporal lobe epilepsy. Espilspsia, 25:729-740

18. Baimbridge KG; Peet,M.J.; McLennan,H.; Church,J. (1991) Bursting response to current-evoked depolarization in rat CA1 pyramidal neurons is correlated with Lucifer yellow dye coupling but not with the presence of calbindin-D28k. Synapse 7: 269-277

19. Baker PF, Blaustein MP, Keynes RD, Manil J, Shaw TI, Steinhardt RA (1969) The ouabain-sensitive fluxes of sodium and potassium in squid giant axons. J Physiol (Lond) 200: 459-496

20. Baldissera, F., Gustafsson, B., (1974) Firing behavior of a neurone model based on the afterhyperpolarization conductance time course.First interval firing. Acta Physiologica Scand. 91:528-544.

21. Balestrino M; Somjen,G.G. (1988) Concentration of carbon dioxide, interstitial pH and synaptic transmission in hippocampal formation of the rat. J Physiol (Lond) 396: 247-266

21. Barnes CA;Rao, G; McNaughton,B.L. (1987) Increased electrotonic coupling in aged rat hippocampus: A possible mechanisms for cellular excitability changes. J Comp Neurol 259: 549-558

22. Ben-Ari Y, Krnjevic K, Reinhardt W (1979) Hippocampal seizures and failure of inhibition. can j physiol pharmacol 57: 1462-1466

23. Bernardo LS; Prince,D.A. (1982) Dopamine modulates a Ca-activated potassium conductance in mammalian hippocampal pyramidal cells. Nature 297: 76-79

24. Bindman LJ; Lippold,O.C.J.; Redfearn,J.W.T. (1964) The action of brief polarizing currents on the cerebral cortex of the rat (1) during current flow and (2) in the production of long-lasting after-effects. J Physiol (Lond) 172: 369-382

25. Bortoff A (1964) Localization of slow potential responses in the Necturus retina. Vision Res 4: 627-635

26. Brismar T; Frankenhaeuser B (1972)Acta Physio Scand 85:237-241

27. Brock LG, Coombs JS, Eccles JC (1952) The recording of potentials from motoneurones with an intracellular electrode. J Physiol (Lond) 117: 431-460

28. Bures J (1957) Ontogenetic development of steady potential differences in cerebral cortex in animals. Electroen Neurophysiol 9: 121-130

29. Bures J, Buresova O, Krivanek J (1974) The Mechanism and Applications of Leaos Spreading Depression of Electroencephalographic Activity. Academia, Prague,

30. Bures J; Buresova,O.; Krivanek,J. (1984) The meaning and significance of Leao's spreading depression. An Acad brasil Cienc 56(4): 385-400

31. Calvin, W., (1972) Synaptic Potential summations and repetitive firing mechanisms: Input-output theory for the recruitment of neurons into epileptic bursting firing patterns. Brain Res 39:71-94

32. Chan CY; Nicholson C (1986) Modulation by applied electric fields of purkinje and stellate cell activity in the isolated turtle cerebellum. J. Physiol. 371:89-114

33. Chater SN; Simpson,K.H. (1988) Effect of passive hyperventilation on seizure duration in patients undergoing electroconvulsive therapy. Br J Anaesth 60: 70-73

34. Church J; Baimbridge,K.G. (1991) Exposure to high-pH medium increases the incidence and extent of dye coupling between rat hippocampal CA1 pyramidal neurons in vitro. J Neurosci 11: 3289-3295

35. Church J; McLennan,H. (1989) Electrophysiological properties of rat CA1 pyramidal neurons in vitro modified by changes in extracellular bicarbonate. J Physiol (Lond) 415: 85-108

36. Connors BW (1984) Initiation of synchronized neuronal bursting in neocortex. Nature 310: 685-687

37. Creutzfeldt OD, Fromm H, Kapp H (1962) Influence of transcortical dc currents on cortical neuronal activity. Exp Neurol 5: 436-452

38. Dalkara T; Krnjevic K; Ropert N; Yim CY (1986) Chemical modulation of ephaptic activation of CA3 hippocampal pyraimds. Neuroscience (17)2;361-370

39. Dietzel I, Heinemann U, Hofmeier G, Lux HD (1980) Transient changes in the size of the extracellular space in the sensorimotor cortex of cats in relation to stimulus-induced changes in potassium concentration. Exp Brain Res 40: 432-439

40. Dingledine R (1984) Brain Slices. Plenum Press, New York, NY

41. Dingledine R, Dodd J, Kelly JS (1980) The in vitro brain slice as a useful neurophysiological preparation for intracellular recording. J Neurosci Methods 2: 323-362

42. Dudek FE; Traub,R.D. (1988) Local synaptic and electrical interactions in the hippocampus: experimental data and computer simulations. In: Byrne JH; Berry,W.O. (ed) Neural models of plasticity. Academic, Orlando,FL, pp 378-402

43. Dudel J (1983) Graded or all-or-none release of transmitter quanta by local depolarization of nerve terminals on crayfish muscle? Pflugers Arch 398: 155-164

44. Franck, JE; Roberts, DL; (1990) Combined kainate and ischemia produces "mesial temporal sclerosis". Neurosci. Let. 118:159-163.

45. Frankenhaeuser B; Hodgkin,A.L. (1957) The action of calcium on the electrical properties of squid axons. J Physiol 137: 218-244

46. Fricke RA; Prince,D.A. (1984) Electrophysiology of dentate gyrus granule cells. J Neurophysiol 51: 195-209

47. Fujii T, Baumgartl H, Lubbers DW (1982) Limiting section thickness of guinea pig olfactory cortical slices studied from tissue po2 values and electrical activities. Pflugers Arch 393: 83-87

48. Furshpan EJ, Furukawa T (1962) Intracellular and Extracellular Responses of the Several Regions of the Mauthner Cell of the Goldfish. J Neurophysiol 25: 732-771

49. Furukawa T, Furshpan EJ (1963) Two inhibitory mechanisms in the mauthner neurons of goldfish. J Neurophysiol 26: 140-176

50. Gardner-Medwin AR (1976) The initiation of action potentials in hippocampal granule cells. Exp Brain Res Suppl 1 1: 218-222

51. Gardner-Medwin AR (1983a) A study of the mechanisms by which potassium moves through brain tissue in the rat. J Physiol 335:353-374

52. Gardner-Medwin AR (1983b) Analysis of potassium dynamics in mammalian brain tissue. J Physiol (Lond) 335: 393-426

53. Gardner-Medwin AR, Coles JA, Tsacopoulos M (1981) Clearance of extracellular potassium: evidence for spatial buffering by glial cells in the retina of the drone. Brain Res 209: 452-457

54. Gardner-Medwin AR, Nicholson C (1983) Changes of extracellular potassium activity induced by electric current through brain tissue in the rat. J Physiol (Lond) 335: 375-392

55. Garthwaite J, Woodhams PL, Collins MJ, Balazs R (1979) On the preparation of brain slices: morphology and cyclic nucleotides. Brain Res 173: 373-377

56. Gjerstad L; Andersen,P.; Langmoen,I.A.; Lundervold,A.; Hablitz,J. (1981) Synaptic triggering of epileptiform discharges in CA1 pyramidal cells in vitro. Acta Physiol Scand 113: 245-252

56. Gloor P, Vera CL, Sperti L (1961a) Investigations on the mechanism of epileptic discharge in the hippocampus. Epilepsia 2 (series 4): 42-63

57. Gloor P, Vera CL, Sperti L, Ray SN (1961b) Investigations on the mechanism of epileptic discharge in the hippocampus. Epilepsia 2: 42-63

58. Gloor P; Sperti,L.; Vera,C. (1964) A consideration of feedback mechanisms in the genesis and maintenance of hippocampal seizure activity. Epilepsia 5: 213-238

59. Granit R, Skoglund CR (1945) Facilitation, inhibition and depression at the "artificial synapse" formed by the cut end of a mammalian nerve. J Physiol (Lond) 103: 435-448

60. Green JD, Maxwell DS (1961) Hippocampal electrical activity I morphological aspects. Electroencephalogr Clin Neurophysiol 13:837-846

61. Green JD (1964) The hippocampus. Physiol Rev. 44:561-608

62. Green JD, Petsche H (1961) Hippocampal electrical activity II virtual generators. Electroenceph Clin Neurophysiol 13: 847-853

63. Haas HE; Konnerth,A. (1983) Histamine and noradrenaline decrease calcium-activated potassium conductance in hippocampal pyramidal cells. Nature 302:432-434

64. Haas HL, Jefferys JG (1984) Low-calcium field burst discharges of CA1 pyramidal neurones in rat hippocampal slices. J Physiol (Lond) 354: 185-201

65. Haas HL; Jefferys JG; Slater NT; Carpenter DO (1984) Modulation of low calcium induced field bursts in the hippocampus by monoamines and cholinomimetics. Pflugers Arch 400:28-33

66. Hablitz JJ (1983) Mechanisms underlying picrotoxin-induced epileptiform activity in the hippocampus. Soc Neurosci 9: 397

67. Hablitz JJ (1984) Picrotoxin-induced epileptiform activity in hippocampus: role of endogenous versus synaptic factors. J Neurophysiol 51: 1011-1027

68. Heinemann, U; Beck, H; Dreier, JP; Ficker, E; Stabell, J; Zhang, CL (1992) The dentate gyrus as a regulated gate for the propagation of epileptiform activity. In The Dentate Gyrus & Its Role in Seizures. Epilepsy Res. Supp. Ed: Ribak CE, Gall CM, Mody I. Chap. 20 pp.273-280

69. Heinemann U; Franceschetti S; Hamon B; Konnerth A; Yaari Y (1985) Effects of anitconvulsants on sponatneous epileptiform activity which develops in the absence of chemical synaptic transmission in hippocampal slices. Br. Res. 325:349-352.

70. Heinemann U; Lux HD; Gutnick MJ (1977) Extracellular free calcium and potassium during paroxysmal activity in the cerebral cortex of the cat. Exp Brain Res 27: 237-243

71. Heinemann U; Konnerth, A; Louvel, J; Lux, HD; Pumain, R (1982) Changes in extracellular free calcium in normal and epileptic sensorimotor cortex of cats. In: Klee MR; Lux,H.D.; Speckmann,E.J. (ed) Physiology and pharmacology of epileptogenic phenomena. Raven Press, New York, pp 29-35

72. Heinemann U; Lux, HD (1977) Ceiling of stimulus induced rises in extracellular potassium concentration in the cerebral cortex of cat. Brain Res 120: 231-249

73. Heinemann U; Neuhaus,S.; Dietzel,I. (1983) Aspects of potassium regulation in normal and gliotic brain tissue. In: Baldey-Moulinier M; Ingvar,H.D.; Meldrum,B.S. (ed) Cerebral blood flow, metabolism and epilepsy. John Libbey, London, pp 271-278

74. Houser, CR (1992) Morphological changes in the dentate gyrus in human temporal lobe epilepsy. In: Mody, I.; Gall, C.M.; Ribak, C.E. (ed.) The dentate gyrus and its role in seizures. , Elsevier Science Pub Epilepsy Res. Supp 7, Chap.16 pp223-234

75. Jackson JH (1870) A study of convulsions. Trans St Andrews Med Grad Assn 3: 1-45

76. Jefferys JGR (1981) Influence of electric fields on the excitability of granule cells in guinea-pig hippocampal slices. J Physiol (Lond) 319: 143-152

77. Jefferys JGR, Haas HL (1982) Synchronized bursting of ca1 hippocampal pyramidal cells in the absence of synaptic transmission. Nature 300: 448-450

78. Johnston D; Brown,T. (1984) The synaptic nature of the paroxysmal depolarizing shift in hippocampal neurons. Ann Neurol Suppl 16: s65-71

79. Kandel E; Spencer,W. (1961) Excitation and inhibition on pyramidal cells during hippocampal seizure. Exp Neurol 4: 162-179

80. Kandel E; Spencer W.; Brinkly FJ (1961) Electrophysiology of hippocampal neurons. I Sequesntial invasion and synaptic organization. Nature 300:448-450

81. Katz B (1969) The release of neural transmitter substances. The Sherrington Lecture (in press)

82. Katz B, Miledi R (1970) Further study of the role of calcium in synaptic transmission. J Physiol (Lond) 207: 789-801

83. Kim, JH; Guimaraes, PO; Shen, MY; Masukawawa, LM; Spencer, DD (1990) Hippocampal neuronal density in temporal lobe epilepsy with and without gliomas. Acta Neuropathol. 80:41-45

84. Knowles W; Funch,P.; Schwartzkroin,P. (1982) Electrotonic and dye coupling in hippocampal CA1 pyramidal cells in vitro. Neuroscience 7: 1713-1722

85. Konnerth A, Heinemann U, Yarri Y (1984) Slow transmission of neural activity in hippocampal area ca1 in absence of active chemical synapses. Nature 307: 69-71

86. Konnerth A, Heinemann U, Yaari Y (1986) Nonsynaptic epileptogenesis in the mammalian hippocampus in vitro. I. Development of seizurelike activity in low extracellular calcium. J Neurophysiol 56: 409-423

87. Konnerth A; Heinemann,U. (1983) Presynaptic involvement in frequency facilitation in the hippocampal slice. Neurosci Lett 42: 255-260

88. Korn H, Faber DS (1980) Electrical field effect interactions in the vertebrate brain. Trends Neurosci jan: 6-9

89. Kuffler SW, Nicholls JG (1976) From Neuron to Brain. Sinauer, Massachusetts.

90. Kuffler SW,, Nicholls JG, Orkand RK (1966) Physiological properties of glial cells in the central nervous system of amphibia. J Neurophysiol 29: 768-787

91. Landcaster, B., Nicholl, R., (1987) Properties of two calcium-activated hyperpolarizations in rat hippocampal neurones. J. Physiol. 389:187-203.

92. Leao AAP (1972) Spreading depression. In: Purpura DP; Penry,J.K.; Walter,R.D. (ed) Experimental models of epilepsy - A manual for the laboratory worker. Raven, New York, pp 173-196

93. Leung LW (1979) Potentials evoked by alvear tract in hippocampal CA1 region of rats: Topographical projections, component anaylsis and correlation with unit activities. J. Neurophysiol 42:1557-1570.

94. Libet B, Gerard RW (1941) Steady potential fields and neurone activity. J Neurophysiol 4: 438-455

95. Lipton P, Whittingham TS (1984) Energy metabolism and brain slice function. In: Dingledine R (ed) Brain slices. Plenum press, New York,

96. Llinas R; Nicholson,C. (1974) Analysis of field potentials in the central nervous system. In: Remond A (ed) Handbook of EEG clinical neurophysiology. Elsevier, Amsterdam, pp 61-92

97. Lomo T (1971) Patterns of Activation in a Monosynaptic Cortical Pathway: The Perforant Path Input to the Dentate Area of the Hippocampal Formation. Exp Brain Res 12: 18-45

98. Lorente de No R (1934) Studies on the structure of the cerebral cortex.II Continuation of the study of the ammonic system. J Psychol Neurol 46: 113-177

99. Lowenstein WR (1981) Junctional intercellular communication: the cell-to-cell membrane channel. Physiol Rev 61: 829-913

100. Madison DV; Nicoli,R.A. (1982) Noradrenaline blocks accommodation of pyramidal cell discharge in the hippocampus. Nature 299: 636-638

101. Madison, D., Nicholl, R., (1984) Control of the repetitive discharge of rat CA1 pyramidal neurons in vitro. J. Physiol. 354:319-331

102. Matsumoto H; Ajmone Marsan,C.A. (1964) Cortical cellular phenomena in experimental epilepsy: interictal manifestations. Exp Neurol 9: 286-304

103. McBain CJ, Traynelis SF, Dingledine R (1990) Regional variation of extracellular space in the hippocampus. Science 249: 674-677

104. McIlwain H (1975) Preparing neural tissue for metabolic study in isolation. In: McIlwain H (ed) . Churchill Livingstone, London, pp 105-132

105. McVicar BA, Dudek FE (1981) Electrotonic coupling between pyramidal cells: a direct demonstration in rat hippocampal slices. Science 213: 782-785

106. Merwarth CR; Sieker,H.O. (1961) Acid-base changes in blood and cerebrospinal fluid during altered ventilation. J Appl Physiol 16: 1016-1018

107. Meyer JS; Gotoh,F.; Tazaki,Y. (1961) Inhibitory actions of carbon dioxide and acetazoleamide in seizure activity. Electroencephalogr Clin Neurophysiol 13: 762-775

108. Millichap JG (1969) Systemic electrolyte and neuroendocrine mechanisms. In: Jasper HH; Ward,A.A.; Pope,A. (ed) Basic mechanisms of the epilepsies. Little, Brown & Co., Boston, pp 709-729

109. Milner PM (1958) Note on a possible correspondence between the scotomas of migraine and spreading depression of Leao. Electroencephalogr Clin Neurophysiol 10: 705

110. Misgeld U, Frotscher M (1982) Dependence of the viability of neurons in hippocampal slices on oxygen supply. Br. Res Bull 8:95-100

111. Neyton J, Trautmann A (1986) Physiological modulation of gap junction permeability. J Exp Biol 124: 93-114

112. Nicholson C; Kraig, RP (1981) The behavior of extracellular ions during spreading depression. In: Zeuthen T (ed) The application of ion-selective microelectrodes. Elsivier\North-Holland Biomed, Amsterdam, pp 217-238

113. OBeirne M, Bulloch AGM, MacVicar BA (1987) Dye and electrotonic coupling between cultured neurons. Neurosci Lett 7: 265-270

114. O'Reilly CN, Richardson TL (1993) Antidromic bursting in the dentate gyrus during low $[Ca^{2+}]_o$ with applied fields. Soc. Neurosci. Abstr. p.1873 (764.20).

115. O'Reilly CN, Richardson TL (1992) A quantitative analysis of field-induced alterations of the granule cell transmembrane potential. Can.J.Physiol.Pharmacol. vol.70:axvii

116. O'Reilly CN, Richardson TL (1992) Further characterization of field induced alterations of evoked potentials in the dentate gyrus. Can.J.Physiol.Pharm. vol.70:axvii

117. Orkand RK; Nicholls,J.G.; Kuffler,S.W. (1966) Effect of nerve impulses on the membrane potential of glial cells in the central nervous system of amphibia. J Neurophysiol 29: 788-806

118. Palay SL, Chan-Palay V (1974) Cerebellar Cortex, Cytology, and Organization. Springer-Verlag, New York,

119. Pokorny J, Schwartzkroin PA (1991) Do hippocampal CA3 cells project into the dentate hilus? Society for Neuroscience Abstracts 17: 52.1(Abstract)

120. Prince DA (1982) Epileptogenesis in hippocampal and neocortical neurons. In: Klee M; Lux,H.D.; Speckmann,E.J. (ed) Physiology and pharmacology of epileptogenic phenomena. Raven Press, New York, pp 151-162

121. Prince DA (1985) Physiological Mechanisms of Focal epileptogenesis. Epilesia 26(sup)s3-14.

122. Purpura DP (1969) Mechanisms of propagation: intracellular studies. In: Jasper HH; Ward,A.A.; Pope,A. (ed) Basic Mechanisms of the Epilepsies. Churchill, London, pp 441-451

123. Purpura DP (1974) Evidence contradicting neuron sensitivity to extracellular fields. Neurosciences Res Prog Bull 12: 143

124. Purpura DP, Malliani A (1966) Spike generation and propagation initiated in dendrites by transhippocampal polarization. Brain Res 1: 403-406

125. Ramon y Cajal S (1911) Histologie du Systeme Nerveux de l'Homme et des Vertebres. Maloine, Paris,

126. Rao ML, Froscher W, Bulau P (1987) Influence of anticonvulsants and flunarizine on the metabolism of thyroid hormones: speculation about the possible role of calmodulin. Clin Neuropharmacol 10: 356-364

127. Richardson , TL, O'Reilly, CN, (1993) Spontaneous low Ca2+ bursting can be blocked or induced by applied fields. Soc. Neruosci. Abstr. p.1872 (764.19)

128. Richardson TL, Turner RW, Miller JJ (1984a) Extracellular fields influence transmembrane potentials and synchronization of hippocampal neuronal activity. Brain Res 294: 255-262

129. Richardson TL, Turner RW, Miller JJ (1984b) Extracellular voltage gradients and ephaptic interactions in the hippocampal formation. Soc Neurosci (Abstract)

130. Richardson TL, Turner RW, Miller JJ (1987) Action-potential discharge in hippocampal CA1 pyramidal neurons: current source-density analysis. J Neurophysiol 58: 981-996

131. Roper SN, Obenaus A, Dudek FE (1992) Osmolality and Non-synaptic epileptiform bursts in rat CA1 and dentate. Ann. Neurology; 89:676-680

132. Sagar, HJ; Oxbury, JM (1987) Hippocampal neuron loss in temporal lobe epilepsy: correlation with early childhood convulsions. Ann. Neurol. 22:334-340

133. Schweitzer, JS; Patrylo, PR; Dudek, FE (1992) Prolonged field bursts in the dentate gyrus: dependence on low Ca^{2+}, high K^{+}, and nonsynaptic mechanisms. J. Neurophys. vol.158, 6:2016-2025.

134. Schwartzkroin PA (1981) To slice or not to slice. In: Kerkut GA, Wheal HV (eds) Electrophysiology of isolated mammalian CNS preparations. Academic Press, New York, pp 82-91

135. Schwartzkroin PA; Scharfman,H.E.; Sloviter,R.S. (1990) Similarities in circuitry between Ammon's horn and dentate gyrus: local interactions and parallel processing. In: . pp 269-286

136. Shepherd GM (1990) The synaptic organization of the brain. Oxford university press, New York,

137. Smith SJ (1991) Neural and glial network interactions: visualization in live brain tissues. Society of Neuroscience Abstracts 598: 278(Abstract)

138. Snow RW, Dudek FE (1984) Electrical fields directly contribute to action potential synchronization during convulsant-induced epileptiform bursts. Brain Res 323: 114-118

139. Snow RW, Dudek FE (1986) Evidence for neuronal interactions by electrical field effects in the ca3 and dentate regions of rat hippocampal slices. Brain Res 367: 292-295

140. Somjen G; Dingledine,R.; Connors,B.; Allen,B. (1981) Extracellular potassium and calcium activities in the mammalian spinal cord, and the effect of changing ion levels on mammalian neural tissues. In: Sykova E; Hnik,P.; Vyklicky,L. (ed) Ion-selective microelectrodes and their use in excitable tissues. Plenum, New York, pp 159-180

141. Somjen GG (1973) Do potassium, glia, and neurons interact? In: Woody CDet al (ed) Cellular mechanisms subserving changes in neuronal activity. Brain Information Services, Los Angeles, pp 79-96

142. Sperti L; Gessi T; Volta F (1966) Extracellular potential field of antidromically activated CA1 pyramidal neurons. Brain Res. 3:343-361

143. Spray DC; Bennett,M.V.L. (1985) Physiology and pharmacology of gap junctions. Annu Rev Physiol 47: 281-313

144. Stinger JL, Lothman EW (1989) Maximal dentate gyrus activation: characteristics and alterations after repeated seizures. J. Neurophysiol. 62, 136-143.

145. Stringer JL, Lothman EW (1990) Maximal dentate activation: a tool to screen compounds for activity against limbic seizures. Epilepsy Res. 5, 169-176.

146. Stringer JL, WIlliamson JM, Lothma EW (1989) Induction of paroxysmal discharges in the dentate gyrus: frequency dependence and relationship to afterdischarge production. J.Neurophysiol. 62,126-135.

147. Stringer JL, Williamson JM, Lothman EW (1991) Maximal dentate activation is produced by amygdala stimulation in unanesthetized rats. Brain Res. 542, 336-342.

148. Stringer JL, Lothman EW (1992) Bilateral maximal dentate activation is critical for the appearance of an aftterdischarge in the dentate gyrus. Neuroscience 46(2) 309-314.

149. Taylor CP, Dudek FE (1982) Synchronous neural afterdischarges in rat hippocampal slices without active chemical synapses. Science 218: 810-812

150. Taylor CP, Dudek FE (1984) Synchronization without active chemical synapses during hippocampal afterdischarges. J Neurophysiol 52: 143-155

151. Taylor CP; Krnjevic K; Ropert N (1984) Facilitation of hippocampal CA1 pyramidal cell firing by electrical fields generated antidromically. Neuroscience (11)1:101-109

152. Treherne JE (1981) Review volume: glial-neurone interactions. J Exp Biol 95: 1-240

153. Turin L; Warner,A.E. (1978) Carbon dioxide reversibly abolishes ionic communication between cells of early amphibian embryos. Nature 270: 56-57

154. Turner, RW, Meyers, DE, Richardson, TL, Barker, JL (1991) The site for initiation of action potential discharge over the somatodendritic axis of rat hippocampal CA1 pyramidal cells. J. Neruoscience 11(7):2270-2280.

155. Urban, L, Aitken, PG, Crain, BJ, Freidman, AH, Somjen, GG, (1993) Correlation between function and structure in "epileptic" human hippocampal tissue maintained in vitro. Epilepsia 34(1):54-60.

156. Varon SS, Somjen GG (1979) Neuron-glial interactions. Neurosciences Res Prog Bull 17: 1-239

157. Warburg O (1923) Versuche anuberebendem carinomgewebe (methoden). Biochem Z, 142: 317-350. In: Brain Slices, Dingledine, R. (1984) Plenum Press, New York

158. Warburg O; Posner K; Negelien E (1924) Uber den Stowechsel der carcinozelle. Mol Parmacol. 6: 13-23. In: Brain Slices, Dingledine,R. (1982) Plenum Press, New York.

159. Winson J (1974) Patterns of hippocampal theta rhythm in the freely moving rat. Electroencephalogr Clin Neurophysiol 36: 291-301

160. Yaari Y, Konnerth A, Heinemann U (1983) Spontaneous epileptiform activity of ca1 hippocampal neurons in low extracellular calcium solutions. Exp Brain Res 51: 153-156

161. Yaari Y, Konnerth A, Heinemann U (1986) Non-synaptic epileptogenesis at the mammalian hippocampus in vitro II. Role of extracellular potassium. J. Neurophysiol 56:424-438.

162. Yaari Y; Jensen,M.S. (1988) Nonsynaptic mechanisms and interictal-ictal transitions in the mammalian hippocampus. In: Dichter M (ed) Mechanisms of epileptogenesis. Plenum, New York, pp 183-197

163. Yamamoto C (1972) Activation of Hippocampal Neurons by Mossy Fiber Stimulation in Thin Brain Sections in Vitro. Exp Brain Res 14: 423-435

166. Yamamoto C, Kawai N (1967) Presynaptic action of acetylcholine in thin sections from the guinea pig dentate gyrus in vitro. Expl Neurol 19: 176-187

165. Yim CC, Krnjevic K, Dalkara T (1986) Ephaptically generated potentials in CA1 neurons of rat's hippocampus in situ. J Neurophysiol 56: 99-122